Chemical Studies on Okinawan Marine Sponges *Agelas* spp.

2019

Lee Sanghoon

Abbreviations

Ac	acetyl
aq.	aqueous
BuOH	butanol
CD	circular dichroism
COSY	correlated spectroscopy
DMSO	dimethyl sulfoxide
2D NMR	two dimensional nuclear magnetic resonance
ESI	electrospray ionization
ext.	extract
fr.	fraction
HMBC	^{1}H-detected heteronuclear multiple bond correlation
HPLC	high performance liquid chromatography
HR	high resolution
HSQC	heteronuclear single quantum coherence
J	coupling constant
Me	methyl
MeOH	methanol
mmu	milli mass unit
MPLC	medium-pressure liquid chromatography
MS	mass spectrometry
n-	normal
NMR	nuclear magnetic resonance
ODS	octadecylsilyl
OMe	methoxy
OR	optical rotation
ROESY	rotating frame nuclear Overhauser effect spectroscopy
sp.	species (the singular form)
spp.	species (the plural form)
TFA	trifluoroacetic acid
UV	ultraviolet
wt.	weight

Contents

Chapter 1.
General Introduction

Natural products have long been an important source of therapeutic agents and/or their lead compounds because of diverse chemical structures and biological activities [1]. Especially, marine collection efforts over the years have focused on obtaining diverse biota to maximize the potential chemical diversity with intriguing biological activities [2]. Although a number of therapeutic agents have been developed based on chemical constituents from plants, mammals, and microorganisms, marine natural products have also made an important contribution to drug discovery. Macroorganisms such as algae, sponges, corals, and other marine invertebrates have been studied for their secondary metabolites, while researches on marine microorganisms are also significantly increasing in the recent years [3].

The global marine pharmaceutical pipeline is very active now. Eight compounds from marine sources have approved as therapeutic agents by the U.S. Food and Drug Administration (FDA) or European Medicines Agency (EMA) (Table 1-1), while several candidates are in different phases of the clinical trials (Table 1-2) [4]. Among approved agents, three marine natural products, ziconotide (Prialt®), trabectedin (Yondelis®), and iota carrageenan (Carragelose®), are on the market without any modification of the original structures (Figure 1-1), whereas the rest of them were modified to optimize for their development [4].

Table 1-1. Marine drugs approved by the FDA and EMA.

Compound (trademark)	NP/D[a]	Original NP/source organism	Target area
Cytarabine (Cytosar-U®; Depocyte®)	D	Spongouridine and spongothymidine /sponge *Cryptotethya crypta*	Cancer
Vidarabine (Vira-A®)	D	Spongouridine and spongothymidine /sponge *Cryptotethya crypta*	Antiviral
Ziconotide (Prialt®)	NP	ω-Conotoxin /marine snail *Conus magus*	Pain
Omega-3-acid ethyl esters	D	Omega-3-fatty acids /fish	Hypertriglyceridemia
Trabectedin (Yondelis®)	NP	Ecteinascidin 743 /tunicate *Ecteinascidia turbinata*	Cancer
Eribulin mesylate (Halaven®)	D	Halichondrin B /sponge *Halichondria okadai*	Cancer
Brentuximab vedotin (Adcetris®)	D	Dolastatin 10 /sea hare *Dolabella auricularia*	Cancer
Iota carrageenan (Carragelose®)	NP	Iota carrageenan /red algae *Eucheuma/Chondrus*	Antiviral

[a]Marine natural product (NP), derivative (D)

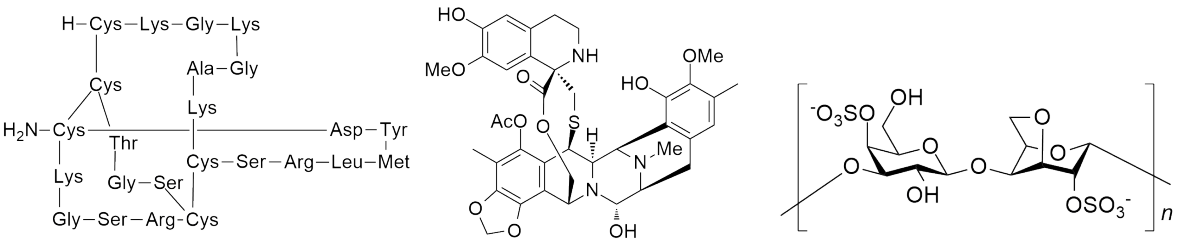

Ziconotide (Prialt®) from marine snail *Conus magus*

Trabectedin (Yondelis®) from tunicate *Ecteinascidia turbinata*

Iota carrageenan (Mono-subunit of Carragelose®) from red algae *Eucheuma* and *Chondrus*

Figure 1-1. Structures of marine-derived drugs approved by the FDA and EMA on the market without modification.

Especially, halichondrin B was initially isolated from marine sponge *Halichondria okadai* as an anticancer agent in 1986 [5]. After it was accepted for preclinical development by the U.S. National Cancer Institute in 1992 [6], total synthesis of halichondrin B was achieved [7]. This results opened for development of a simplified synthetic analog, eribulin (Figure 1-2). It showed greater activity against lung and breast tumors in animal studies than either the parent molecule halichondrin B or paclitaxel (Taxol®), an anticancer agent derived from the bark of Pacific yew, *Taxus brevifolia* [8]. In 2010, eribulin was approved by the FDA as an anticancer drug, and this is marketed by Eisai Co. under the trademark Halaven® [9a], and has also received approval to market in Japan in 2011 [9b].

Table 1-2. Representative candidates of marine natural products or their derivatives in clinical trials by the FDA and EMA.

Candidate	NP/D[a]	Source organism	Target area	Status EMA 2016	Status FDA 2016
Plitidepsin	NP	tunicate *Aplidium albicans*	Cancer	Phase Ⅲ	Phase Ⅲ
Squalamine	NP	shark *Squalus acanthias*	Neovascular AMD[b]	Phase Ⅲ	Phase Ⅲ
Lurbinectedin	D	tunicate *Ecteinascidia turbinata*	Cancer	Phase Ⅲ	Phase Ⅲ
Plinabulin	D	halimide analog	Cancer	None	Phase Ⅲ
Tetrodotoxin	NP	pufferfish symbiotic bacteria	Chronic pain	None	Phase Ⅲ

[a]Marine natural product (NP), derivative (D)

[b]Neovascular age-related macular degeneration

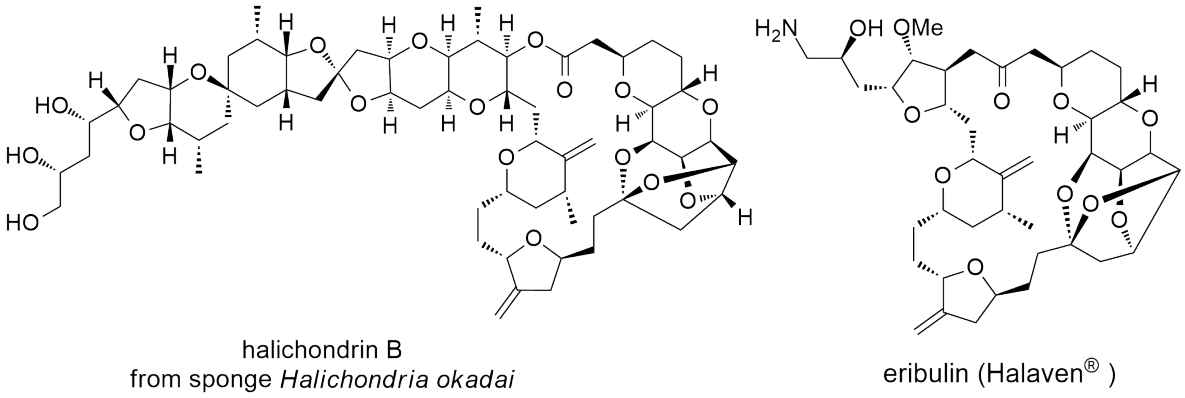

Figure 1-2. Structures of halichondrin B and eribulin.

In alignment with the pharmaceutical industry, the cosmeceuticals, a combination of cosmetic and pharmaceutical industry have attracted increased attention because of their beneficial effects on human beauty and health. Bioactive secondary metabolites derived from marine organisms have diverse functional roles, and these properties can be applied to the development of cosmeceuticals [10].

Sponges (phylum Porifera) are the oldest multicellular animals (Metazoa), and more than 8,000 species have discovered under the sea around the world to date [11]. A simple analogy of a sponge is a flexible balloon containing a gelatinous ground substance, a roving cell population, water canals and water pumping stations, and organic and/or inorganic structures producing a definite body form [12]. The marine sponge is bounded on the exterior surface by a unicellular layer (exopinacoderm), called the ectosome, composed of special epithelial cells (pinacocytes). Internally, the choanosome, the sponge is excavated by water current canals, also lined by a single layer of cells (porocytes) forming the endopinacoderm. Water pumping station are found at certain locations along the water canals, lined by special collar cells with a flagellum, unique to the Porifera [13].

Sessile organisms such as sponges and other marine invertebrates (including corals and ascidians) rely on their secondary metabolites as a form of defense against predators and competitors. Interestingly, the metabolites appear to be produced by sponge-associated microorganisms. Through some observations such as nutrition providers and percentage of bacteria from sponges, some ecologists argued that microorganisms may help defend their host sponges against disease-causing bacteria. Though unculturable symbiotic microorganisms occupy more than 40% of sponge tissue volume, scientists are still not exactly sure the true producer of natural products isolated from marine sponges [14].

Intense researches on constituents of marine sponges have been carried out to give abundant structurally unique natural products with intriguing bioactivities such as purealin

(ATPase modulator) [15], calyculin A (cytotoxicity) [16], and theonezolide A (microtubule reorganization) [17] (Figure 1-3). Therefore, marine sponges are excellent sources for natural product chemists since their diversity of unique chemical structure with biological activities [18].

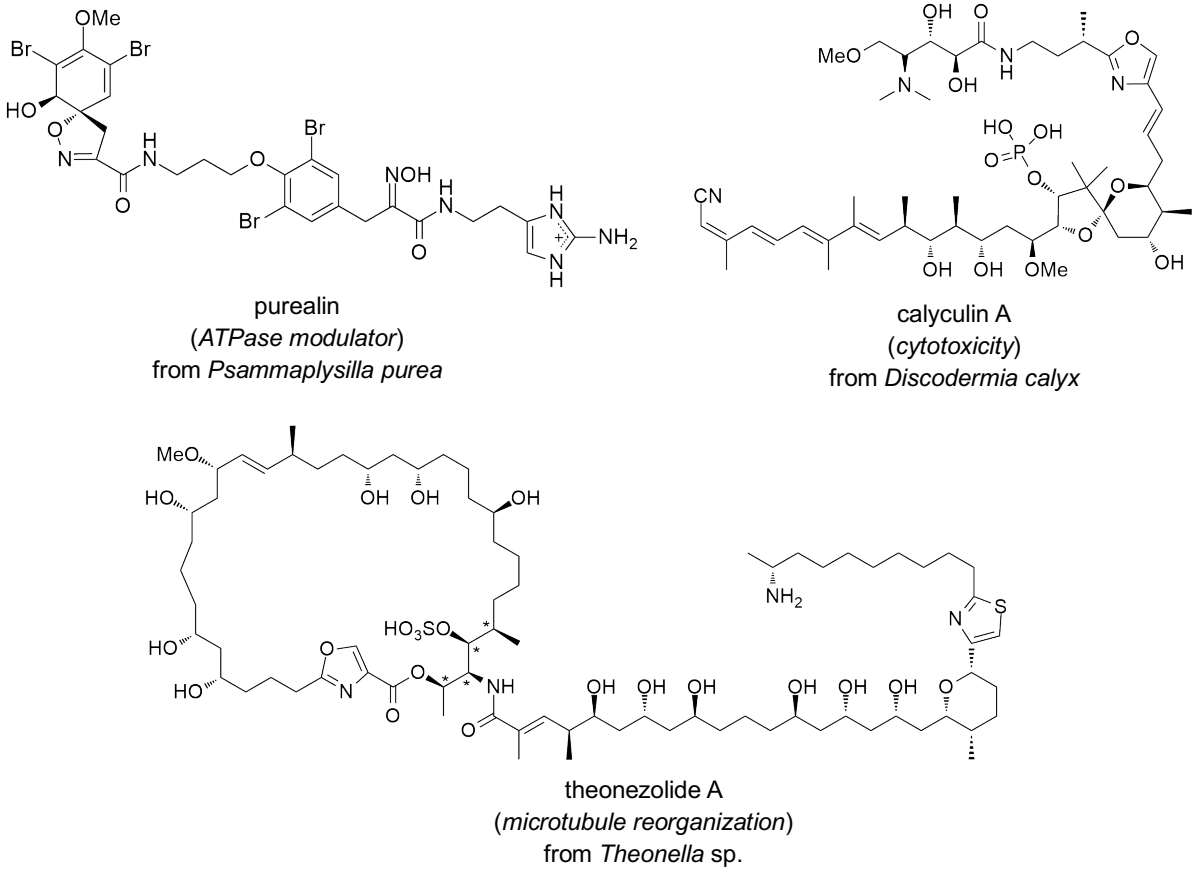

Figure 1-3. Representative natural products from marine sponges.

Marine sponges belonging to the genus *Agelas* are a rich source of interesting natural products such as diterpene alkaloids and bromopyrrole alkaloids (Figure 1-4), which have been used as taxonomically characteristic compounds of *Agelas* sponges [19]. A study showed that bromopyrrole alkaloids were produced by not symbiotic bacterial populations but the sponge cells [20].

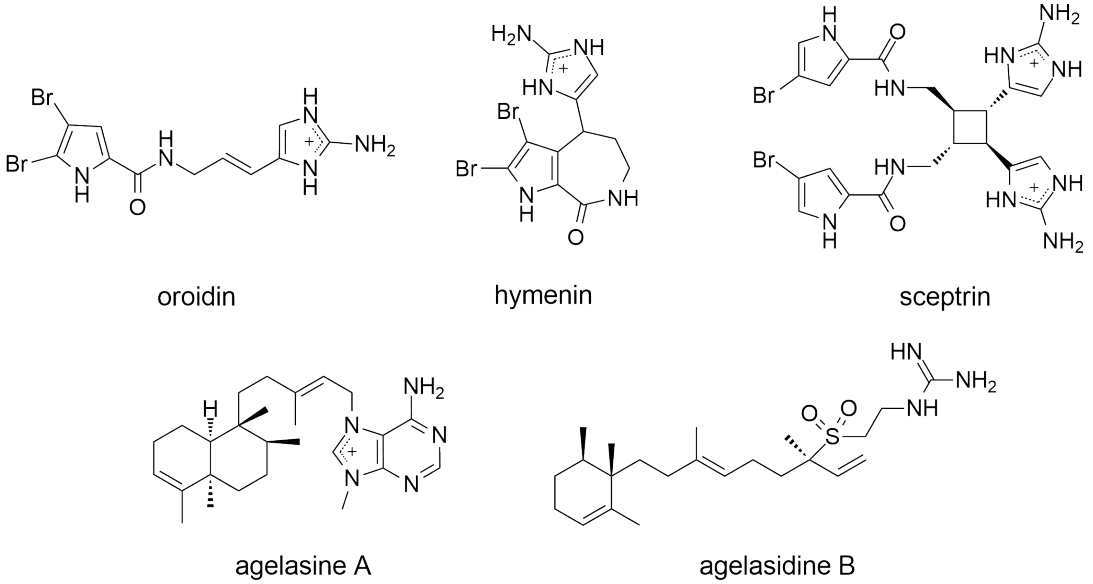

Figure 1-4. Representative secondary metabolites from marine sponges *Agelas* spp.

In our continuing search for structurally unique secondary metabolites from marine sponges, constituents of four *Agelas* sponges (SS-12, SS-1302, SS-159, and SS-516) collected at Okinawa prefecture, Japan, were investigated. From the extract of SS-12, two new diterpene alkaloids, agelamasines A (**1**) and B (**2**), and six known diterpene alkaloids (**3**–**8**) were isolated (Figure 1-5). Three new bicyclic (**9**–**11**) and three new linear (**12**–**14**) bromopyrrole alkaloids were isolated from SS-1302, together with four known natural products (**15**–**18**) (Figure 1-6). From the extracts of SS-159, 13 known bromopyrrole alkaloids (**19**–**31**) were isolated, while two new linear bromopyrrole alkaloids (**32** and **33**) were isolated from SS-516, along with two known bromopyrrole alkaloids (**34** and **35**) (Figures 1-6 and 1-7).

In this thesis, the isolation and structure elucidation of the new diterpene alkaloids and bromopyrrole alkaloids are described.

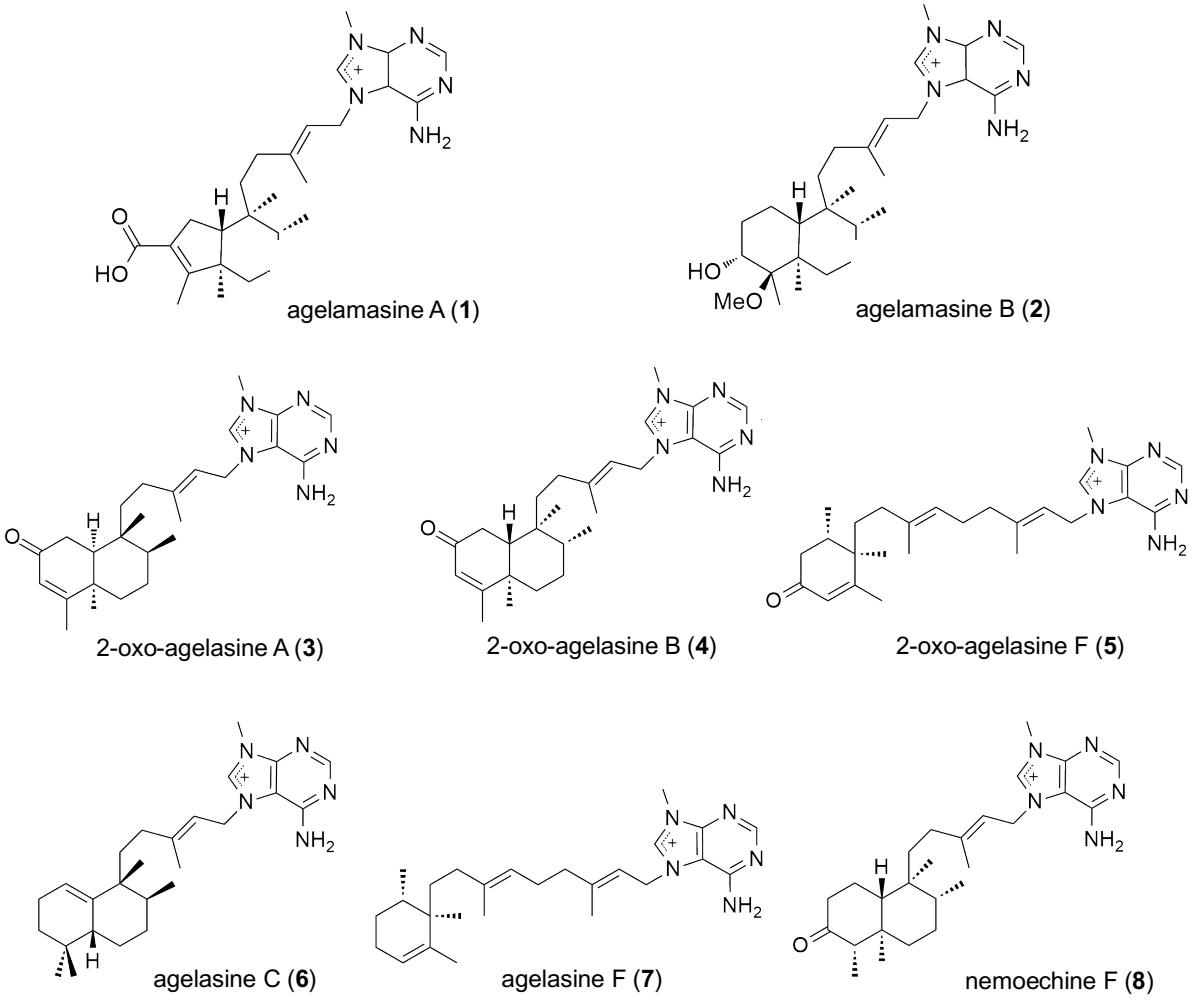

Figure 1-5. Isolated diterpene alkaloids from an Okinawan marine sponge *Agelas* sp. (SS-12).

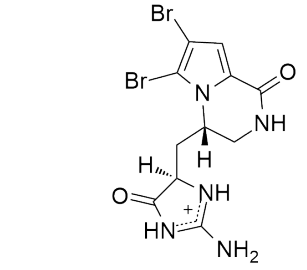

agesamide C (**9**)

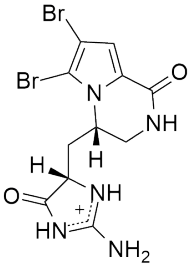

agesamide D (**10**)

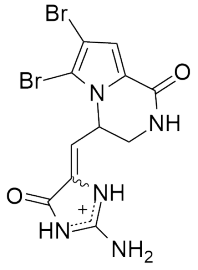

agesamide E (**11**)

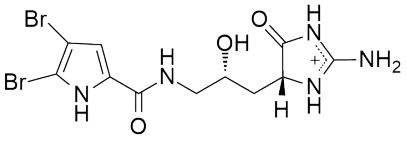

9-hydroxydihydrodispacamide (**12**)

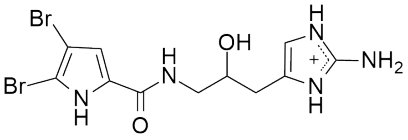

9-hydroxydihydrooroidin (**13**)

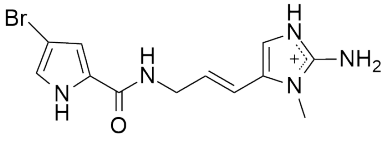

9-(*E*)-keramadine (**14**)

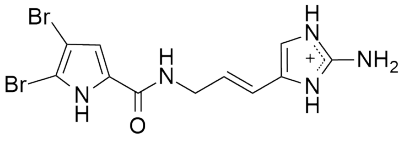

oroidin (**15**)

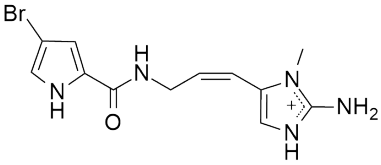

keramadine (**16**)

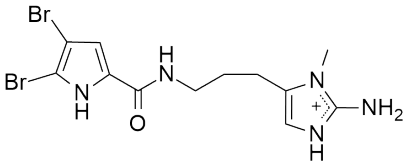

2-bromo-9,10-dihydrokeramadine (**17**)

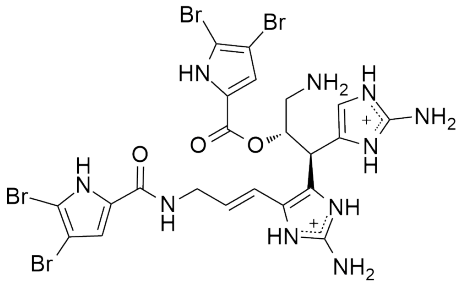

nagelamide L (**18**)

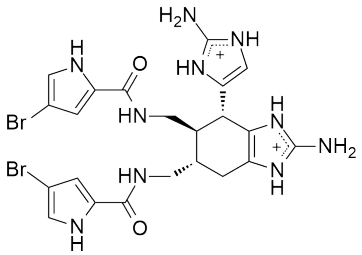

ageliferin (**19**)

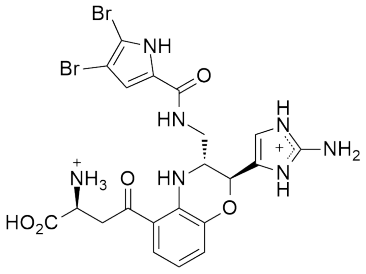

agelamadin C (**20**)

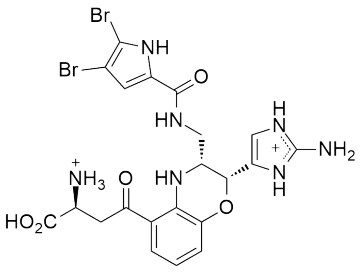

agelamadin D (**21**)

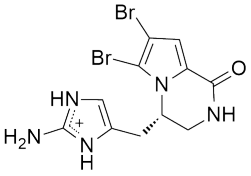

cyclooroidin (**22**)

Figure 1-6. Isolated bromopyrrole alkaloids from Okinawan marine sponges *Agelas* spp. (SS-1302, SS-159, and SS-516).

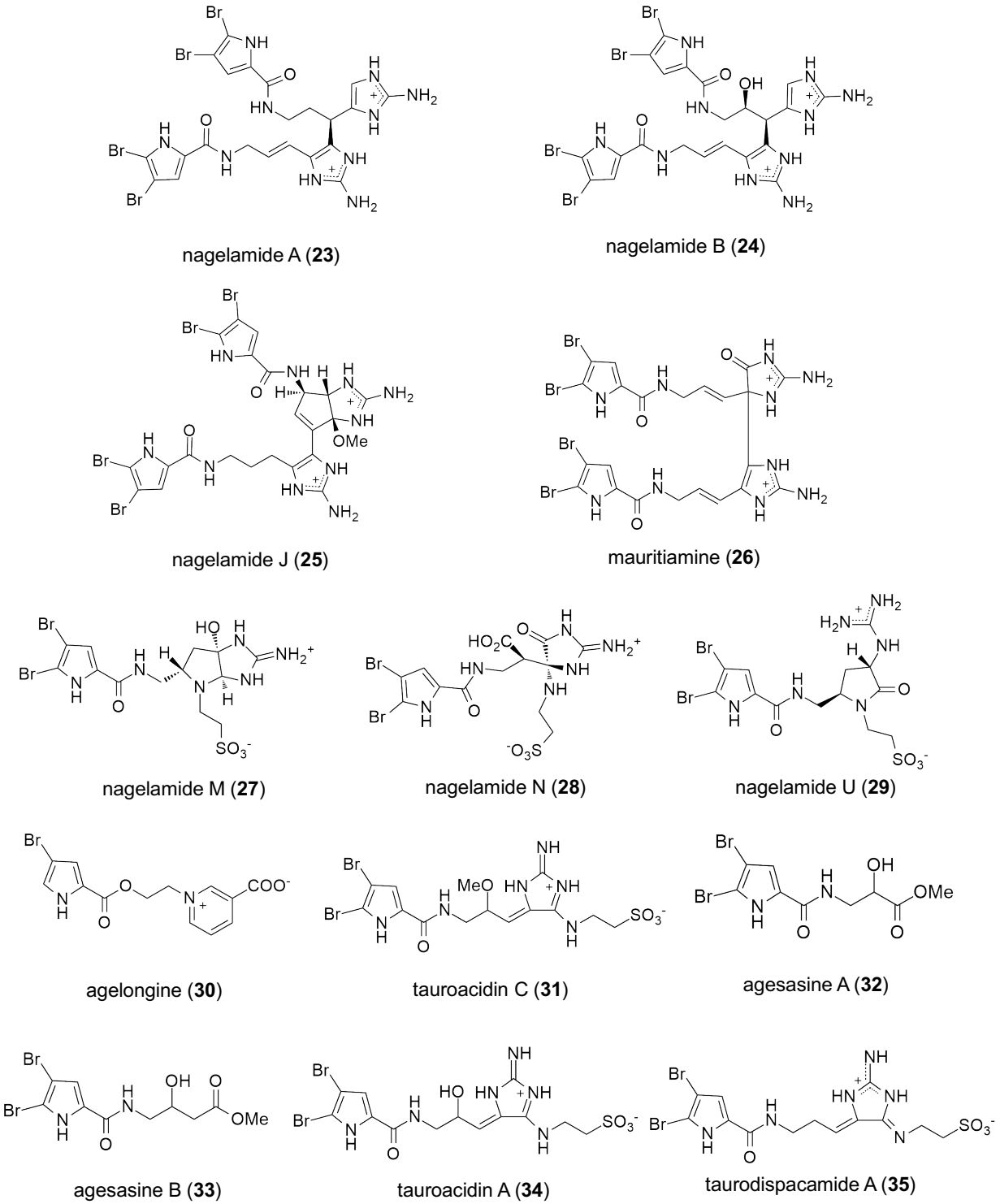

Figure 1-7. Isolated bromopyrrole alkaloids from Okinawan marine sponges *Agelas* spp. (SS-1302, SS-159, and SS-516).

Chapter 2.
New Diterpene Alkaloids from Marine Sponge *Agelas* sp.

2.1. Introduction

Living organisms produce thousands of low molecular weight organic compounds with diverse chemical structures. Among them, terpenes are the largest group of natural products [21]. Approximately 5,000 natural diterpenes derived from the parent geranylgeranyl pyrophosphate are known [22]. Since Cullen and Devlin reported the isolation of agelasine, *N*-methyladenine derivative of an unidentified diterpene as a constituent of the marine sponge *Agelas dispar* in 1975, a number of mono or bicyclic diterpenes having a polar functionality such as hypotaurocyamine and *N*-methyladenine have been reported [23].

The representative monocyclic diterpene alkaloids, agelasidine C and agelasine E, have been isolated from an Okinawan marine sponge *Agelas nakamurai.* They represent partially hydrogenated and rearranged axerophthene skeleton substituted by a hypotaurocyamine and an *N*-methyladenine moieties, respectively, at the end of the chains [22]. In addition, bicyclic diterpene alkaloids possessing halimene, labdane, and clerodane skeletons have reported to date (Figure 2-1).

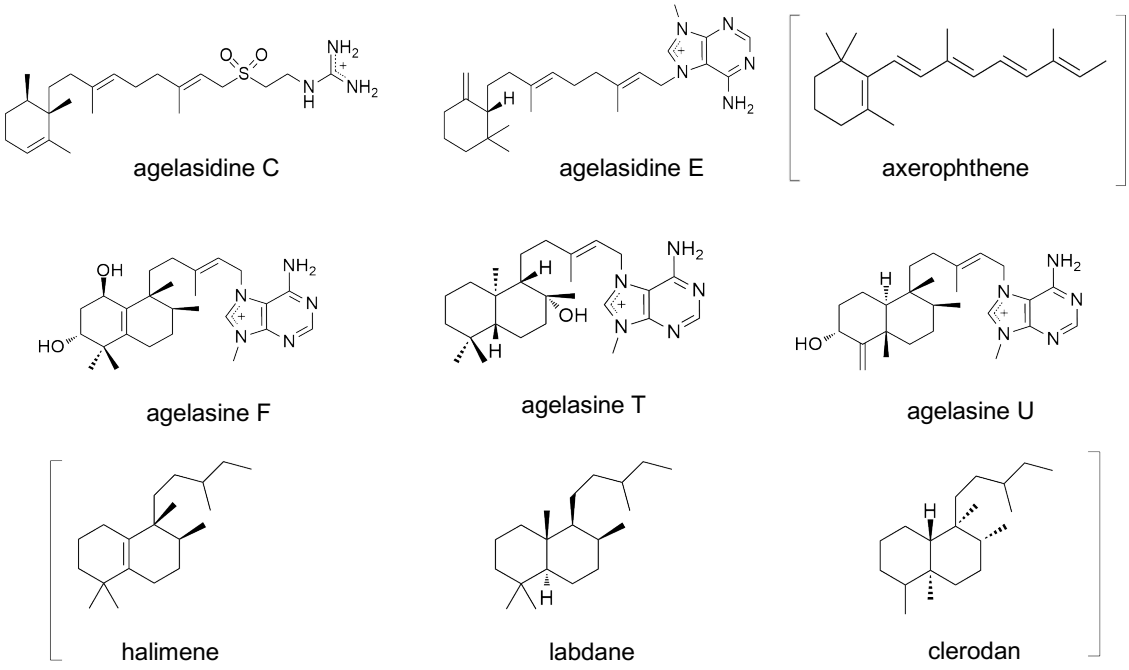

Figure 2-1. Diterpene alkaloids from marine sponges.

Diterpene alkaloids isolated from marine sponges *Agelas* spp. exhibit various bioactivities such as antimicrobial [24], antibiofilm formation [25], antiproliferative [26], antiprotozoal [27], and antifouling [28] activities. A research showed antimicrobial activity of bicyclic diterpene alkaloids, agelasines B, C, and D (Figure 2-2), against *Mycobacterium* sp. in the dormant state [29]. Another study showed a diterpene alkaloid with a brominated pyrrole ester moiety, agelasine G (Figure 2-2), inhibited protein tyrosine phosphatase (PTP) 1B activity. In contrast, ageline B, a debromo derivative of agelasine G (Figure 2-2), was inactive in spite of its structural similarity to agelasine G, indicating that the bromine atom at the pyrrole ring plays an important role in the PTP1B inhibitory activity [30].

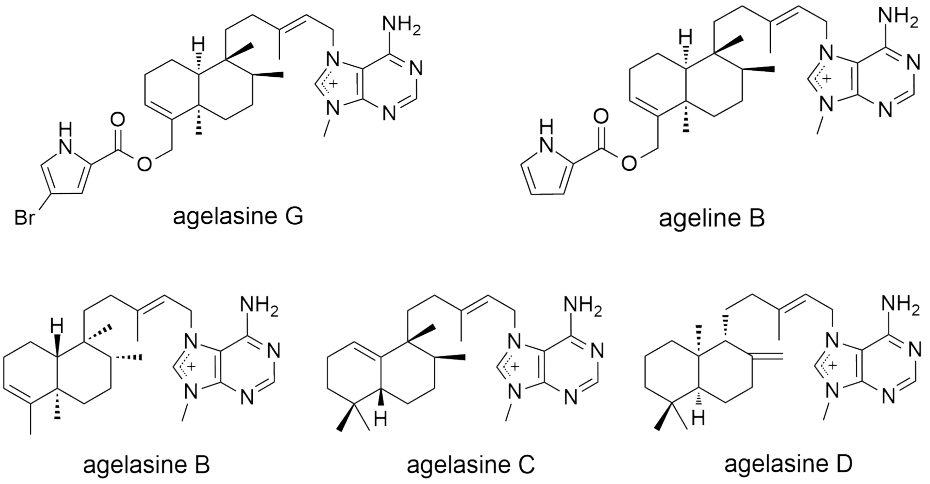

Figure 2-2. Examples of bioactive diterpene alkaloids from sponges *Agelas* spp.

2.2. Extraction and Isolation

The sponge *Agelas* sp. (SS-12, 1.96 kg, wet weight) was extracted with MeOH at room temperature to give the extract (95.8 g), which was partitioned between *n*-hexane and 90% MeOH aq. to remove hydrophobic components. The 90% MeOH aq.-soluble materials were further partitioned with *n*-BuOH and water. Chromatographic separations of a part (23.2 g) of the *n*-BuOH-soluble materials (43.0 g) gave eight diterpene alkaloids including two new compounds, agelamasines A (**1**, 1.7 mg) and B (**2**, 2.2 mg) (Scheme 1).

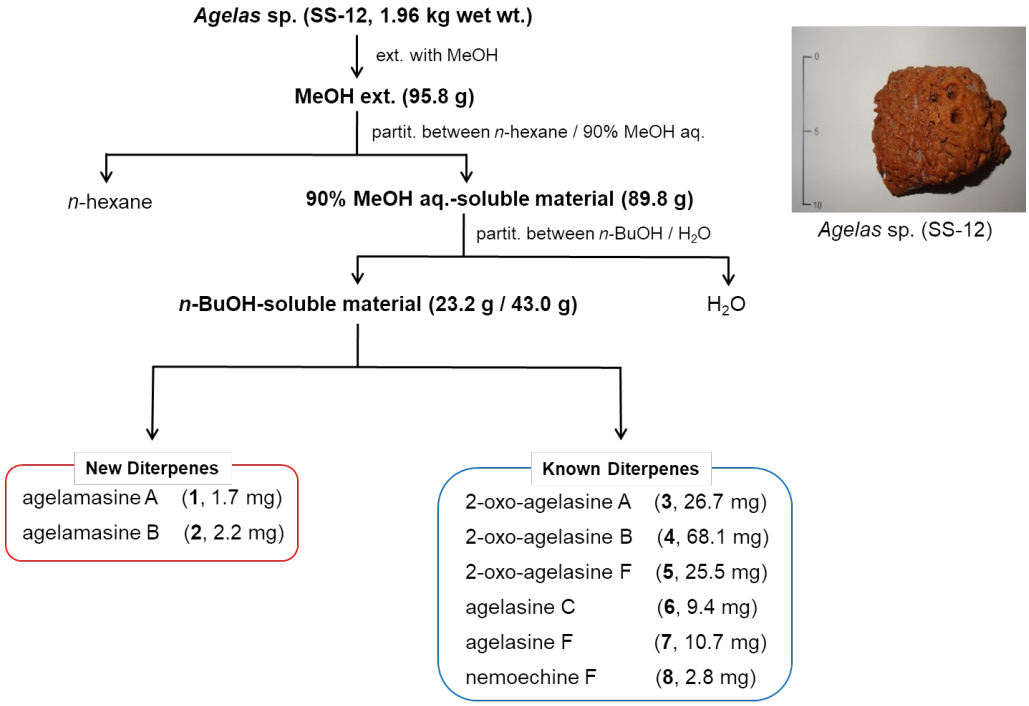

Scheme 1. Isolation scheme of agelamasines A (**1**) and B (**2**) from a marine sponge *Agelas* sp. (SS-12).

2.3. Identification of Known Diterpene Alkaloids

Compounds **3**–**8** were identified as 2-oxo-agelasine A (**3**) [31], 2-oxo-agelasine B (**4**) [32], 2-oxo-agelasine F (**5**) [31], agelasine C (**6**) [23], agelasine F (**7**) [23], and nemoechine F (**8**) [33] by comparison of their spectroscopic data with those reported in the literature (Figure 2-3). Among these, **3**, **4**, **6**, and **8** are bicyclic diterpene alkaloids with *cis*-clerodane, *trans*-clerodane, halimane, and *tran*-clerodane skeletons, respectively, while **5** and **7** are monocyclic diterpene alkaloids. The diterpene alkaloids (**3**–**8**) had an *N*-methyladenine moiety, in common.

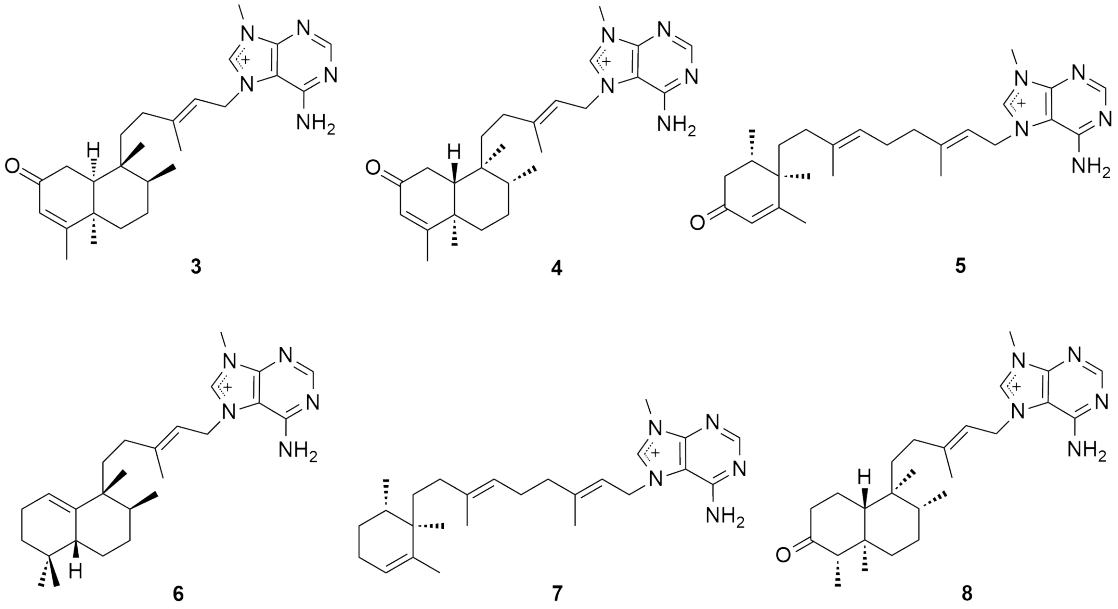

Figure 2-3. Known diterpene alkaloids from a marine sponge *Agelas* sp. (SS-12).

2.4. Structure Elucidation of New Diterpene Alkaloids

2.4.1. Agelamasine A (**1**)

Agelamasine A (**1**) {$[\alpha]_D^{28}$ +12.7 (*c* 0.1, MeOH)} was isolated as a pale yellow amorphous solid. The molecular formula of **1** was elucidated to be $C_{26}H_{38}N_5O_2$ by the HRESIMS (*m/z* 474.2877 $[M–H+Na]^+$, Δ+3.2 mmu). The ^{1}H NMR spectrum showed the signals of one trisubstituted olefin, two sp^3 methines, six sp^3 methylenes, one secondary methyl, and four tertiary methyls, together with the characteristic resonances due to an *N*-methyladenine moiety (H-2', H-8', and *N*-Me) (Figure 2-4 and Table 2-1); these spectral features were similar to those found in diterpene alkaloids from *Agelas* marine sponges [31,34,35]. The ^{13}C NMR spectrum displayed 20 carbon signals including two sp^3 quaternary carbons, two double bonds, and one carboxyl group, along with the resonances due to the *N*-methyladenine moiety. The chemical shifts of C-2 (δ_C 127.6), C-3 (δ_C 170.4), and C-4 (δ_C 167.1) implied the presence of an α,β-unsaturated carboxylic acid (Table 2-1).

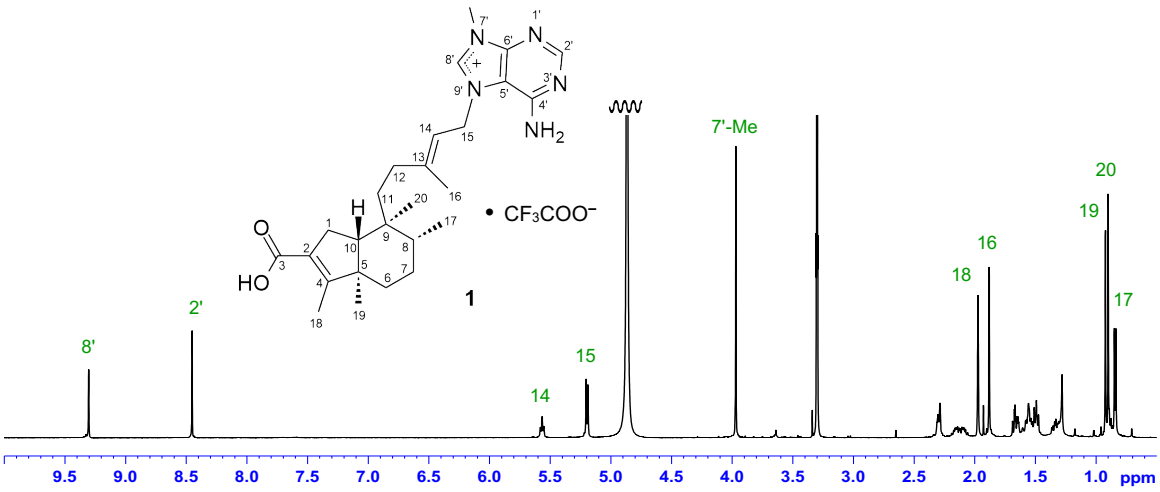

Figure 2-4. ^{1}H NMR spectrum of agelamasine A (**1**) as a TFA salt form in CD_3OD (500 MHz).

Analysis of the ^{1}H-^{1}H COSY and HMBC spectra revealed the presence of a prenyl moiety (C-12–C-16) and a hexahydroindene ring (C-1, C-2, and C-4–C-10) with four methyl groups at C-4, C-5, C-8, and C-9 (Figure 2-5). The presence of the carboxy group at C-2 was suggested by a ^4J HMBC correlation for H_3-18 with C-3 in the HMBC spectrum with a delay value for J_{CH} = 5 Hz. A similar ^4J long-range correlation has been observed in the HMBC spectrum of a related known diterpene [36]. The carboxy group at C-2 was also supported by resemblance of the ^{13}C chemical shifts for C-1–C-10 and C-17–C-20 in **1** with those corresponding positions in related known diterpenes [37,38]. A ^{1}H-^{1}H COSY cross-peak of H_2-11 and H_2-12 and an HMBC correlation for H_3-20 with C-11 showed the connectivity between C-9 to C-12 via C-11. HMBC correlations for H_2-15 with C-5' and

Table 2-1. ^{1}H and ^{13}C NMR data for agelamasines A (**1**) and B (**2**) as a TFA salt form in CD_3OD.

Position	**1**		**2**	
	^{13}C	^{1}H (*J* in Hz)	^{13}C	^{1}H (*J* in Hz)
1	30.7	2.30 (2H, m)	17.5	1.58, 1.28 (each 1H, m)
2	127.6	–	31.2	1.83, 1.60 (each 1H, m)
3	170.4	–	71.1	3.76 (1H, brs)
4	167.1	–	81.0	–
5	51.6	–	43.7	–
6	35.8	1.65, 1.33 (each 1H, m)	33.1	1,76, 1.22 (each 1H, m)
7	29.5	1.55 (2H, m)	27.9	1.43, 1.28 (each 1H, m)
8	38.7	1.54 (1H, m)	37.3	1.43 (1H, m)
9	39.0	–	39.8	–
10	55.5	1.68 (1H, m)	41.0	1.97 (1H, brd, 11.2)
11	39.3	1.49 (2H, t, 8.6)	38.0	1.52, 1.40 (each 1H, m)
12	34.5	2.12 (2H, m)	34.6	2.06 (2H, m)
13	149.9	–	150.3	–
14	115.4	5.57 (1H, t, 7.0)	115.3	5.55 (1H, t, 7.0)
15	48.6	5.20 (2H, d, 7.0)	48.7	5.19 (2H, d, 7.0)
16	17.1	1.88 (3H, s)	17.1	1.87 (3H, s)
17	15.5	0.84 (3H, d, 6.3)	16.5	0.79 (3H, d, 6.0)
18	11.7	1.97 (3H, s)	14.4	1.14 (3H, s)
19	17.3	0.92 (3H, s)	18.2	1.13 (3H, s)
20	18.5	0.90 (3H, s)	19.0	0.75 (3H, s)
4-OMe			50.1	3.16 (3H, s)
2'	157.1	8.45 (1H, s)	157.1	8.45 (1H, s)
4'	154.1	–	154.2	–
5'	111.2	–	111.2	–
6'	151.0	–	150.9	–
8'	142.0	9.30 (1H, s)	141.9	9.32 (1H, s)
N-Me	32.0	3.97 (3H, s)	32.0	3.97 (3H, s)

C-8' indicated the connectivity of C-15 with N-9' of the *N*-methyladenine moiety. The *E*-geometry of the double bond at C-13 was established by ROESY correlations for H_2-15 with H_3-16 and for H-14 with H_2-12. Therefore, the gross structure of **1** was elucidated as shown in Figure 2-5.

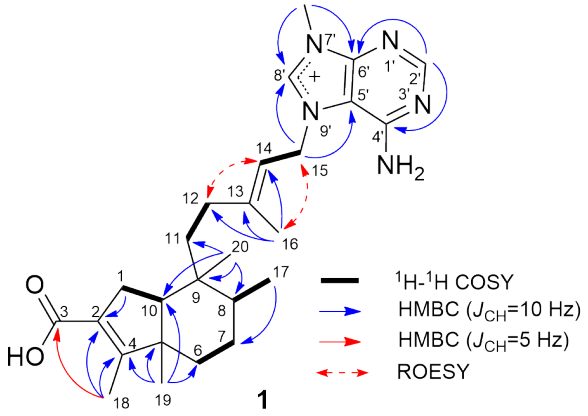

Figure 2-5. Selected 2D NMR correlations for agelamasine A (**1**).

ROESY cross-peaks of H_3-20/H-7α, H_3-19/H_3-20, and H-8/H-10 were indicative of the axial orientations of Me-19, Me-20, H-8, and H-10, as well as the *trans*-fusion of the hexahydroindene ring (Figure 2-6). Therefore, the relative stereochemistry of agelamasine A (**1**) was assigned as shown in Figure 2-6.

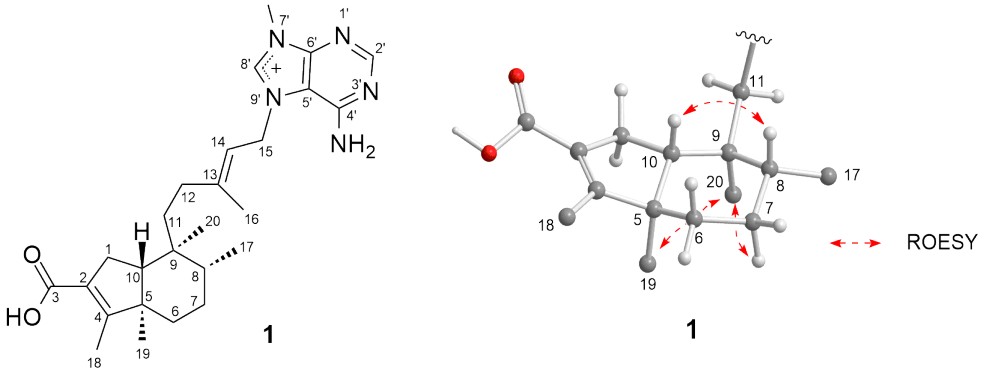

Figure 2-6. Structure of agelamasine A (**1**), and selected ROESY correlations and relative stereochemistry for the bicyclic core of **1** (protons of methyl groups were omitted).

2.4.2. Agelamasine B (**2**)

Agelamasine B (**2**) was obtained as a pale yellow amorphous solid. The molecular formula of **2** was established to be $C_{27}H_{44}N_5O_2$ by the HRESIMS (*m/z* 470.3533 $[M]^+$, Δ+3.8 mmu). The bicyclic diterpene moiety of **2** was deduced as a *trans*-clerodane skeleton by comparison of the 1D NMR spectra (Figure 2-7 and Table 2-1) with the literature data [23,31]. The presence of a hydroxy group at C-3 and a methoxy group at C-4 were revealed by the chemical shifts of C-3 (δ_C 71.1) and C-4 (δ_C 81.0) as well as HMBC correlations for a methoxy proton signal with C-4 and H_3-18 with C-3 and C-4 (Figure 2-8). Thus, the planar structure of agelamasine B (**2**) was assigned as shown in Figure 2-8.

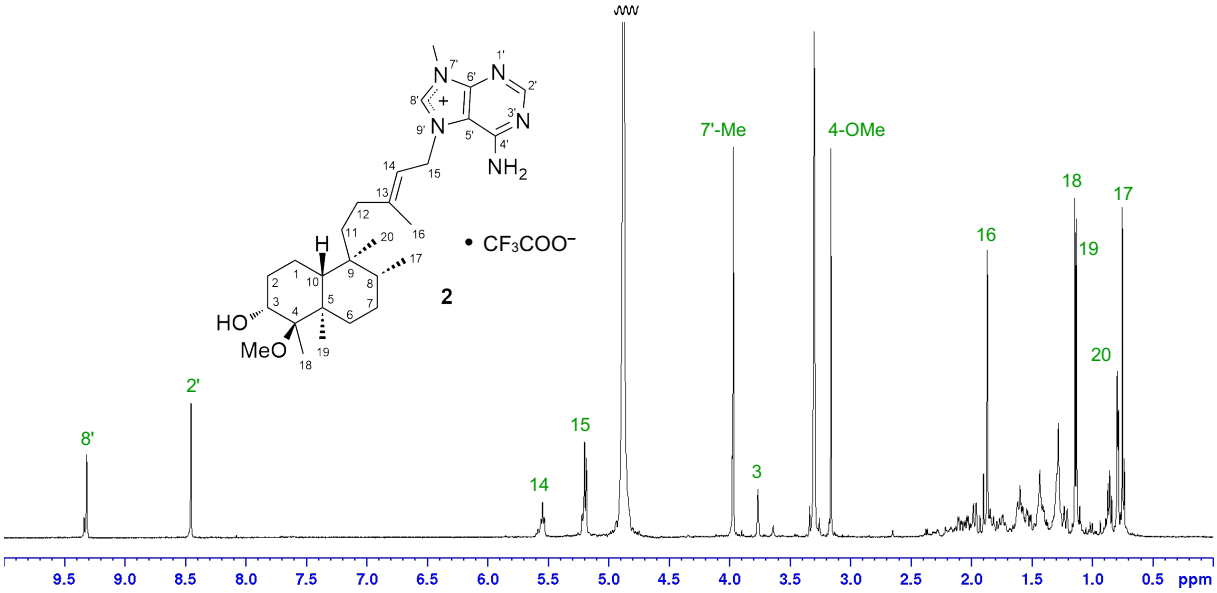

Figure 2-7. ^{1}H NMR spectrum of agelamasine B (**2**) as a TFA salt form in CD_3OD (500 MHz).

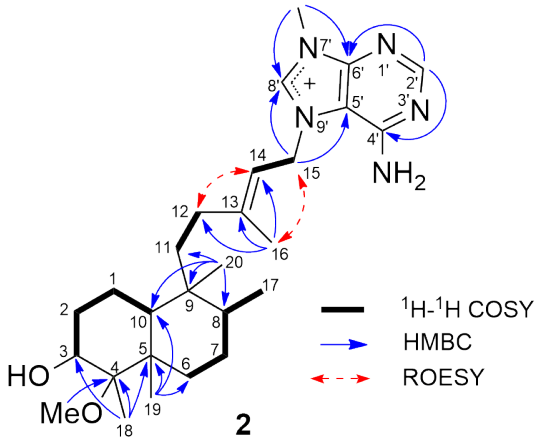

Figure 2-8. Selected 2D NMR correlations for agelamasine B (**2**).

The relative stereochemistry of agelamasine B (**2**) was assigned by interpretation of the ROESY spectrum (Figure 2-9). The *trans*-fusion of the decaline ring (C-1 to C-10) and the axial orientations of H-8, H-10, Me-19, and Me-20 were indicated by ROESY correlations of H-8/H-10 and H_3-19/H_3-20. ROESY cross-peaks of H-10/OMe-4, H-2β/OMe-4, OMe-4/H-3, and H_3-18/H-3 suggested the β-orientations of OMe-4 and H-3. Accordingly, the relative stereochemistry of agelamasine B (**2**) was elucidated as shown in Figure 2-9.

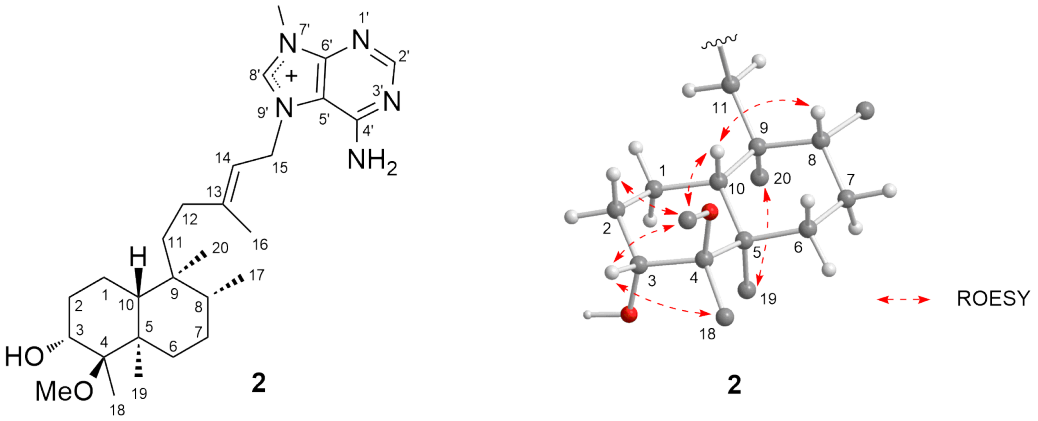

Figure 2-9. Structure of agelamasine B (**2**), and selected ROESY correlations and relative stereochemistry for the bicyclic core of **2** (protons of methyl groups are omitted).

2.5. Summary

An Okinawan marine sponge *Agelas* sp. (SS-12) was investigated to isolate two new diterpene alkaloids, agelamasines A (**1**) and B (**2**) (Figure 2-10). Their structures were

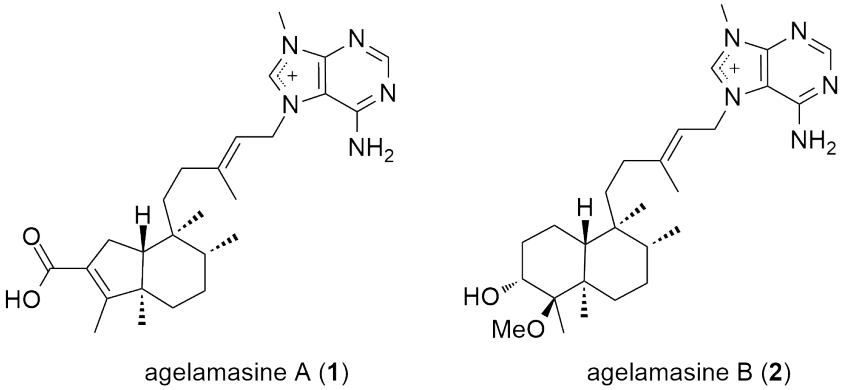

Figure 2-10. New diterpene alkaloids agelamasines A (**1**) and B (**2**) from Okinawan marine sponge *Agelas* sp. (SS-12).

assigned by detailed spectroscopic analyses. Agelamasine A (**1**) had an unique structure with a rearranged (4→2)-*abeo*-clerodane skeleton. Although several rearranged clerodane diterpenes have been isolated from terrestrial plants so far, agelamasine A (**1**) is the first diterpene alkaloid possessing the rearranged (4→2)-*abeo*-clerodane skeleton from a marine source. The biogenethic pathway of solidagonal acid, a diterpene with the rearranged (4→2)-*abeo*-clerodane skeleton, has been proposed [39]. Similarly, **1** might be generated from a plausible precursor with clerodane skeleton, agelasine B [23], via oxidative cleavage followed by aldol condensation (Figure 2-11).

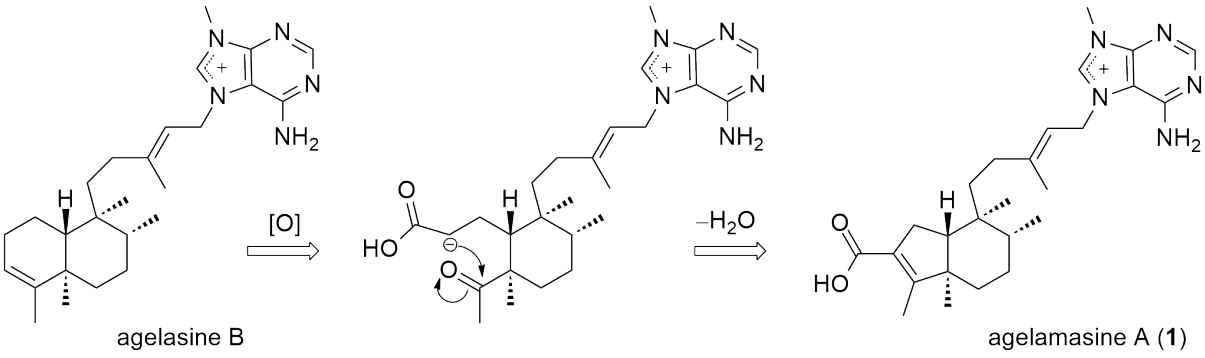

Figure 2-11. Possible biogenetic pathway of agelamasine A (**1**).

Chapter 3.
New Bromopyrrole Alkaloids from Marine Sponges *Agelas* spp.

3.1. Introduction

Bromopyrrole alkaloids family comprises hundreds of secondary metabolites originating from marine sponges exclusively [40]. These natural products have been isolated from various sponge species belonging to the *Agelasidae*, *Axinellidae*, *Dyctionellidae*, and *Hymeniacidonidae* families [40]. Ecological role of bromopyrrole alkaloids was firstly observed as an antifeedant properties in 1996. Polycyclic and dimeric bromopyrrole alkaloids, produced by cyclization and/or dimerization of linear monomeric bromopyrrole alkaloids, have attracted widespread interest as challenging targets for total synthesis by virtue of their fascinating highly functionalized structures with a high N:C ratio (1:2) [40–42].

Oroidin and hymenidin are the representative linear monomeric bromopyrrole alkaloids. Typically, the bromopyrrole alkaloids consist of a mono or dibrominated pyrrole carboxamide moiety and an aminoimidazole moiety linked through a C_3 unit (Figure 3-1).

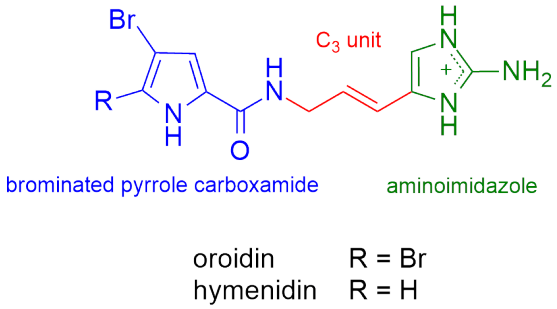

Figure 3-1. Structure of representative monomeric bromopyrrole alkaloids, oroidin and hymenidin.

The reported biosynthetic hypotheses for formation of the brompyrrole alkaloid building blocks, clathrodin and its brominated derivatives, are originated from proteinogenic amino acids [42]. The postulated key steps rely on several plausible precursors isolated from phylogenetically related sponges or isolated together with other higher order bromopyrrole alkaloids. While it seems reasonable to speculate that the pyrrole-2-carboxylic acid unit is derived from proline oxidation (Figure 3-2a), several alternative possibilities have been suggested for the origin of the 2-amino-5-(3-amino)-propylimidazole unit including diketopiperazine intermediates (Figure 3-2b) [42].

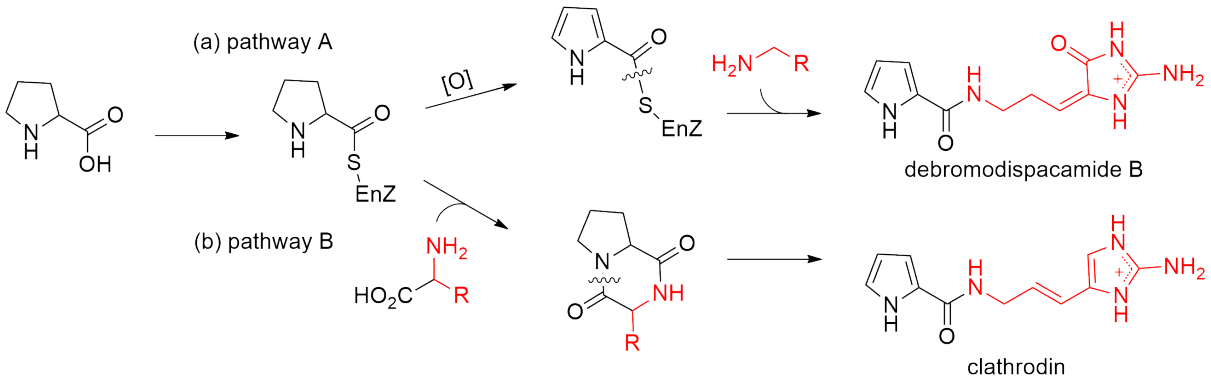

Figure 3-2. Possible routes to debromodispacamide B and clathrodin via (a) pathway A: pyrrole oxidation and nucleophilic addition to an activated acyl pyrrole (b) pathway B: dipeptide-based synthesis through diketopiperazines and intramolecular rearrangements.

Ability of a given enzyme, proton exchange reactions, tautomeric equilibria of the aminopropenylimidazole portion of oroidin or hymenidin are hypotheses for the formation of cyclized dimers and polycyclic monomers such as sceptrin, ageliferin, massadine, and hymenin (Figure 3-3) [40]. Sceptrin is a dimeric bromopyrrole alkaloid formally made up by two hymenidin subunits. The biogenetic hypothesis derives sceptrin from hymenidin via an enzyme-mediated [2+2]-cycloaddition. Ageliferin is also a dimeric bromopyrrole alkaloid. Biogenetically, it might be derived from two molecules of hymenidin via [4+2]-cycloaddition that infers chirality to achiral precursors. Massadine might be derived from two molecules of oroidin forming two C-C bonds and one ether linkage. A cyclized bromopyrrole alkaloid, hymenin, might be generated by intramolecular cyclization via C-4/C-10 [40].

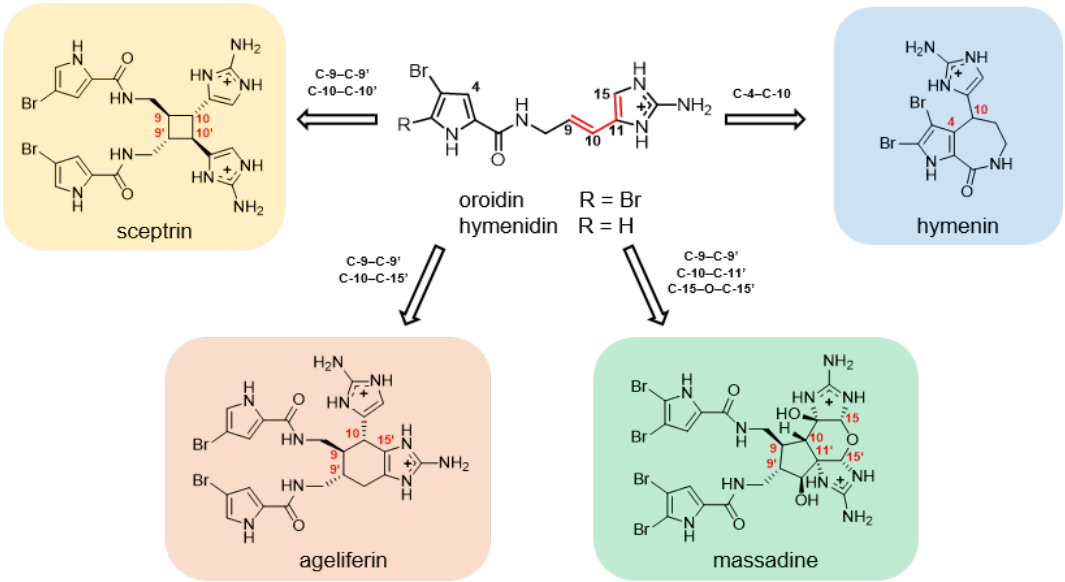

Figure 3-3. Biosynthetic hypothesis of polycyclic and dimeric bromopyrrole alkaloids.

Previously, our research group have reported a series of bromopyrrole alkaloids such as agelamadins A–F, nagelamides U–Z, and several linear bromopyrrole alkaloids (Figure 3-4) [43–48]. In this study, the extracts of Okinawan marine sponges *Agelas* spp. (SS-1302, SS-159, and SS-516) were investigated to isolate eight new bromopyrrole alkaloids (**9**–**14**, **32**, and **33**), together with 19 known bromopyrrole alkaloids.

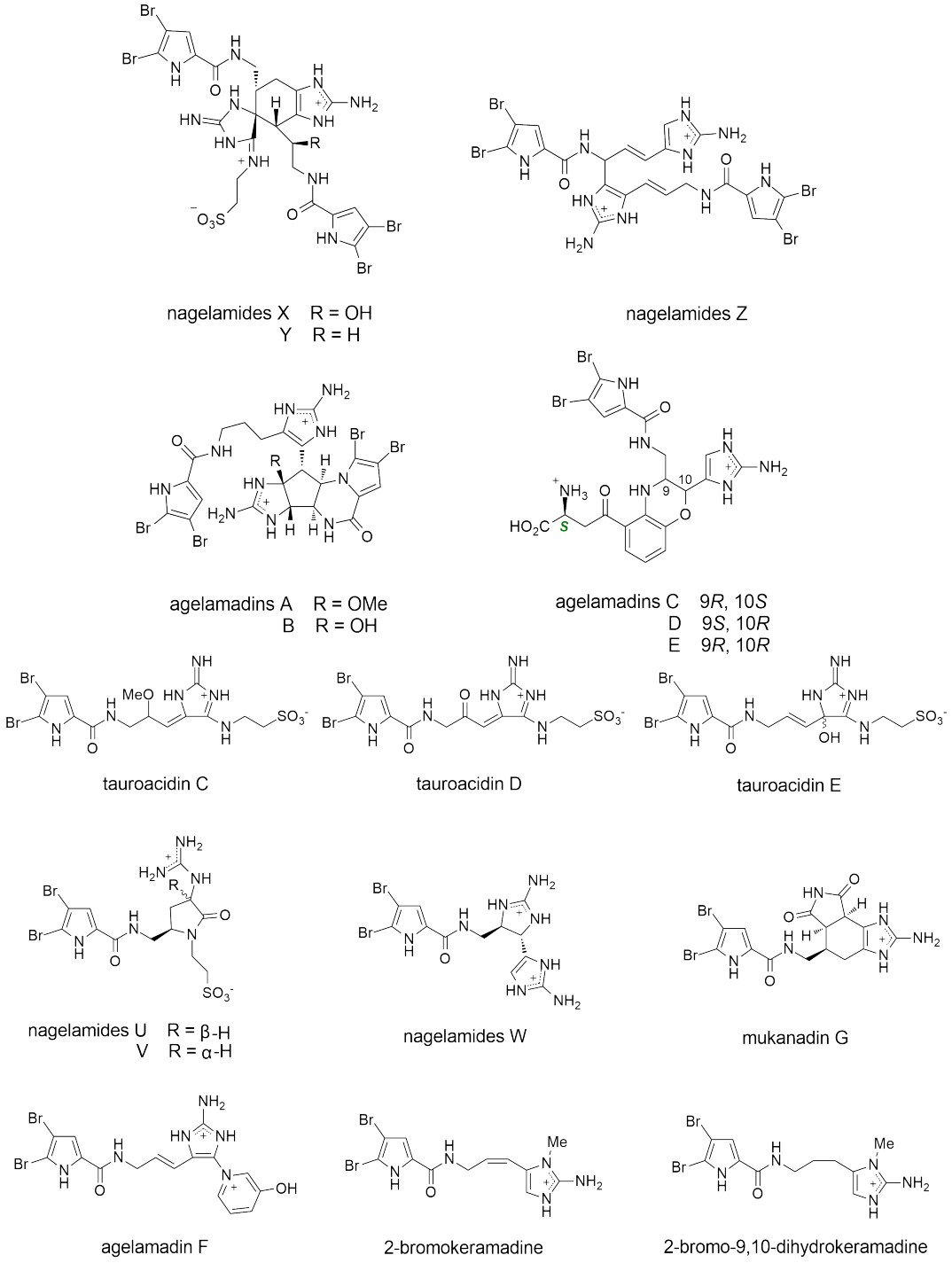

Figure 3-4. Bromopyrrole alkaloids previously isolated from Okinawan marine sponges *Agelas* spp. by our group.

3.2. Extraction and Isolation

3.2.1. Extraction and Isolation of SS-1302

A marine sponge *Agelas* sp. (SS-1302, 3.42 kg, wet weight), collected in Okinawa, Japan, was extracted with MeOH at room temperature to give the extract (197.1 g). The methanolic extract was partitioned between *n*-hexane and 90% MeOH aq. The 90% MeOH aq.-soluble materials were further partitioned with *n*-BuOH and water. The *n*-BuOH-soluble materials (58.0 g) were separated by column chromatographies to give six new bromopyrrole alkaloids, agesamides C (**9**, 26.4 mg), D (**10**, 16.6 mg), and E (**11**, 3.6 mg), 9-hydroxydihydrodispacamide (**12**, 5.0 mg), 9-hydroxydihydrooroidin (**13**, 2.1 mg), and 9-(*E*)-keramadine (**14**, 3.1 mg), together with four known bromopyrrole alkaloids (**15**–**18**) (Scheme 2).

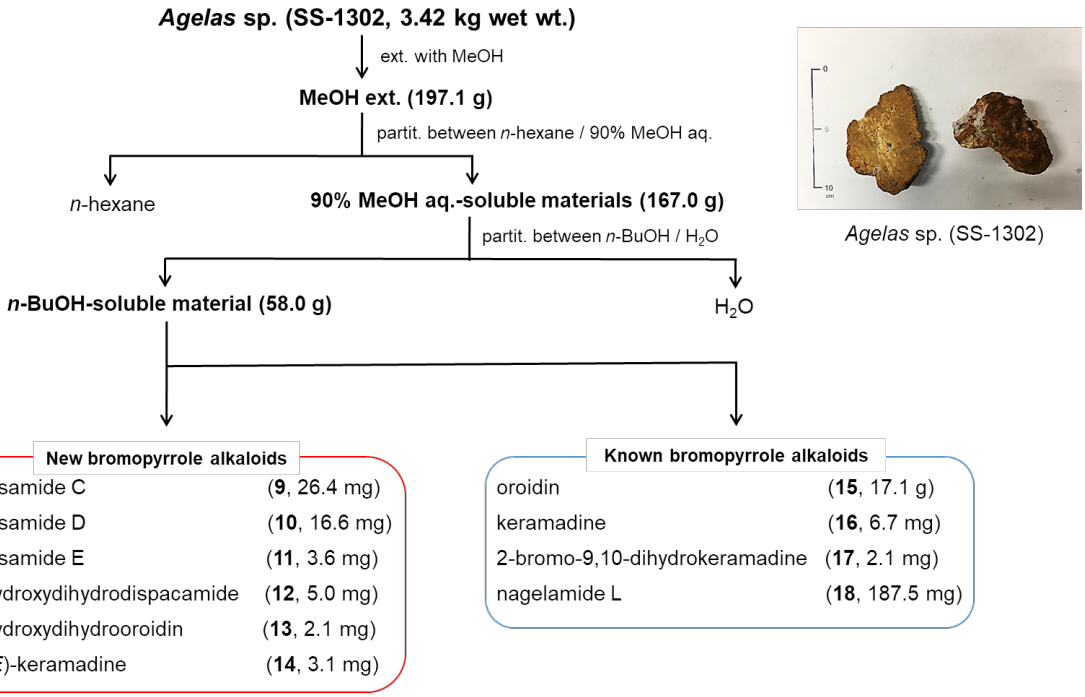

Scheme 2. Isolation scheme of new bromopyrrole alkaloids (**9**–**14**) from a marine sponge *Agelas* sp. (SS-1302).

3.2.2. Extraction and Isolation of SS-159

A marine sponge *Agelas* sp. (SS-159, 3.78 kg, wet weight) was extracted with MeOH, to give an extract, which was partitioned with *n*-hexane and 50% MeOH aq. The 50% MeOH aq.-soluble materials were further partitioned with *n*-BuOH and water. The *n*-BuOH-soluble materials (147.3 g) were subjected to various column chromatographies to give 13 known bromopyrrole alkaloids (**19**–**31**) (Scheme 3).

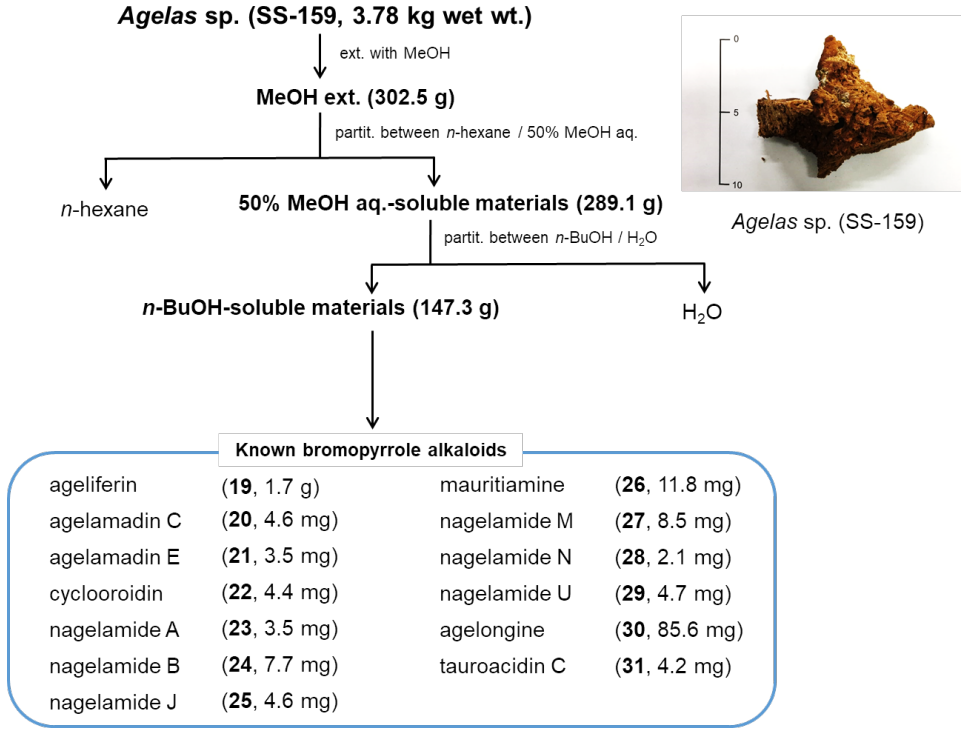

Scheme 3. Isolation scheme of bromopyrrole alkaloids (**19**–**31**) from a marine sponge *Agelas* sp. (SS-159).

3.2.3. Extraction and Isolation of SS-516

An Okinawan marine sponge *Agelas* sp. (SS-516, 5.22 kg, wet weight) was extracted with MeOH. The methanol extract was partitioned between *n*-hexane and 90% MeOH aq. Repeated chromatographic separations of the 90% MeOH aq.-soluble materials gave two new bromopyrrole alkaloids, agesasines A (**32**, 2.5 mg) and B (**33**, 2.2 mg). Two known bromopyrrole alkaloids (**34** and **35**) were also isolated (Scheme 4).

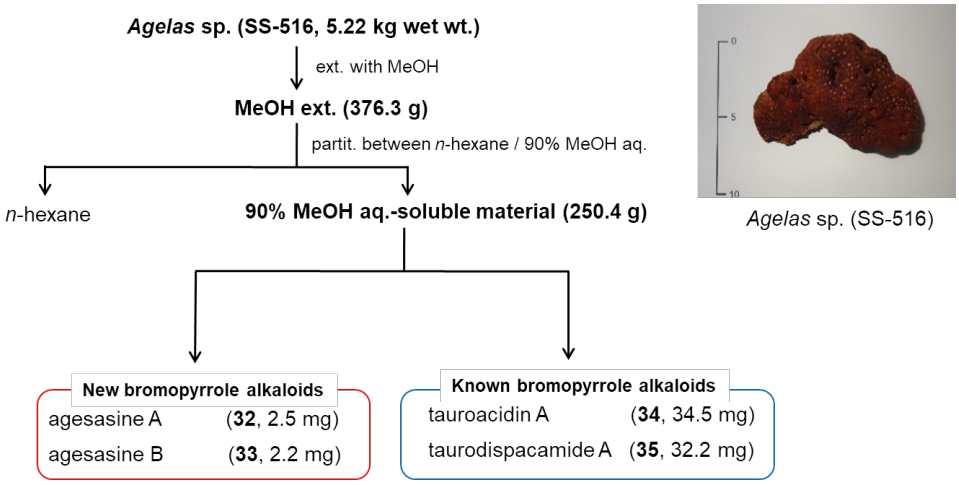

Scheme 4. Isolation scheme of new bromopyrrole alkaloids agesasines A (**32**) and B (**33**) from a marine sponge *Agelas* sp. (SS-516).

3.3. Identification of Known Bromopyrrole Alkaloids

3.3.1. Identification of Known Bromopyrrole Alkaloids from SS-1302

Compounds **15**–**18** isolated from SS-1302 were identified as monomeric linear bromopyrrole alkaloids, oroidin (**15**) [49,50], keramadine (**16**) [51], 2-bromo-9,10-dihydrokeramadine (**17**) [48], and a dimeric bromopyrrole alkaloid with a dibromopyrrole carboxylate moiety, nagelamide L (**18**) [52], by comparing their spectral data with those described in the literature (Figure 3-5).

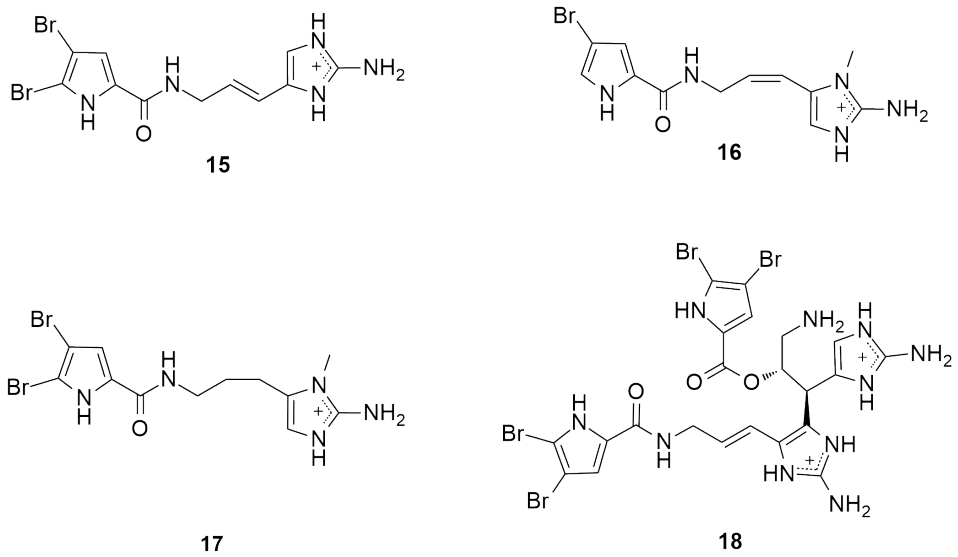

Figure 3-5. Known bromopyrrole alkaloids from *Agelas* sp. (SS-1302).

3.3.2. Identification of Known Bromopyrrole Alkaloids from SS-159

Compounds **19**–**31** isolated from SS-159 were identified as dimeric bromopyrrole alkaloids, ageliferin (**19**) [53], nagelamides A (**23**) [54], B (**24**) [54], and J (**25**) [55], and mauritiamine (**26**) [56], conjugates of monomeric bromopyrrole alkaloid and hydroxykynurenine, agelamadins C (**20**) [44], and E (**21**) [44], a bicyclic monomeric bromopyrrole alkaloid, cyclooroidin (**22**) [57], linear monomeric bromopyrrole alkaloids nagelamides M (**27**) [58], N (**28**) [58], and U (**29**) [46], agelongine (**30**) [59], and tauroacidin C (**31**) [48], by comparison of their physicochemical data with those reported in the literature (Figure 3-6).

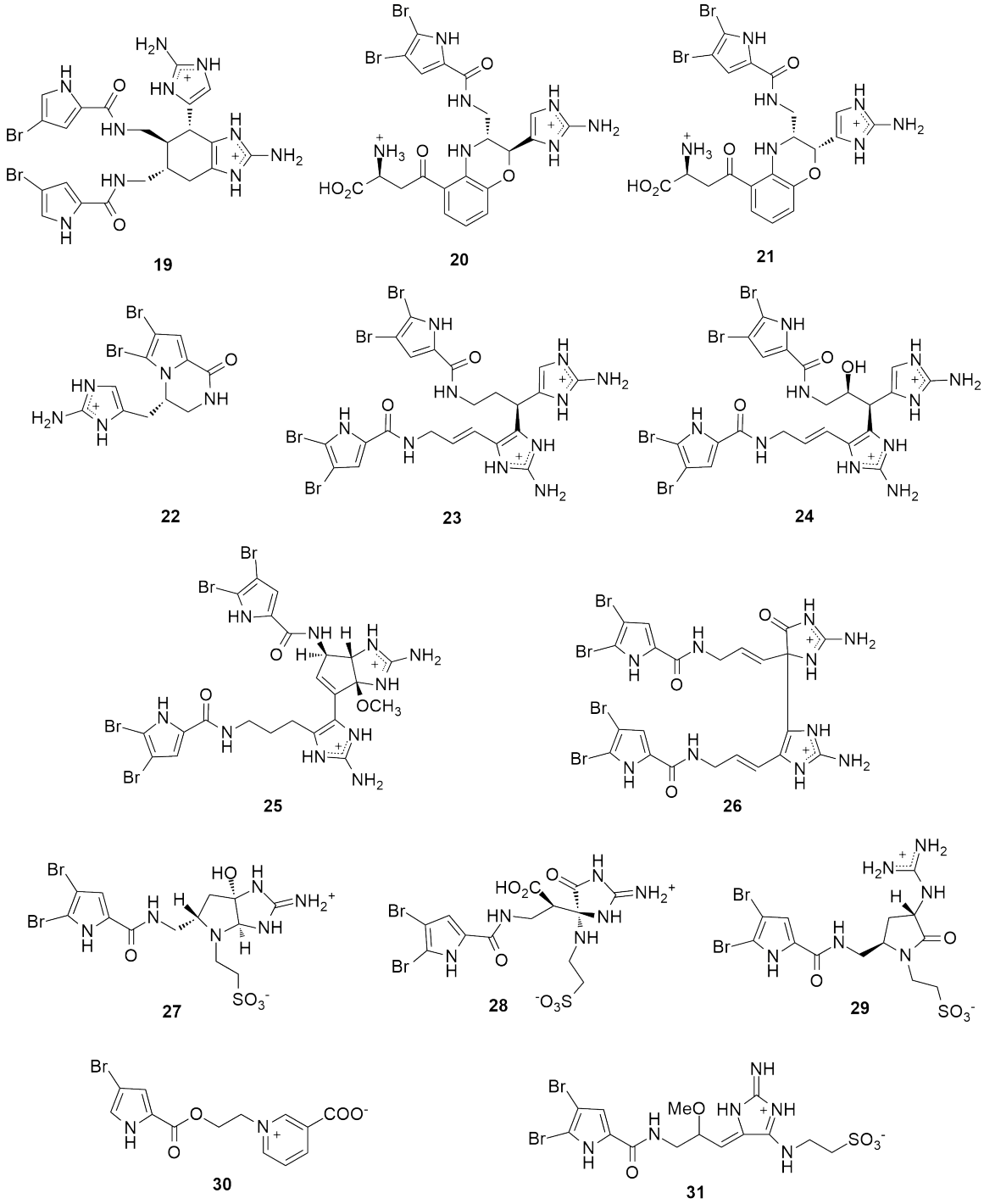

Figure 3-6. Known bromopyrrole alkaloids from *Agelas* sp. (SS-159).

3.3.3. Identification of Known Bromopyrrole Alkaloids from SS-516

Compounds **34** and **35** isolated from SS-516 were identified as linear monomeric alkaloids with a taurine moiety, tauroacidin A (**34**) [60] and taurodispacamide A (**35**) [54], by comparisons of their spectroscopic data with those described in the literature (Figure 3-7).

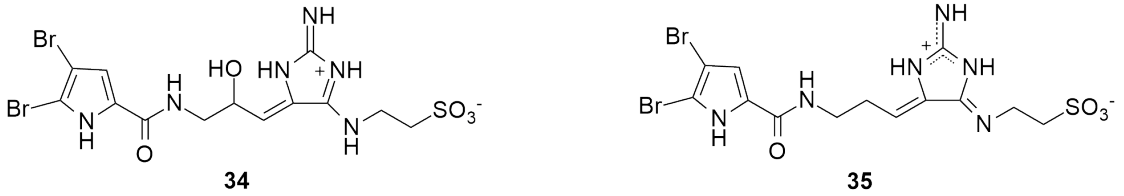

Figure 3-7. Known bromopyrrole alkaloids from *Agelas* sp. (SS-516).

3.4. Structure Elucidation of New Bromopyrrole Alkaloids

3.4.1. Agesamides C–E (**9**–**11**)

Agesamide C (**9**) was obtained as a pale yellow amorphous solid. The ESIMS showed ion peaks at *m/z* 404, 406, and 408 (1:2:1, $[M]^+$), implying the existence of two bromine atoms in the molecule. The molecular formula of **9** was established by the HRESIMS to be $C_{11}H_{12}N_5O_2Br_2$ (*m/z* 403.9388 $[M]^+$, Δ+3.0 mmu).

The gross structure of **9** was elucidated as follows. The existence of a 2,3-dibromopyrrole carboxamide moiety was deduced by ^1H and ^{13}C NMR data (δ_H 7.91 and 6.86; δ_C 157.9, 125.9, 114.4, 105.9, and 99.7). The ^1H NMR spectrum also showed signals of an sp^3 methylene (δ_H 3.76 and 3.53, H_2-8), and an sp^3 methine (δ_H 4.59, H-9) (Figure 3-8, Table 3-1). ^1H-^1H COSY cross-peaks of 7-NH/H_2-8 and H_2-8/H-9, and HMBC correlations of H_2-8/C-6, and of H-9/C-5, and C-2 revealed the existence of a pyrroloketopiperazine moiety (C-2–C-9) (Figure 3-9). In addition, the presence of an aminoimidazolone moiety was suggested by HMBC correlations for H-11/C-13, and C-15, and for 12-NH/C-13, and C-15.

The connectivity of these partial structures through an sp^3 methylene (CH_2-10) were assigned by ^1H-^1H COSY cross-peaks of H-9/H_2-10 and H_2-10/H-11. Thus, the planar structure of agesamide C (**9**) was assigned as shown in Figure 3-9.

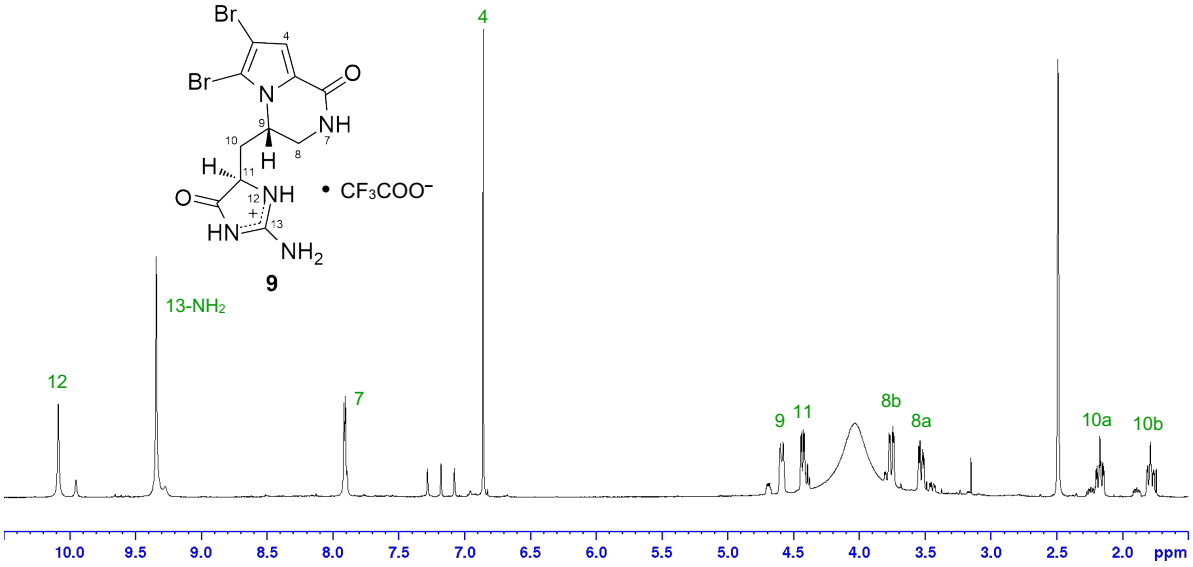

Figure 3-8. ^1H NMR spectrum of agesamide C (**9**) as a TFA salt form in DMSO-d_6 (500 MHz).

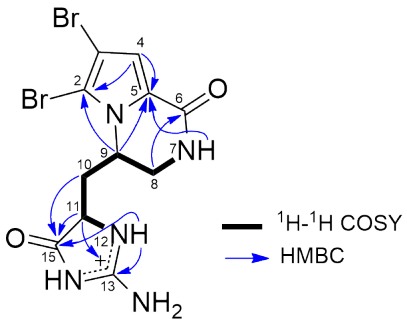

9 and **10**

Figure 3-9. Selected 2D NMR correlations and the gross structure for agesamides C (**9**) and D (**10**).

Agesamide D (**10**) had the same molecular formula, $C_{11}H_{12}N_5O_2Br_2$, as that of **9** (*m/z* 403.9315 $[M]^+$, Δ–4.3 mmu). Resemblance of ^1H and ^{13}C NMR data for **10** and **9** (Figures 3-9 and 3-10, Table 3-1) suggested the diastereomeric relationship of **10** and **9**. This was supported by interpretation of the 2D NMR spectra (Figure 3-9).

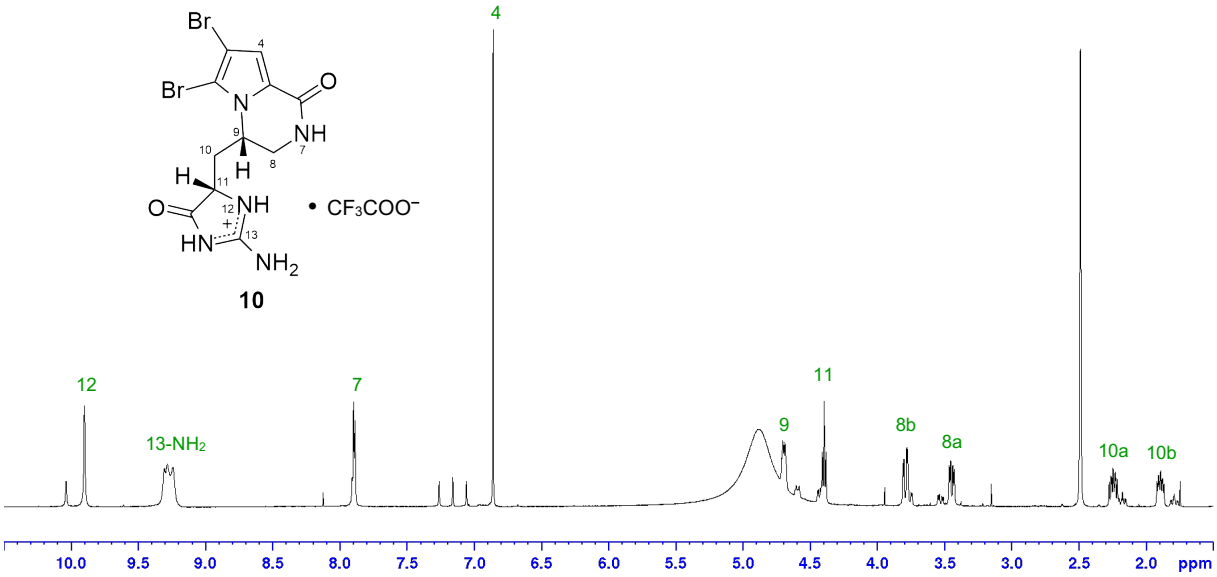

Figure 3-10. ^1H NMR spectrum of agesamide D (**10**) as a TFA salt form in DMSO-d_6 (500 MHz).

The relative stereochemistry of agesamides C (**9**) and D (**10**) were assigned by ROESY analyses. ROESY correlations for H-8a/H-11 and H-10a, H-10a/H-11, and for H-9/H-10b and H-8b were observed in each case (Figure 3-11). However, 12-NH correlated with H-10b in **9**, while a correlation 12-NH/H-10a was observed in **10** (Figure 3-11). Therefore, the relative configurations of 9*S** and 11*R** for **9** and 9*S** and 11*S** for **10** were deduced.

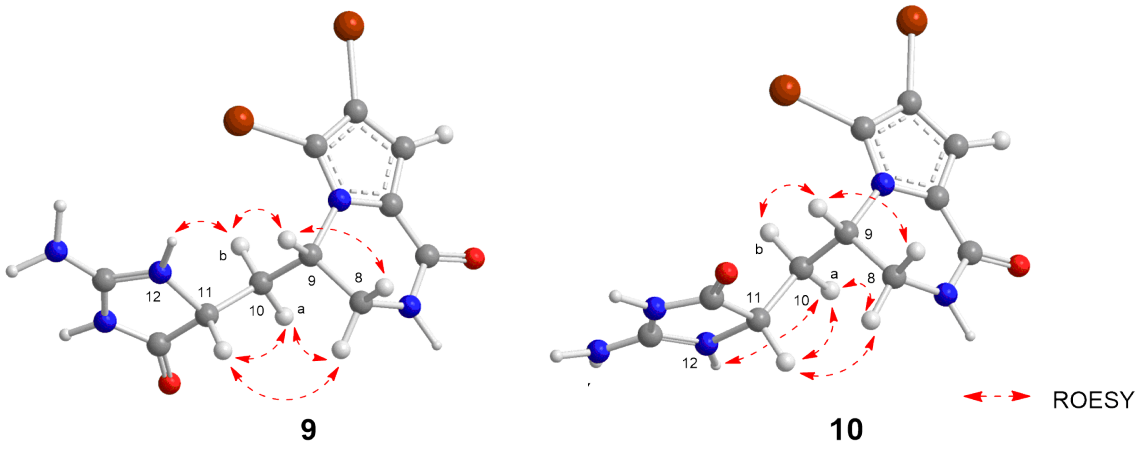

Figure 3-11. Selected ROESY correlations and relative configurations for agesamides C (**9**) and D (**10**).

Agesamide E (**11**) was isolated as a pale yellow amorphous solid, and the HRESIMS revealed the molecular formula of **11** to be $C_{11}H_{10}N_5O_2Br_2$ (*m/z* 401.9177 $[M]^+$, Δ–2.4 mmu). Though the ^1H and ^{13}C NMR spectra (Table 3-1) of **11** were reminiscent of those of **9**, the signals of a double bond (CH-10 and C-11) in **11** were discerned in place of the sp^3 methylene (CH_2-10) and sp^3 methine (CH-11) signals in **9** (Figures 3-8 and 3-12). Given 2D

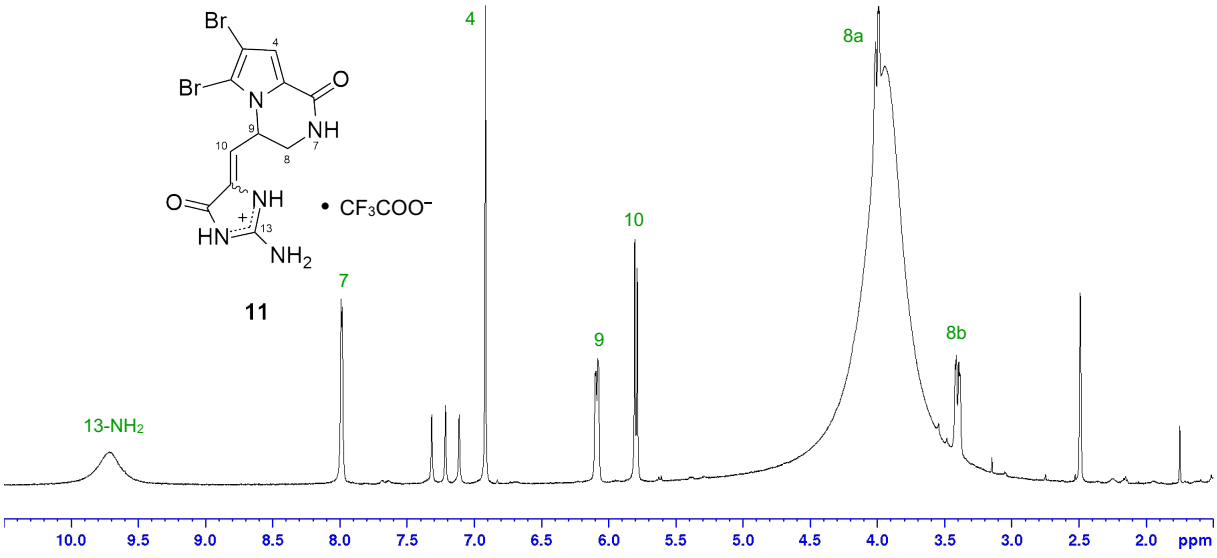

Figure 3-12. ^1H NMR spectrum of agesamide E (**11**) as a TFA salt form in DMSO-d_6 (500 MHz).

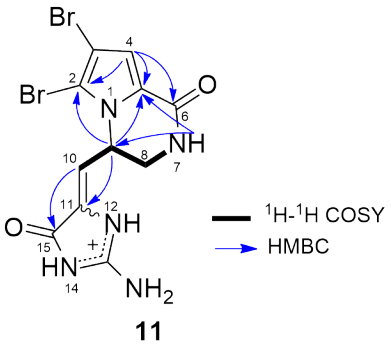

Figure 3-13. Selected 2D NMR correlations and the gross structure for agesamide E (**11**).

NMR correlations depicted in Figure 3-13, the planar structure of **11** was deduced to be a dehydro derivative of **9**. The geometry of the double bond (C-10/C-11) could not be assigned since interchangeable proton signals of 12-NH and 14-NH were not detected in the ^{1}H NMR spectrum. The optical resolution of **11** using chiral HPLC column resulted in the separation of enantiomers {(+)-**11**, t_R 27.1 min; (–)-**11**, t_R 31.8 min}, the ratio of which was approximately 1:1 (Figure 3-14). Therefore, **11** was concluded to be a racemate.

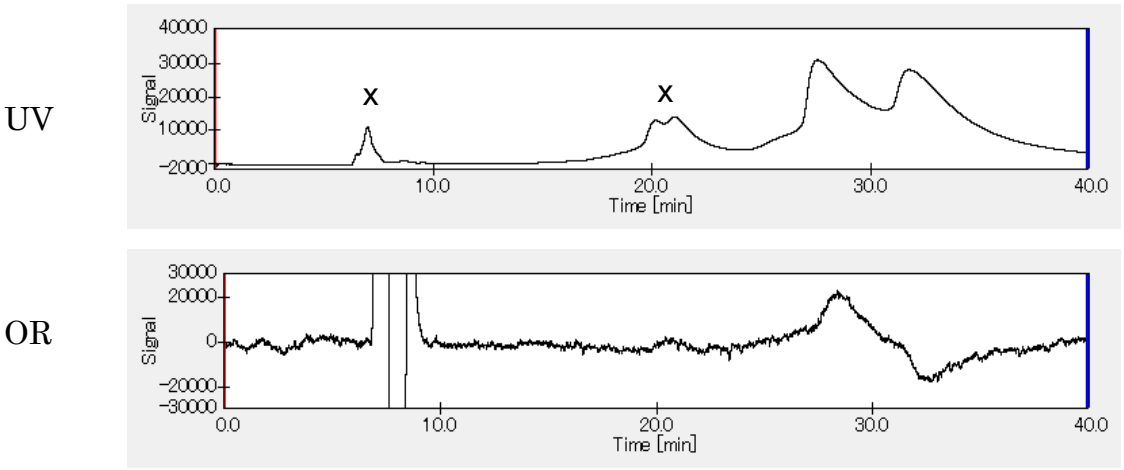

Figure 3-14. Chromatogram of chiral HPLC analysis for agesamide E (**11**).

Table 3-1. ^{1}H and ^{13}C NMR data for agesamides C–E (**9**–**11**) as TFA salt forms in DMSO-d_6.

Position	**9**		**10**		**11**	
	^{13}C	^{1}H (*J* in Hz)	^{13}C	^{1}H (*J* in Hz)	^{13}C	^{1}H (*J* in Hz)
2	105.9	–	106.1	–	107.1	–
3	99.7	–	99.8	–	100.4	–
4	114.4	6.86 (1H, s)	114.5	6.86 (1H, s)	115.2	6.92 (1H, s)
5	125.9	–	125.9	–	125.8	–
6	157.9	–	157.8	–	158.1	–
7	–	7.91 (1H, d, 5.3)	–	7.89 (1H, d, 5.3)	–	7.99 (1H, d, 4.4)
8	41.0	3.76 (1H, dd, 13.7, 3.6)	42.1	3.79 (1H, dd, 13.6, 3.9)	45.4	4.00 (1H, dd, 13.0, 3.3)
		3.53 (1H, dd, 13.7, 5.3)		3.45 (1H, dd, 13.6, 5.3)		3.40 (1H, dd, 13.0, 4.4)
9	50.7	4.59 (1H, m)	50.4	4.70 (1H, m)	49.1	6.09 (1H, dd, 9.3, 3.3)
10	33.1	2.17 (1H, ddd, 14.1, 10.7, 3.9)	32.9	2.24 (1H, ddd, 14.1, 9.4, 6.8)	116.7	5.80 (1H, d, 9.3)
		1.78 (1H, ddd, 14.1, 10.5, 3.1)		1.89 (1H, ddd, 14.1, 7.2, 4.5)		
11	55.9	4.44 (1H, dd, 10.5, 3.7)	56.1	4.40 (1H, brt, 7.2)	130.0	–
12	–	10.09 (1H, brs)	–	9.90 (1H, brs)	–	*nd*
13	158.7	–	158.7	–	156.6	–
14	–	*nd*	–	*nd*	–	*nd*
15	174.5	–	174.8	–	164.0	–
13-NH_2	–	9.34 (2H, brs)	–	9.28 (2H, brs)	–	9.72 (2H, brs)

nd: not detected.

3.4.2. 9-Hydroxydihydrodispacamide (**12**)

9-Hydroxydihydrodispacamide (**12**) was obtained as a pale yellow amorphous solid. The presence of two bromine atoms in **12** was revealed by the molecular ion peaks at 422, 424, and 426 (1:2:1) in the ESIMS. The HRESIMS showed the ion peak at *m/z* 443.9319 ($[M–H+Na]^+$, Δ+3.6 mmu), suggesting the molecular formula of $C_{11}H_{14}N_5O_3Br_2$, larger by 16 mass units than dihydrodispacamide [61]. The ^1H and ^{13}C NMR spectra of **12** were similar to those of dihydrodispacamide, except for the presence of a hydroxy methine signal (δ_H 3.79; δ_C 66.3, CH-9) in **12** (Figure 3-15, Table 3-2) in place of the sp^3 methylene seen in dihydrodispacamide. Therefore, **12** was deduced as a hydroxylated derivative of dihydrodispacamide.

The presence of the hydroxy group at C-9 was confirmed by ^1H-^1H COSY cross-peaks of H_2-8/H-9 and H-9/H_2-10 (Figure 3-16).

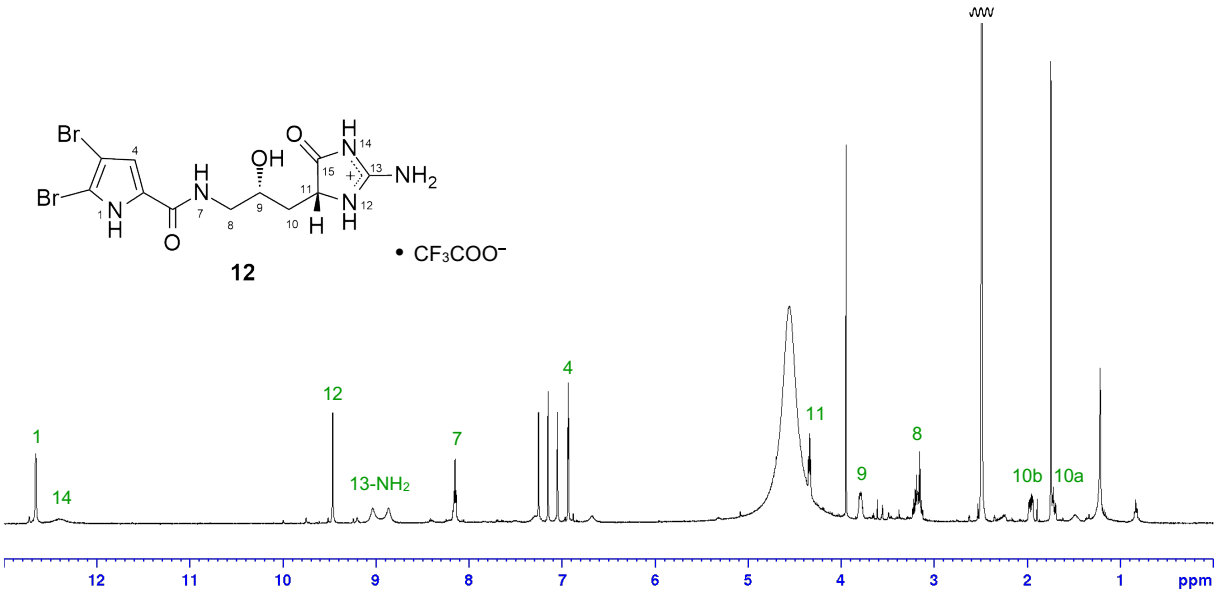

Figure 3-15. ^1H NMR spectrum of 9-hydroxydihydrodispacamide (**12**) as a TFA salt form in DMSO-d_6 (500 MHz).

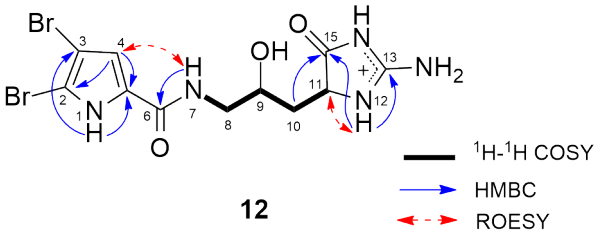

Figure 3-16. Selected 2D NMR correlations and the gross structure for 9-hydroxydihydrodispacamide (**12**).

Table 3-2. ^{1}H and ^{13}C NMR data for 9-hydroxydihydrodispacamide (**12**) as TFA salt forms in DMSO-d_6.

Position	**12**	
	^{13}C	^{1}H (J in Hz)
1	–	12.66 (1H, brs)
2	104.7	–
3	98.0	–
4	113.1	6.94 (1H, d, 2.8)
5	128.3	–
6	159.3	–
7	–	8.15 (1H, t, 5.9)
8	45.3	3.18 (2H, m)
9	66.3	3.79 (1H, m)
10	34.8	1.96 (1H, ddd, 14.4, 5.5, 2.6)
		1.71 (1H, ddd, 14.4, 10.9, 5.5)
11	56.8	4.34 (1H, t, 5.5)
12	–	9.47 (1H, brs)
13	158.2	–
14	–	12.41 (1H, brs)
15	175.6	–
13-NH_2	–	8.95 (2H, br)

Based on the ^{1}H-^{1}H coupling constants and ROESY correlations, the relative configurations for C-9/C-10 and C-10/C-11 of **12** were assigned. A large value for $^{3}J_{H\text{-}10a/H\text{-}9}$ (10.9 Hz) and a small value for $^{3}J_{H\text{-}10b/H\text{-}9}$ (2.6 Hz) indicated the *anti* and *gauche* relationships for H-10a/H-9 and H-10b/H-9, respectively (Figure 3-17a). Values for $^{3}J_{H\text{-}10b/H\text{-}11}$ and $^{3}J_{H\text{-}10a/H\text{-}11}$ (each 5.5 Hz) suggested that H-11 was *gauche* to both H-10a and H-10b (Figure 3-17b). Given ROESY correlations for H_2-8/H_2-10, H-9/H-10b, H-9/H-11, H_2-10/H-11, and H-10b/12-NH, the relative configurations of C-9 and C-11 were assigned as both *R**.

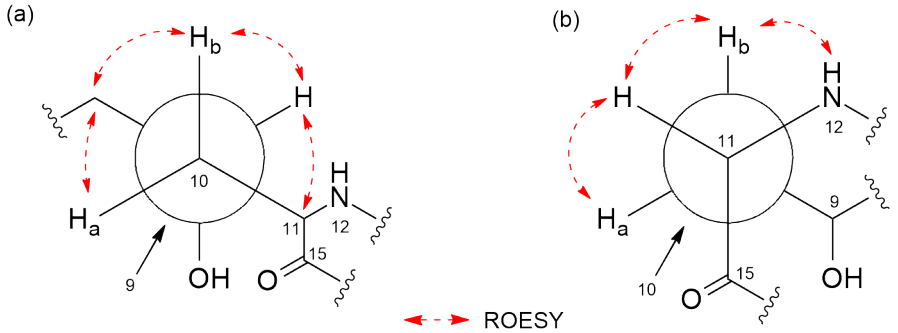

Figure 3-17. Selected ROESY correlations and projections for (**a**) C-9 to C-10 (**b**) C-10 to C-11 bonds of 9-hydroxydihydrodispacamide (**12**).

The specific rotation value (≈ 0) of 9-hydroxydihydrodispacamide (**12**) indicated **12** to be a racemate. The optical resolution of **12** using chiral HPLC column resulted in the separation of enantiomers (t_R 12.5 and 14.3 min), the ratio of which was approximately 1:1 (Figure 3-18). Thus, 9-hydroxydihydrodispacamide (**12**) was concluded to be a racemate.

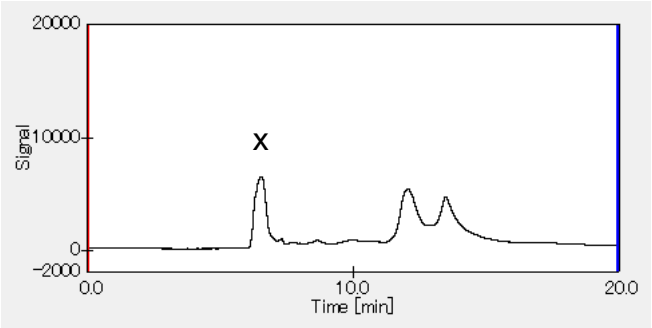

Figure 3-18. Chromatogram of chiral HPLC analysis for 9-hydroxydihydrodispacamide (**12**).

3.4.3. 9-Hydroxydihydrooroidin (**13**)

9-Hydroxydihydrooroidin (**13**) was obtained as a pale yellow amorphous solid. The ^{1}H and ^{13}C NMR spectra (Table 3-3) implied that **13** was related to dihydrooroidin [61]. The HRESIMS showed the ion peak at *m/z* 405.9478 ($[M]^{+}$), larger by 16 mass units than dihydrooroidin, implying the existence of a hydroxy group in the molecule. Moreover, the signal of a hydroxy methine (δ_H 3.76 and δ_C 68.4, CH-9) was observed in **13** in place of an sp^3 methylene seen in dihydrooroidin (Figure 3-19).

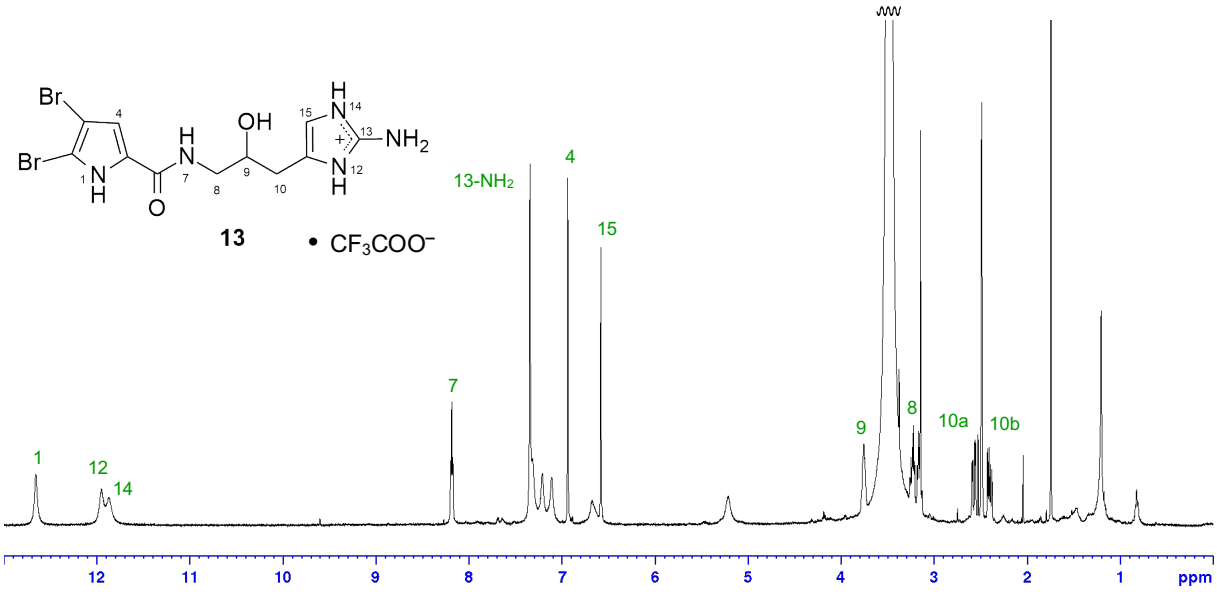

Figure 3-19. ^{1}H NMR spectrum of 9-hydroxydihydrooroidin (**13**) as a TFA salt form in DMSO-d_6 (500 MHz).

The presence of the hydroxy group at C-9 was confirmed by analysis of the ^{1}H-^{1}H COSY spectrum (Figure 3-20). Thus, the structure of **13** was assigned to be 9-hydroxydihydrooroidin.

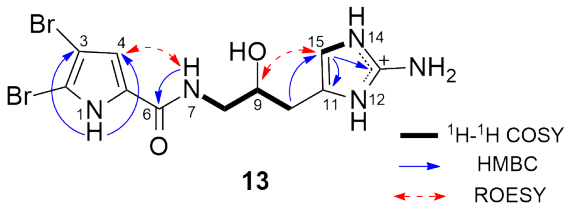

Figure 3-20. Selected 2D NMR correlations and the gross structure for 9-hydroxydihydrooroidin (**13**).

Table 3-3. ^{1}H and ^{13}C NMR data for 9-hydroxydihydrooroidin (**13**) as a TFA salt form in DMSO-d_6.

Position	**13**	
	^{13}C	^{1}H (*J* in Hz)
1	–	12.66 (1H, brs)
2	104.8	–
3	98.2	–
4	113.2	6.94 (1H, s)
5	128.4	–
6	159.4	–
7	–	8.16 (1H, t, 5.6)
8	44.8	3.23 (1H, m)
		3.16 (1H, m)
9	68.4	3.76 (1H, m)
10	30.1	2.57 (1H, dd, 15.2, 4.2)
		2.40 (1H, dd, 15.2, 7.8)
11	124.3	–
12	–	11.95 (1H, brs)
13	147.1	–
14	–	11.87 (1H, brs)
15	110.1	6.58 (1H, brs)
13-NH_2	–	7.35 (2H, brs)

3.4.4. 9-(*E*)-Keramadine (**14**)

The 1D NMR spectra (Table 3-4) of 9-(*E*)-keramadine (**14**) were similar to those of keramadine [51]. Though keramadine has the *Z*-olefin, the coupling constant of H-10 was 16.1 Hz in **14** (Figure 3-21), indicating the *E* configuration of the double bond in **14**.

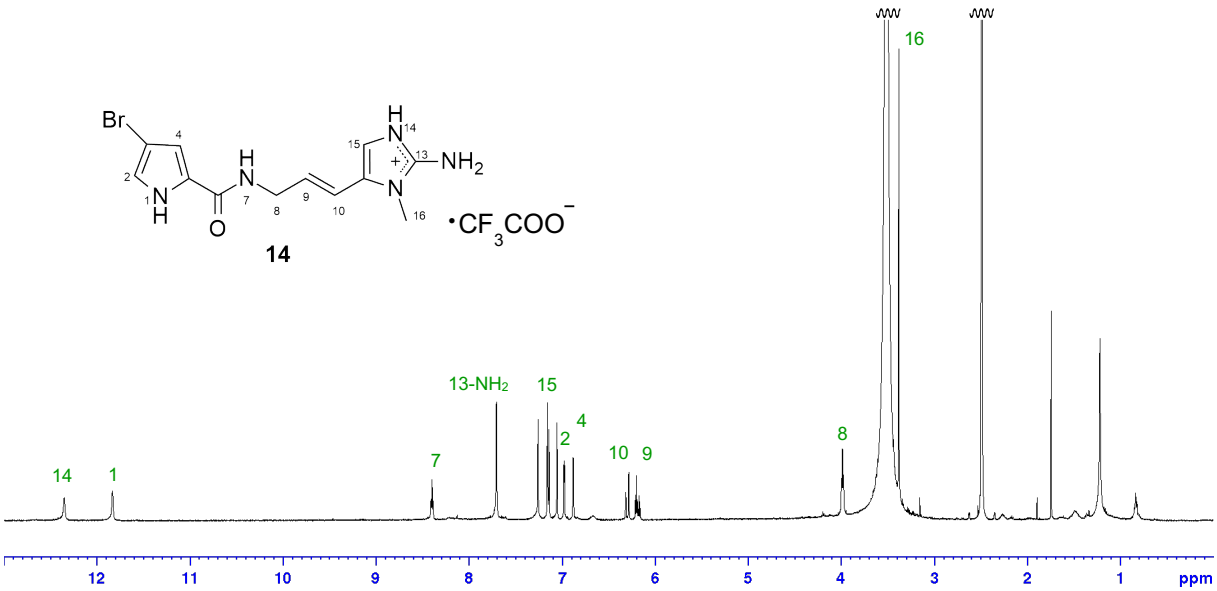

Figure 3-21. ^{1}H NMR spectrum of 9-(*E*)-keramadine (**14**) as a TFA salt form in DMSO-d_6 (500 MHz).

The *E* geometry was also underpinned by ROESY correlations for H-9/H-15 and H-10/H_3-16 (Figure 3-22). This is the first isolation of 9-(*E*)-keramadine from natural source, whereas the synthesis of 9-(*E*)-keramadine has been reported to date [62].

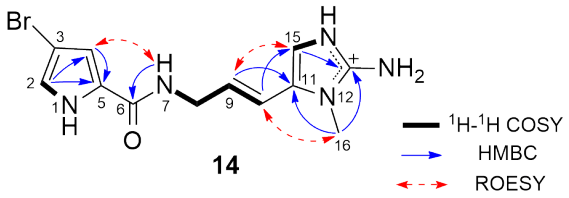

Figure 3-22. Selected 2D NMR correlations and the gross structure for 9-(*E*)-keramadine (**14**).

Table 3-4. ^{1}H and ^{13}C NMR data for 9-(*E*)-keramadine (**14**) as a TFA salt form in DMSO-d_6.

Position	**14**	
	^{13}C	^{1}H (*J* in Hz)
1	–	11.83 (1H, brs)
2	121.6	6.98 (1H, dd, 2.9, 1.6)
3	95.2	–
4	111.8	6.92 (1H, s)
5	126.9	–
6	159.7	–
7	–	8.40 (1H, t, 5.5)
8	40.4	3.99 (2H, t, 5.5)
9	130.8	6.19 (1H, dt, 16.1, 5.5)
10	115.3	6.30 (1H, d, 16.1)
11	126.6	–
12	–	–
13	146.9	–
14	–	12.35 (1H, brs)
15	109.4	7.14 (1H, brs)
16	29.8	3.38 (3H, s)
13-NH_2	–	7.71 (2H, brs)

3.4.5. Agesasines A (**32**) and B (**33**)

Agesasine A (**32**) has the molecular formula of $C_9H_{10}N_2O_4Br_2$, as determined by the HRESIMS (*m/z* 390.8889 $[M+Na]^+$, Δ–1.6 mmu). The ^1H and ^{13}C NMR spectra displayed the signals of one sp^3 oxymethine, one sp^3 methylene, one methoxy group, and one carboxy carbon as well as resonances due to a dibrominated pyrrole carboxamide moiety (Figure 3-23, Table 3-5).

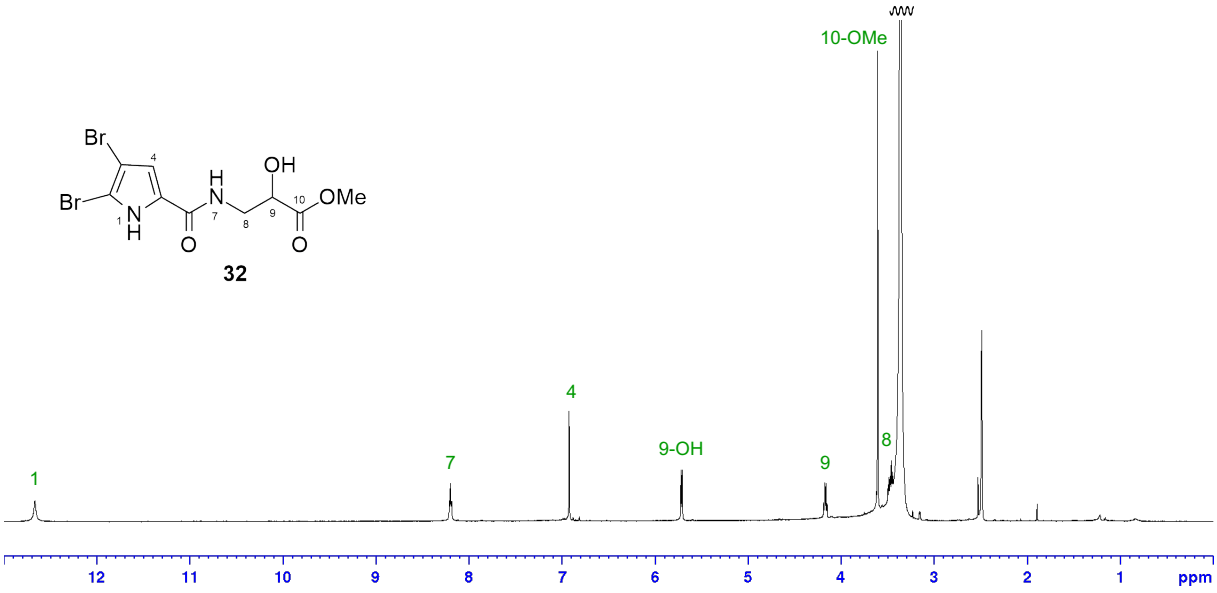

32

Figure 3-23. ^1H NMR spectrum of agesasine A (**32**) in DMSO-d_6 (500 MHz).

The connectivities from 7-NH to 9-OH were revealed by interpretation of the ^1H-^1H COSY spectrum (Figure 3-24). HMBC correlations for methoxy protons and H_2-8 with C-9 suggested the presence of a methxoxy carbonyl group at C-9. Thus, the planar structure of agesasine A (**32**) was elucidated as shown in Figure 3-24.

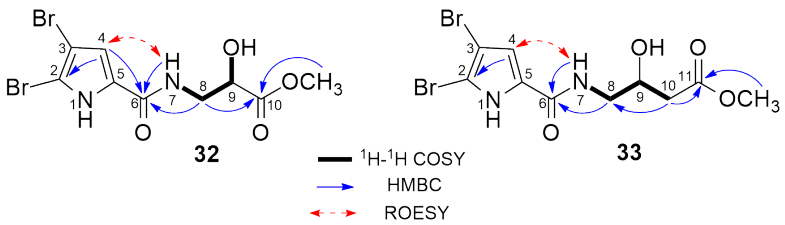

Figure 3-24. Selected 2D NMR correlations and the gross structure for agesasines A (**32**) and B (**33**).

Agesasine B (**33**) gave the 1D NMR spectra closely correlated with those of **32** (Figure 3-25). The molecular formula was established by the HRESIMS to be $C_{10}H_{12}N_2O_4Br_2$ (*m*/*z* 380.9063 $[M–H]^-$, Δ–2.3 mmu). The ^{13}C NMR spectrum showed an additional sp^3 methylene carbon signal (δ_C 40.6, CH_2-10) as compared with that of **32** (Table 3-5). The connectivities of 7-NH to CH_2-10 were assigned by ^1H-^1H COSY and HMBC analysis (Figure 3-24). Thus, the gross structure of **33** was elucidated as shown in Figure 3-25.

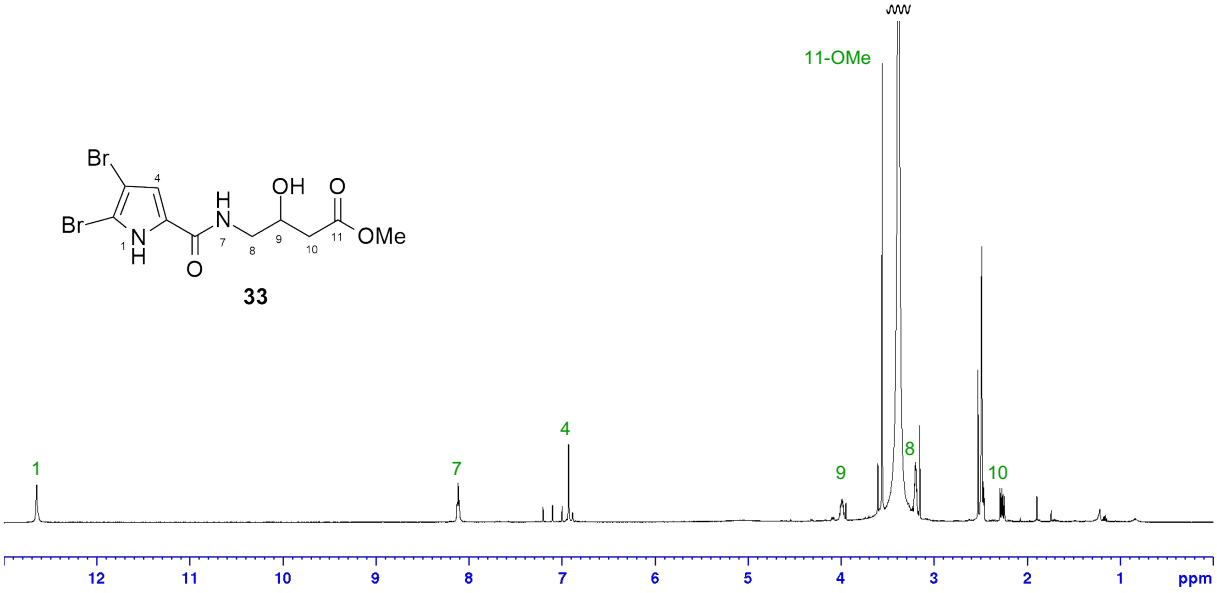

Figure 3-25. ^1H NMR spectrum of agesasine B (**33**) in DMSO-d_6 (500 MHz).

Table 3-5. ^1H and ^{13}C NMR data for agesasines A (**32**) and B (**33**) in DMSO-d_6.

Position	**32**		**33**	
	^{13}C	^1H (*J* in Hz)	^{13}C	^1H (*J* in Hz)
1	–	12.67 (1H, brs)	–	12.65 (1H, brs)
2	104.8	–	104.7	–
3	98.0	–	98.0	–
4	113.1	6.93 (1H, brs)	113.0	6.93 (1H, d, brs)
5	128.1	–	128.3	–
6	159.3	–	159.3	–
7	–	8.20 (t, 5.8)	–	8.12 (1H, t, 5.5)
8	42.7	3.46 (1H, m)	44.9	3.20 (2H, m)
		3.36 (1H, m)		
9	69.3	4.17 (1H, q, 6.1)	66.6	3.99 (1H, m)
10	173.1	–	40.6	2.49 (1H, m)
				2.27 (1H, dd, 8.8, 15.2)
11			171.8	–
9-OH	–	5.71 (1H, d, 5.9)	–	*nd*
10-OMe	51.8	3.61 (3H, brs)		
11-OMe			51.4	3.56 (3H, brs)

nd: not detected.

Since specific rotation values of agesasines **A** (**32**) and B (**33**) (each ≈ 0) implied **32** and **33** to be racemates, optical resolutions of **32** and **33** by chiral HPLC column were carried out. The optical resolution of **32** using chiral HPLC column resulted in the separation of enantiomers (t_R 27.5 and 29.0 min), whose ratio of which was approximately 1:1 (Figure 3-26). Therefore, **32** was concluded to be a racemate. Agesasine B (**33**) was also deduced to be a racemate due to resemblance biogenetic pathway of **32**, although the optical resolution of agesasine B (**33**) could not be achieved in spite of attempts at various separation conditions.

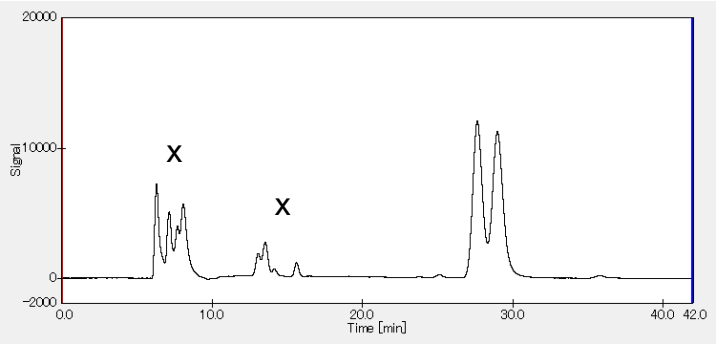

Figure 3-26. Chromatogram of chiral HPLC analysis for agesasine A (**32**).

3.5. Summary

Eight new bromopyrrole alkaloids, agesamides C–E (**9**–**11**), 9-hydroxydihydrodispacamide (**12**), 9-hydroxydihydrooroidin (**13**), 9-(*E*)-keramadine (**14**), and agesasines A (**32**) and B (**33**) were isolated from Okinawan marine sponges *Agelas* spp. (SS-1302 and SS-516) (Figure 3-27). The absolute configurations of **9**–**13**, **32**, and **33** could not be assigned, since any Cotton effects were not observed in their CD spectra. Taking their specific rotation values ($[\alpha]_D \approx 0$ in each case) into account, **9**–**13**, **32**, and **33** were concluded to be racemates.

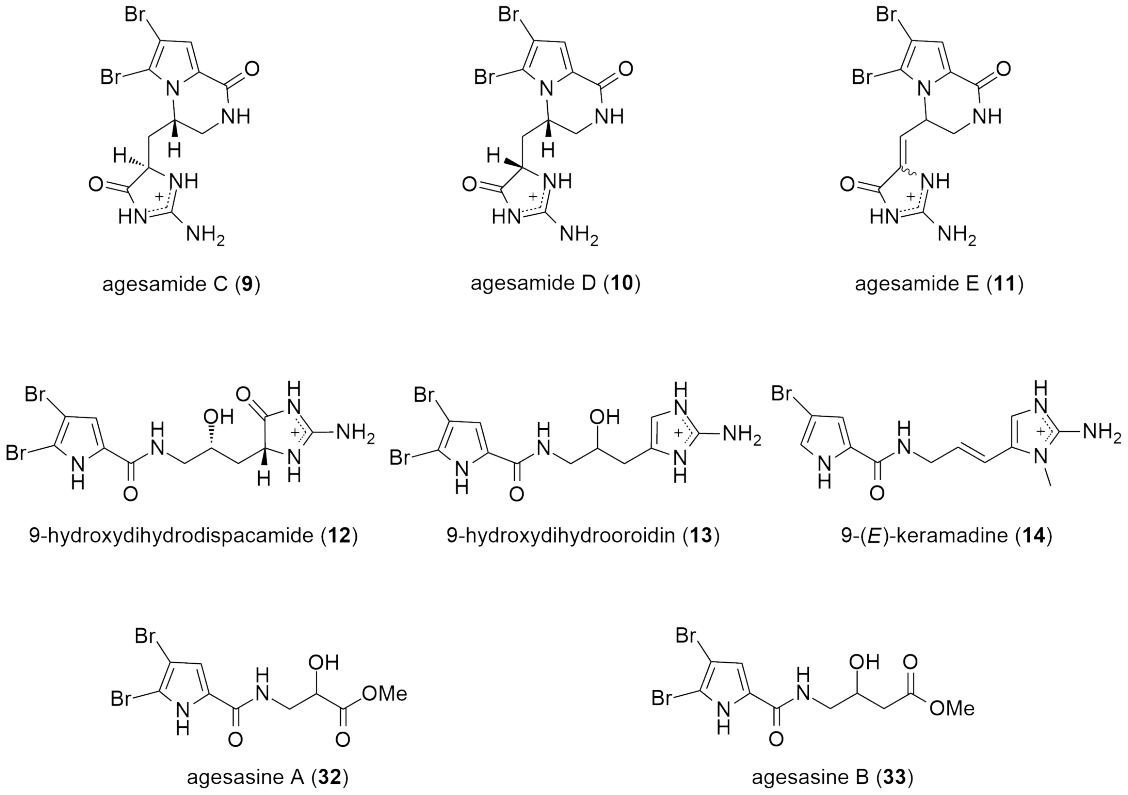

Figure 3-27. Isolated new bromopyrrole alkaloids from Okinawan marine sponges *Agelas* spp. (SS-1302 and SS-516).

In addition, 19 known bromopyrrole alkaloids, oroidin (**15**), keramadine (**16**), 2-bromo-9,10-dihydrokeramadine (**17**), ageliferin (**19**), agelamadines C (**20**), and E (**21**), cyclooroidin (**22**), mauritiamine (**26**), agelongine (**30**), tauroacidins A (**34**), and C (**31**), taurodispacamide A (**35**), nagelamides A (**23**), B (**24**), J (**25**), L (**18**), M (**27**), N (**28**), and U (**29**), were obtained from marine sponges *Agelas* spp. (SS-1302, SS-159, and SS-516).

Agesamides C–E (**9**–**11**) are new bromopyrrole alkaloids possessing pyrroloketopiperazine and aminoimidazolone moieties. Furthermore, it is the first example of a cyclized bromopyrrole alkaloid with an aminoimidazolone ring from nature resource.

Agesasines A (**32**) and B (**33**) are rare bromopyrrole alkaloids lacking an

aminoimidazole moiety, whereas several alkaloids with such structural feature have been isolated from marine sponges *Agelas* spp. collected off the South China Sea [63,64].

Chapter 4.
Conclusion

This research focused on searching new secondary metabolites from Okinawan marine sponges *Agelas* spp. The chemical constituents of four *Agelas* spp. (SS-12, SS-1302, SS-159, and SS-516) were explored, resulting in the isolation and characterization of two new diterpene alkaloids and eight new bromopyrrole alkaloids together with 25 known marine natural products.

Chemical study on the extract of SS-12 led to the isolation of two new diterpene alkaloids, agelamasines A (**1**) and B (**2**). Agelamasine A (**1**) is a diterpene alkaloids with a rearranged (4→2)-*abeo*-clerodane skeleton. Although several diterpenes with the rearranged (4→2)-*abeo*-clerodane carbon skeleton have been reported from terrestrial plants, it is the first example of a diterpene possessing an alkaloidal partial structure *N*-methyladenine from a marine source.

Eight new bromopyrrole alkaloids were isolated from the methanol extracts of SS-1302 and SS-516. Their structures were determined by spectroscopic data and conformational analysis. Agesamides C–E (**9**–**11**) are new bromopyrrole alkaloids possessing pyrroloketopiperazine and aminoimidazolone moieties. Agesasines A (**32**) and B (**33**) are rare bromopyrrole alkaloids lacking an aminoimidazole moiety, whereas several alkaloids with such carbon skeleton have been obtained from marine sponges *Agelas* spp. collected off the South China Sea.

Chapter 5.
Experimental Section

5.1. General Experimental Procedures

Specific rotations were obtained on a JASCO P-2200 digital polarimeter. UV and CD spectra were measured by a Hitachi U-3900H and a JASCO J-1500 spectrophotometers, respectively. NMR spectra were run on a Bruker AVANCE-500 spectrometer using tetramethylsilane as an internal standard. The HMBC spectra observed with delay values for J_{CH}=10 or 5 Hz. ESIMS and HRESIMS were recorded on a Waters SQD2 2695 and Waters LCT PREMIER 2695, respectively. Column chromatographies were performed with silica gel 60N (63-210 μm, Kanto Kagaku, Japan) and Diaion HP-20 (Mitsubishi Chemical, Japan). MPLC was carried out on Toyopearl HW-40F (TOSOH), MIC gel CHP 20P (37-75 μm, Mitsubishi Chemical, Japan), and Biotage SNAP Cartridge KP-C18-HS (Biotage). HPLC was performed on YMC Hydrosphere C18 (10 i.d. × 250 mm and 20 i.d. × 250 mm; 5 μm, YMC), COSMOSIL πNAP (10 i.d. × 250 mm and 20 i.d. × 250 mm; 5 μm, Nacalai Tesque), Gel-Permeation Chromatography (GPC, Asahipak GS-310 2G, SHOWA DENKO), COSMOSIL 5C_{18}-AR-II (10 i.d. × 250 mm; 5 μm, Nacalai Tesque), COSMOSIL 5C_{18}-MS-II (10 i.d. × 250 mm; 5 μm, Nacalai Tesque), and YMC-triart C18 (10 i.d. × 250 mm; 5 μm, YMC). Optical resolution was performed on chiral HPLC (Chiral ART Cellulose-SB, 4.6 i.d. × 250 mm, YMC, flow rate 0.5 mL/min, UV 254 nm) at 35 °C.

5.2. Experimental Procedure of Chapter 2

5.2.1. Material

The sponge *Agelas* sp. (SS-12), collected in Okinawa, Japan, was kept frozen until used. The voucher specimen is deposited at the Graduate School of Pharmaceutical Sciences, Tokushima University.

5.2.2. Extraction and Isolation

The Okinawan marine sponge *Agelas* sp. (SS-12, 1.96 kg, wet weight) was extracted with MeOH. The extract (95.8 g), which was partitioned between *n*-hexane and 90% MeOH aq. The 90% MeOH aq.-soluble materials were further partitioned with *n*-BuOH and water. The *n*-BuOH-soluble materials (43.0 g) were subjected to MPLC on a Toyopearl HW-40F column (MeOH/TFA) to give seven fractions (frs. A1−7). Fractionation of fr. A5 by an ODS column on MPLC (MeOH/H_2O/TFA, 30:70:0.1−100:0:0.1) gave five fractions (frs. A5.1−5.5). Fr.

A5.5 was applied to a silica gel column ($CHCl_3$/MeOH/H_2O/TFA, 95:5:0.1–0:100:0.1) to give seven fractions (frs. A5.5.1–7). Fr. A5.5.6 was separated by an ODS column on MPLC (MeOH/H_2O/TFA, 60:40:0.1–100:0:0.1) to give eight fractions (frs. A5.5.6.1–8). Fr. A5.5.6.5 was loaded on ODS HPLC (Hydrosphere C18, flow rate 7.0 mL/min, UV detection at 254 nm, eluent MeCN/H_2O/TFA, 35:65:0.1) to give 10 fractions (frs. A5.5.6.5.1–10). Fr. A5.5.6.5.9 was purified using ODS HPLC (COSMOSIL πNAP, 3.0 mL/min, 254 nm, MeCN/H_2O/TFA, 35:65:0.1) to afford agelamasine B (**2**, 2.2 mg) and nemoechine F (**8**, 2.8 mg), while purification of fr. A5.5.6.5.10 with the same condition afforded agelamasine A (**1**, 1.7 mg). Fr. A5.5.6.4 was loaded on ODS HPLC (Hydrosphere C18, 7.0 mL/min, 254 nm, MeCN/H_2O/TFA, 30:70:0.1) to furnish 2-oxo-agelasines A (**3**, 26.7 mg), B (**4**, 68.1 mg), and F (**5**, 25.5 mg). Fr. A5.5.6.7 was purified by ODS HPLC (Hydrosphere C18, 7.0 mL/min, 254 nm, MeCN/H_2O/TFA, 47:53:0.1) to give agelasines C (**6**, 9.4 mg) and F (**7**, 10.7 mg).

5.2.3. Agelamasine A (**1**)

A pale yellow amorphous solid; $[\alpha]_D^{28}$ +12.7 (*c* 0.1, MeOH); HRESIMS: *m*/*z* 474.2877 $[M–H+Na]^+$ (calcd for $C_{26}H_{38}N_5O_2Na$, 474.2845); UV (MeOH) λ_{max} 224 (ε 8,800) and 265 (870, sh) nm; ^1H and ^{13}C NMR data (Table 2-1).

5.2.4. Agelamasine B (**2**)

A pale yellow amorphous solid; $[\alpha]_D^{20}$ –2.8 (*c* 0.1, MeOH); HRESIMS: *m*/*z* 470.3533 $[M]^+$ (calcd for $C_{27}H_{44}N_5O_2$, 470.3495); UV (MeOH) λ_{max} 224 (ε 10,200) and 260 (1,400, sh) nm; ^1H and ^{13}C NMR data (Table 2-1).

5.3. Experimental Procedure of Chapter 3

5.3.1. Material

The marine sponges *Agelas* spp. (SS-1302, SS-159, and SS-516) were collected in Okinawa, Japan. The voucher specimens were deposited in the Graduate School of Pharmaceutical Sciences, Tokushima University.

5.3.2. Extraction and Isolation of SS-1302

The Okinawan marine sponge *Agelas* sp. SS-1302 (3.42 kg, wet weight) was extracted with MeOH to give the extract (197.1 g). The extract was partitioned with *n*-hexane and 90% MeOH aq. The 90% MeOH aq.-soluble materials were further partitioned between *n*-BuOH and water. The *n*-BuOH-soluble materials (58.0 g) were separated by chromatography on a

silica gel column ($CHCl_3$/MeOH/TFA, 90:10:0.1–50:50:0.1) to give six fractions (frs. B1–6) including oroidin (**15**, 17.1 g, fr. B5).

Fr. B4 was subjected to MPLC on a Toyopearl HW-40F column (MeOH/H_2O/TFA, 10:90:0.1–90:10:0.1), a MCI gel CHP 20P column (MeOH/H_2O/TFA, 50:50:0.1–90:10:0.1) to yield seven fractions (frs. B4.4.1–7). Fr. B4.4.3 was loaded to MPLC with an ODS column (MeCN/H_2O/TFA, 10:90:0.1–60:40:0.1) to give six fractions (frs. B4.4.3.1–6), and then fr. B4.4.3.3 was purified by ODS HPLC (COSMOSIL 5C_{18}-MS-II, 20 i.d. × 250 mm, MeCN/H_2O/TFA, 17:83:0.1). Purification of fr. B4.4.3.3.2 by an ODS HPLC (Hydrosphere C18, 10 i.d. × 250 mm, MeCN/H_2O/TFA, 13:87:0.1) afforded 9-hydroxydihydrodispacamide (**12**, 5.0 mg), 9-(*E*)-keramadine (**14**, 3.1 mg), and keramadine (**16**, 6.7 mg). 9-Hydroxydihydrooroidin (**13**, 2.1 mg) was isolated from fr. B4.4.3.3.3 by reversed phase HPLCs {Hydrosphere C18 (10 i.d. × 250 mm) and YMC-Triart PFP (10 i.d. × 250 mm) with MeCN/H_2O/TFA (13:87:0.1 and 16:84:0.1, respectively)}. Fr. B4.4.4 was separated by an ODS column on MPLC (MeCN/H_2O/TFA, 10:90:0.1–50:50:0.1) to give six fractions (frs. B4.4.4.1–6). Fr. B4.4.4.4 was purified by ODS HPLC (COSMOSIL 5C_{18}-AR-II, 10 i.d. × 250 mm, MeCN/H_2O/TFA, 14:86:0.1), and then further purified by reversed phase HPLC (YMC-Triart PFP, 10 i.d. × 250 mm, MeCN/H_2O/TFA, 20:80:0.1) to furnish agesamide E (**11**, 3.6 mg). Fr. B4.4.4.5 was separated by GPC (Asahipak GS-310 2G, MeOH/TFA, 100:0.1) to afford seven fractions (frs. B4.4.4.5.1–7). Fr. B4.4.4.5.2 was purified by ODS HPLC column (Hydrosphere C18, 10 i.d. × 250 mm, MeCN/H_2O/TFA, 15:85:0.1) to furnish 2-bromo-9,10-dihydrokeramadine (**17**, 2.1 mg).

Fr. B5 was subjected to MPLC on a Toyopearl HW-40F column (MeOH/H_2O/TFA, 10:90:0.1–90:10:0.1), resulting in eight fractions (frs. B5.1–5.8). Fr. B5.3 was passed through an MCI gel CHP 20P column (MeOH/H_2O/TFA, 10:90:0.1–100:0:0.1) to give eight fractions (frs. B5.3.1–5.3.8). Fr. B5.3.4 was subject to an ODS column (MeOH/H_2O/TFA, 10:90:0.1–90:10:0.1) to yield six fractions (frs. B5.3.4.1–5.3.4.6) with nagelamide L (**18**, 187.5 mg, fr. B5.3.4.5), and then frs. B5.3.4.3 was separated by GPC (Asahipak GS-310 2G, MeOH/TFA, 100:0.1) to afford four fractions (frs. B5.3.4.3.1–4). Fr. B5.3.4.3.4 was purified by ODS HPLC (YMC-Triart C18, 20 i.d. × 250 mm, MeCN/H_2O/TFA, 17:83:0.1) to afford agesamides C (**9**, 26.4 mg) and D (**10**, 16.6 mg).

5.3.3. Agesamide C (**9**)

A pale yellow amorphous solid; $[\alpha]_D^{18} \approx 0$ (*c* 0.10, MeOH); UV (MeOH) λ_{max} 227 (ε 3,990) and 282 (2,160) nm; ESIMS: *m/z* 404, 406, and 408 (1:2:1) $[M]^+$; HRESIMS: *m/z* 403.9388 $[M]^+$ (calcd for $C_{11}H_{12}N_5O_2{}^{79}Br_2$, 403.9358); ^1H and ^{13}C NMR data (Table 3-1).

5.3.4. Agesamide D (**10**)

A pale yellow amorphous solid; $[\alpha]_D^{18} \approx 0$ (*c* 0.10, MeOH); UV (MeOH) λ_{max} 227 (ε 4,880) and 282 (2,640) nm; ESIMS: *m/z* 404, 406, and 408 (1:2:1) $[M]^+$; HRESIMS: *m/z* 403.9315 $[M]^+$ (calcd for $C_{11}H_{12}N_5O_2{}^{79}Br_2$, 403.9358); ^1H and ^{13}C NMR data (Table 3-1).

5.3.5. Agesamide E (**11**)

A pale yellow amorphous solid; $[\alpha]_D^{24} \approx 0$ (*c* 0.10, MeOH); UV (MeOH) λ_{max} 251 (ε 10,220) and 286 (6,880) nm; ESIMS: *m/z* 424, 426, and 428 (1:2:1) $[M–H+Na]^+$; HRESIMS: *m/z* 401.9177 $[M]^+$ (calcd for $C_{11}H_{10}N_5O_2{}^{79}Br_2$, 401.9201); ^1H and ^{13}C NMR data (Table 3-1). Optical resolution of agesamide E (**11**) was performed on chiral HPLC (Chiral ART Cellulose-SB, YMC, 4.6 i.d. × 250 mm, flow rate 0.5 mL/min, UV 254 nm) at 35 °C with eluent MeOH/MeCN/H_2O/H_3PO_4 (8:2:90:0.1) to give each enantiomers {(+)-**11**, t_R 27.1 min; (–)-**11**, 31.8 min} in the integral ratio of ca. 1:1.

5.3.6. 9-Hydroxydihydrodispacamide (**12**)

A pale yellow amorphous solid; $[\alpha]_D^{27} \approx 0$ (*c* 0.10, MeOH); UV (MeOH) λ_{max} 223 (ε 3,890) and 275 (3,380) nm; ESIMS: *m/z* 422, 424, and 426 (1:2:1) $[M]^+$; HRESIMS: *m/z* 443.9319 $[M–H+Na]^+$ (calcd for $C_{11}H_{13}N_5O_3Na\,{}^{79}Br_2$, 443.9283); ^1H and ^{13}C NMR data (Table 3-2). Optical resolution of 9-hydroxydihydrodispacamide (**12**) was performed on chiral HPLC (Chiral ART Cellulose-SB, YMC, 4.6 i.d. × 250 mm, flow rate 0.5 mL/min, UV 254 nm) at 35 °C with eluent MeOH/MeCN/H_2O/H_3PO_4 (16:4:80:0.1) to give each enantiomers (t_R 12.5 and 14.3 min) in the integral ratio of ca. 1:1.

5.3.7. 9-Hydroxydihydrooroidin (**13**)

A pale yellow amorphous solid; $[\alpha]_D^{27} \approx 0$ (*c* 0.10, MeOH); UV (MeOH) λ_{max} 276 (ε 3,850) nm; ESIMS: *m/z* 406, 408, and 410 (1:2:1) $[M]^+$; HRESIMS: *m/z* 405.9478 $[M]^+$ (calcd for $C_{11}H_{14}N_5O_2{}^{79}Br_2$, 405.9514); ^1H and ^{13}C NMR data (Table 3-3).

5.3.8. 9-(*E*)-Keramadine (**14**)

A pale yellow amorphous solid; UV (MeOH) λ_{max} 271 (ε 3,280) nm; ESIMS: *m/z* 324 and 326 (1:1) $[M]^+$; HRESIMS: *m/z* 324.0467 $[M]^+$ (calcd for $C_{12}H_{15}N_5O^{79}Br$, 324.0460); ^1H and ^{13}C NMR data (Table 3-4).

5.3.9. Extraction and Isolation of SS-159

The sponge *Agelas* sp. SS-159 (3.78 kg, wet weight) was extracted with MeOH. The extract was partitioned with *n*-hexane and 90% MeOH aq. The 90% MeOH aq.-soluble materials were partitioned between *n*-BuOH and water. The *n*-BuOH-soluble materials (147.3 g) were separated by chromatography on a silica gel column ($CHCl_3$/MeOH/TFA, 80:20:0.1–50:50:0.1) to give seven fractions (frs. C1–7).

Fr. C6 was separated by an ODS column on MPLC (MeOH/H_2O/TFA, 10:90:0.1–100:0:0.1) to afford seven fractions (frs. C6.1–7). Fr. C6.3 was subjected to MPLC with an ODS column to give five fractions (frs. C6.3.1–5). Fr. C6.3.3 was separated by GPC (Asahipak GS-310 2G, MeOH/TFA, 100:0.1) to afford six fractions (frs. C6.3.3.1–6). Fr. C6.3.3.2 was purified by ODS HPLC (COSMOSIL 5C_{18}-MS-II, 20 i.d. × 250 mm, MeCN/H_2O/TFA, 22:78:0.1) to furnish agelmadins C (**20**, 4.6 mg) and E (**21**, 3.5 mg), while purification of fr. C6.3.3.3 with the same condition afforded cyclooroidin (**22**, 4.4 mg). Fractionation of fr. C6.5 by an ODS column on MPLC (MeCN/H_2O/TFA, 10:90:0.1–70:30:0.1) gave seven fractions (frs. C6.5.1–6.5.7). Fr. C6.5.5 was separated by GPC (Asahipak GS-310 2G, MeOH/TFA, 100:0.1) to afford three fractions (frs. C6.5.5.1–3). Fr. C6.5.5.1 was loaded on ODS HPLC (Hydrosphere C18, 20 i.d. × 250 mm, MeCN/H_2O/TFA, 28:72:0.1) to furnish nagelamides A (**23**, 3.5 mg) and J (**25**, 4.6 mg). Fr. C6.5.5.2 was purified by ODS HPLC (Hydrosphere C18, 20 i.d. × 250 mm, MeCN/H_2O/TFA, 30:70:0.1) to furnish nagelamide B (**24**, 7.7 mg) and mauritiamine (**26**, 11.8 mg).

Fr. C7 was applied to MPLC on a Toyopearl HW-40F column (MeOH/H_2O/TFA, 10:90:0.1–100:0:0.1) to yield five fractions (frs. C7.1–5). Fr. C7.4 was separated by GPC (Asahipak GS-310 2G, MeOH/TFA, 100:0.1) to afford eight fractions (frs. C7.4.1–8) include ageliferin (**19**, 1.7 g, fr. C7.4.4). Fr. C7.4.6 was purified by ODS HPLC (COSMOSIL 5C18-MS-II, 20 i.d. × 250 mm, MeCN/H_2O/TFA, 15:85:0.1) to give in 13 fractions (frs. C7.4.6.1–13) including nagelamides M (**27**, 8.5 mg, fr. C7.4.6.6), N (**28**, 2.1 mg, fr. C7.4.6.3), and U (**29**, 4.7 mg, fr. C7.4.6.9), and tauroacidin C (**31**, 4.2 mg, fr. C7.4.6.13). Fr. C7.3 was subject on an ODS column (MeOH/H_2O/TFA,

10:90:0.1–80:20:0.1) to yield seven fractions (frs. C7.3.1–7.3.7). Agelongine (**30**, 85.6 mg) was isolated from fr. C7.3.4 by GPC (Asahipak GS-310 2G, MeOH/H_2O/TFA, 70:30:0.1).

5.3.10. Extraction and Isolation of SS-516

The sponge *Agelas* sp. SS-516 (5.22 kg, wet weight) was extracted with MeOH to afford the extract (376.3 g). The extract was concentrated, and partitioned with *n*-hexane and 90% MeOH aq. The 90% MeOH aq.-soluble materials (250.4 g) were subjected to Diaion HP-20P (MeOH/H_2O, 0:100–100:0) to give six fractions (frs. D1–6). Fr. D3 was subjected to silica column ($CHCl_3$/MeOH/TFA, 95:5:0.1–80:20:0.1) to yield 12 fractions (frs. D3.1–12). Fr. D3.7 was subjected to MPLC with an ODS column to give 11 fractions (frs. D3.7.1–11), and then fr. D3.7.7 was purified by ODS HPLC (Hydrosphere C18, 20 i.d. × 250 mm, MeCN/H_2O/TFA, 35:65:0.1) to furnish agesasines A (**32**, 2.5 mg), and B (**33**, 2.2 mg). Fr. D3.11 was separated by an ODS column on MPLC (MeCN/H_2O/TFA, 5:95:0.1–80:20:0.1) to give five fractions (frs. D3.11.1–5). Fr. D3.11.3 was loaded to MPLC with an ODS column (MeCN/H_2O/TFA, 20:80:0.1) to afford tauroacidin A (**34**, 124.1 mg) and taurodispacamide A (**35**, 34.5 mg).

5.3.11. Agesasine A (**32**)

A pale yellow amorphous solid; $[\alpha]_D^{27} \approx 0$ (*c* 0.10, MeOH); UV (MeOH) λ_{max} 275 (ε 4,910) nm; HRESIMS: *m/z* 390.8889 $[M+Na]^+$ (calcd for $C_9H_{10}N_2O_4Na^{79}Br_2$, 390.8905); ^1H and ^{13}C NMR data (Table 3-5). Optical resolution of agesasine A (**32**) was performed on chiral HPLC (Chiral ART Cellulose-SB, YMC, 4.6 i.d. × 250 mm, flow rate 0.5 mL/min, UV 254 nm) at 35 °C with eluent MeOH/MeCN/H_2O/H_3PO_4 (30:10:60:0.1) to give each enantiomers (t_R 27.5 and 29.0 min) in the integral ratio of ca. 1:1.

5.3.12. Agesasine B (**33**)

A pale yellow amorphous solid; $[\alpha]_D^{29} \approx 0$ (*c* 0.10, MeOH); UV (MeOH) λ_{max} 274 (ε 3,140) nm; HRESIMS: *m/z* 380.9063 $[M–H]^-$ (calcd for $C_{10}H_{11}N_2O_4^{79}Br_2$, 380.9086); ^1H and ^{13}C NMR data (Table 3-5).

Acknowledgements

First of all, I am greatly appreciate to Professor Yoshiki Kashiwada. If he did not accept me as a Ph.D. candidate in this laboratory, I could not experience this great opportunity. Moreover, he supported me in several aspects such as research and daily life in Japan. I would like to express my appreciation from bottom of my heart.

I am also deeply grateful to Associate Professor Naonobu Tanaka. He guided, taught, and trained me for my researches during my Ph.D. course. Because of his kindness, I could get a lot of knowledge about marine natural products field. I really appreciate him.

Also, I wish to thank to Emeritus Professor Jun'ichi Kobayashi (Hokkaido University). He supported me his amazing Okinawan marine sponges for my research. Without his supports, it was difficult to start to study marine natural products. I would like to appreciate Emeritus Professor Jun'ichi Kobayashi again.

In addition, I appreciate Otsuka Toshimi Scholarship Foundation. They provided me the wonderful scholarship since 2017. It was very valuable to research and living during my doctoral degree course. Because of their support, I did not have any worries in my daily life. I will never forget their support.

I would like to thank to members of the Laboratory of Pharmacognosy, Tokushima University. I got accustomed to living in Tokushima because their help. Thank to them that I can get good memories in this laboratory.

Finally, I am really appreciate my family. They always pray and support me all day and night since I came to Tokushima. Without their support, I cannot imagine to finish this Ph.D. course. I would like to thank to my family again.

All glory to God.

March 2019

Sanghoon Lee

References

[1] Dias, D.A.; Urban, S.; Roessner, U. *Metabolites* **2012**, *2*, 303–306.

[2] Blunt, J.W.; Carroll, A.R.; Copp, B.R.; Davis, R.A.; Keyzers, R.A.; Prinsep M.R. *Nat. Prod. Rep.* **2018**, *35*, 8–53.

[3] Calado, R.; Leal, M.C.; Gaspar, H.; Santos, S.; Marques, A.; Nunes, M.L.; Vieira, H. Grand Challenges in Marine Biotechnology Chapter 9. **2018**, Springer International Publishing AG, 317–403.

[4] Martins, A.; Vieira, H.; Gaspar, H.; Santos, S. *Mar. Drugs* **2014**, *12*, 1066–1101.

[5] Hirata, Y.; Uemura, D. *Pure Appl. Chem.* **1986**, *58*, 701–710.

[6] Success Story: Halichondrin B (NSC 609395) E7389 (NSC 707389).
https://dtp.cancer.gov/timeline/flash/success_stories/s4_halichondrinb.htm

[7] Aicher, T.D.; Buszek, K.R.; Fang, F.G.; Forsyth, C.J.; Jung, S.H.; Kishi, Y.; Matelich, M.C.; Scola, P.M.; Spero, D.M.; Yoon, S.K. *J. Am. Chem. Soc.* **1992**, *114*, 3162–3164.

[8] Towle, M.J.; Salvato, K.A.; Budrow, J.; Wels, B.F.; Kuznetsov, G.; Aalfs, K.K.; Welsh, S.; Zheng, W.; Seletsky, B.M.; Palme, M.H.; Habgood, G.J.; Singer, L.A.; DiPietro, L.V.; Wang Y.; Chen, J.J.; Quincy, D.A.; Davis, A.; Yoshimatsu, K.; Kishi, Y.; Yu, M.J.; Littlefield, B.A. *Cancer Res.* **2001**, *61*, 1013–1021.

[9] Eisai Co., Ltd.

(a) https://www.eisai.com/news/news201064.html

(b) https://www.eisai.com/news/news201155.html

[10] Thomas, N.V.; Kim, S-K. *Mar. Drugs* **2013**, *11*, 146–164.

[11] Laport, M.S.; Santos, O.C.S.; Muricy, G. *Curr. Pharm. Biotechnol.* **2009**, *10*, 86–105.

[12] Mehbub, M.F.; Lei, J.; Franco, C.; Zhang, W. *Mar. Drugs* **2014**, *12*, 4539–4577.

[13] Hooper, J.N.A. Sponguide: Guide to Sponge Collection and Identification. **2000**, Queensland Museum, 1–129.

[14] Vogel, G. *Science* **2008**, *320*, 1028–1030.

[15] Nakamura, H.; Wu, H.; Kobayashi, J.; Nakamura, Y.; Ohizumi, Y.; Hirata, Y. *Tetrahedron Lett.* **1985**, *26*, 4517–4520.

[16] Kato, Y.; Fusetani, N.; Matsunaga, S.; Hashimoto, K.; Fujita, S.; Furuya, T. *J. Am. Chem. Soc.* **1986**, *108*, 2780–2781.

[17] Mitsui-Saito, M.; Ohkubo, S.; Obara, Y.; Yanagisawa, T.; Kobayashi, J.; Ohizumi, Y.; Nakahata, N. *Thromb. Res.* **2003**, *108*, 133–138.

[18] Perdicaris, S.; Vlachoglanni, T.; Valavanidis, A. *Nat. Prod. Chem. Res.* **2013**, *1*, 1–8.

[19] Braekman, J-C.; Daloze, D.; Stoller, C.; Van Soest, R.W.M. *Biochem. Syst. Ecol.* **1992**, *20*, 417–431.

[20] Richelle-Maurer, E.; De Kluijver, M.J.; Feio, S.; Gaudencio, S.; Gaspar, H.; Gomez, R.; Tavares, R.; Van de Vyver, G.; Van Soest, R.M.W. *Biochem. Syst. Ecol.* **2003**, *31*, 1073–1091.

[21] Gershenzon, J.; Dudareva, N. *Nat. Chem. Biol.* **2007**, *3*, 408–414.

[22] Breitmaier, E. Terpenes in chapter 4. **2006**, Wiley-VCH, 52–69.

[23] Wu, H.; Nakamura, H.; Kobayashi, J.; Kobayashi, M.; Ohizumi, Y.; Hirata, Y. *Bull. Chem. Soc. Jpn.* **1986**, *59*, 2495–2504.

[24] Yang, F.; Hamann, M.T.; Zou, Y.; Zhang, M-Y.; Gong, X-B.; Xiao, J-R.; Chen, W-S.; Lin, H-W. *J. Nat. Prod.* **2012**, *75*, 774–778.

[25] Stowe, S.D.; Richards, J.J.; Tucker, A.T.; Thompson, R.; Melander, C.; Cavanagh, J. *Mar. Drugs* **2011**, *9*, 2010–2035.

[26] Kwon, O-S.; Kim, D.; Kim, H.; Lee, Y-J.; Lee, H-S.; Sim, C.J.; Oh, D-C.; Lee, S.K.; Oh, K-B.; Shin, J. *Mar. Drugs* **2018**, *16*, Doi:10.3390/md16120513

[27] Tasdemir, D.; Topaloglu, B.; Perozzo, R.; Brun, R.; O'Nell, R.; Carballerial, N.M.; Zhang, X.; Tonge, P.J.; Linden, A.; Ruedi, P. *Bioorg. Med. Chem.* **2007**, *15*, 6834–6845.

[28] Hattori, T.; Adachi, K.; Shizuri, Y. *J. Nat. Prod.* **1997**, *60*, 411–413.

[29] Arai, M.; Yamano, Y, Setiawan, A.; Kobayashi, M. *ChemBioChem* **2014**, *15*, 117–123.

[30] Yamazaki, H.; Kanno, S.; Abdjul, D.B.; Namikoshi, M. *Bioorg. Med. Chem. Lett.* **2017**, *27*, 2207–2209.

[31] Abdjul, D.B.; Yamazaki, H.; Kano, S.; Takahashi, O.; Kirikoshi, R.; Ukai, K.; Namikoshi, M. *J. Nat. Prod.* **2015**, *78*, 1428–1433.

[32] Calcul, L.; Tenney, K.; Ratnam, J.; McKerrow, J.H.; Crews, P. *Aust. J. Chem.* **2011**, *63*, 915–921.

[33] Li, T.; Wang, B.; de Voogd, N.J.; Tang, X.; Wang, Q.; Chu, M.; Li, P.; Li, G. *Chin. Chem. Lett.* **2016**, *27*, 1048–1051.

[34] Pettit, G.R.; Tang, Y.; Zhang, Q.; Bourne, G.T.; Arm, C.A.; Leet, J.E.; Knight, J.C.; Pettite, R.K.; Chapuis, J.; Doubek, D.L.; Ward, F.J.; Weber, C.; Hooper, J.N.A. *J. Nat. Prod.* **2013**, *76*, 420–424.

[35] Kubota, T.; Iwai, T.; Takahashi-Nakaguchi, A.; Fromont, J.; Gonoi, T.; Kobayashi, J. *Tetrahedron* **2012**, *68*, 9738–9744.

[36] Tori, M.; Katto, A.; Sono, M. *Phytochemistry* **1999**, *52*, 487–493.

[37] Wu, T.H.; Cheng, Y.Y.; Chen, C.J.; Ng, L.T.; Chou, L.C.; Huang, L.J.; Chen, Y.H.; Kuo,

S.C.; El-Shazly, M.; Wu, Y.C.; Chang, F.R.; Liaw, C.C. *Molecules* **2014**, *19*, 2049–2060.

[38] Bomm, M.D.; Zukerman-Schpector, J.; Lopes, L.M.X. *Phytochemistry* **1999**, *50*, 455–461.

[39] Bohlmann, F.; Singh, P.; Singh, R.K.; Joshi, K.C.; Jakupovic, J. *Phytochemistry* **1985**, *24*, 1114–1115.

[40] Forte, B.; Malgesini, B.; Piutti, C.; Quartieri, F.; Scolaro, A.; Papeo, G. *Mar. Drugs* **2009**, *7*, 705–753.

[41] Weinreb, S.M. *Nat. Prod. Rep.* **2007**, *24*, 931–948.

[42] Al-Mourabit, A.; Zancanella, M.A.; Tilvi, S.; Romo, D. *Nat. Prod. Rep.* **2011**, *28*, 1229–1260.

[43] Kusama, T.; Tanaka, N.; Sakai, K.; Gonoi, T.; Fromont, J.; Kashiwada, Y.; Kobayashi, J. *Org. Lett.* **2014**, *16*, 3916–3918.

[44] Kusama, T.; Tanaka, N.; Sakai, K.; Gonoi, T.; Fromont, J.; Kashiwada, Y.; Kobayashi, J. *Org. Lett.* **2014**, *16*, 5176–5179.

[45] Tanaka, N.; Kusama, T.; Takahashi-Nakaguchi, A.; Gonoi, T.; Fromont, J.; Kobayashi, J. *Org. Lett.* **2013**, *15*, 3262–3265.

[46] Tanaka, N.; Kusama, T.; Takahashi-Nakaguchi, A.; Gonoi, T.; Fromont, J.; Kobayashi, J. *Tetrahedron Lett.* **2013**, *54*, 3794–3796.

[47] Kusama, T.; Tanaka, N.; Kashiwada, Y.; Kobayashi, J. *Tetrahedron Lett.* **2015**, *56*, 4502–4504.

[48] Kusama, T.; Tanaka, N.; Takahashi-Nakaguchi, A.; Gonoi, T.; Fromont, J.; Kobayashi, J. *Chem. Pharm. Bull.* **2014**, *5*, 499–503.

[49] Forenza, S.; Minale, L.; Riccio, R.; Fattorusso, E. *J. Chem. Soc., Chem. Commun.* **1971**, 1129–1130.

[50] Garcia, E.E.; Benjamin, L.E.; Frayer, R.J. *J. Chem. Soc., Chem. Commun.* **1973**, 78–79.

[51] Nakamura, H.; Ohizumi, Y.; Kobayashi, J.; Hirata, Y. *Tetrahedron Lett.* **1984**, *25*, 2475–2478.

[52] Araki, A.; Kubota, T.; Tsuda, M.; Mikami, Y.; Fromont, J.; Kobayashi, J. *Org. Lett.* **2008**, *10*, 2099–2102.

[53] Kobayashi, J.; Tsuda, M.; Murayama, T.; Nakamura, H.; Ohizumi, Y.; Ishibashi, M.; Iwamura, M.; Ohta, T.; Nozoe, S. *Tetrahedron* **1990**, *46*, 5579–5586.

[54] Endo, T.; Tsuda, M.; Okada, T.; Mitsuhashi, S.; Shima, H.; Kikuchi, K.; Mikami, Y.; Fromont, J.; Kobayashi, J. *J. Nat. Prod.* **2004**, *67*, 1262–1267.

[55] Araki, A.; Tsuda, M.; Kubota, T.; Mikami, Y.; Fromont, J.; Kobayashi, J. *Org. Lett.* **2007**, *9*, 2369–2371.

[56] Tsukamoto, S.; Kato, H.; Hirota, H.; Fusetani, N. *J. Nat. Prod.* **1996**, *59*, 501–503.

[57] Fattorusso, E.; Taglialatela-Scafati, O. *Tetrahedron Lett.* **2000**, *41*, 9917–9922.

[58] Kubota, T.; Araki, A.; Ito, J.; Mikami, Y.; Fromont, J.; Kobayashi, J. *Tetrahedron* **2008**, *64*, 10810–10813.

[59] Cafieri, F.; Fattorusso, E.; Mangoni, A.; Taglialatel-Scafati, O. *Bioorg. Med. Chem. Lett.* **1995**, *5*, 799–804.

[60] Kobayashi, J.; Inaba, K.; Tsuda, M. *Tetrahedron* **1997**, *53*, 16697–16682.

[61] Olofoson, A.; Yakushijin, K.; Horne, D.A. *J. Org.Chem.* **1988**, *63*, 1248–1253.

[62] Daninos-Zeghal, S.; Al Mourabit, A.; Ahond A.; Poupat, C.; Potier, P. *Tetrahedron* **1997**, *53*, 7605–7614.

[63] Zhu, Y.; Wang, Y.; Gu, B-B.; Yang, F.; Jiao, W-H.; Hu, G-H.; Yu, H-B.; Han, B-N.; Zhang, W.; Shen, Y.; Lin, H-W. *Tetrahedron* **2016**, *72*, 2964–2971.

[64] Chu, M-J.; Tang, X-L.; Qin, G-F.; de Voogd, N.J.; Li, P-L.; Li, G-Q. *Chin. Chem. Lett.* **2017**, *28*, 1210–1213.

Supporting Information

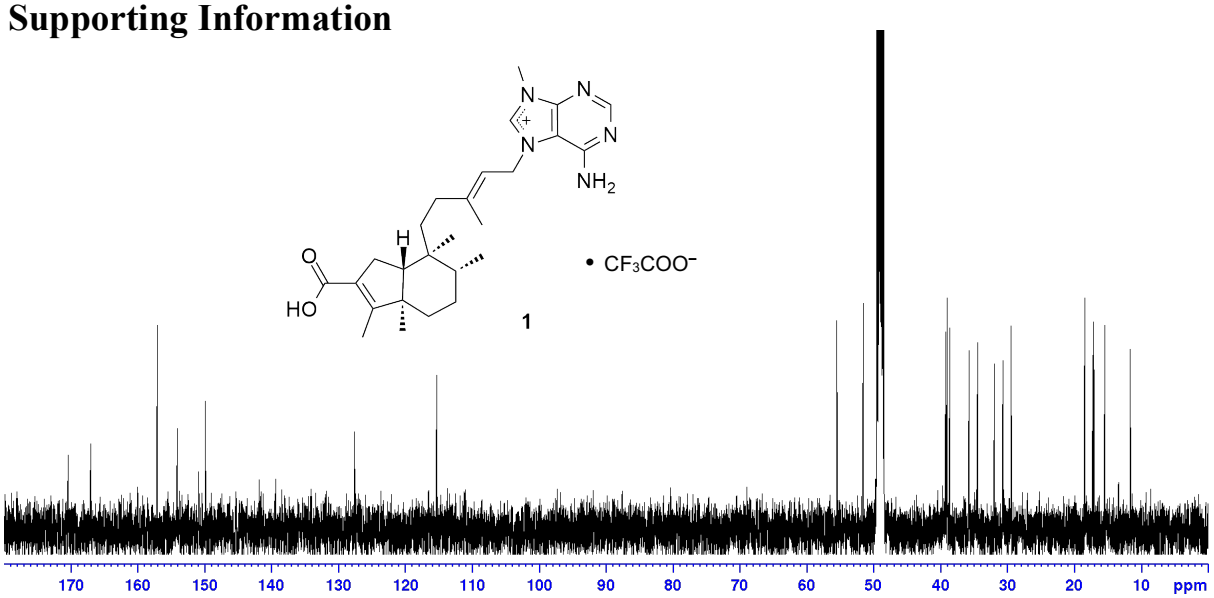

Figure S1. ^{13}C NMR spectrum of agelamasine A (**1**) as a TFA salt form in CD_3OD (125 MHz).

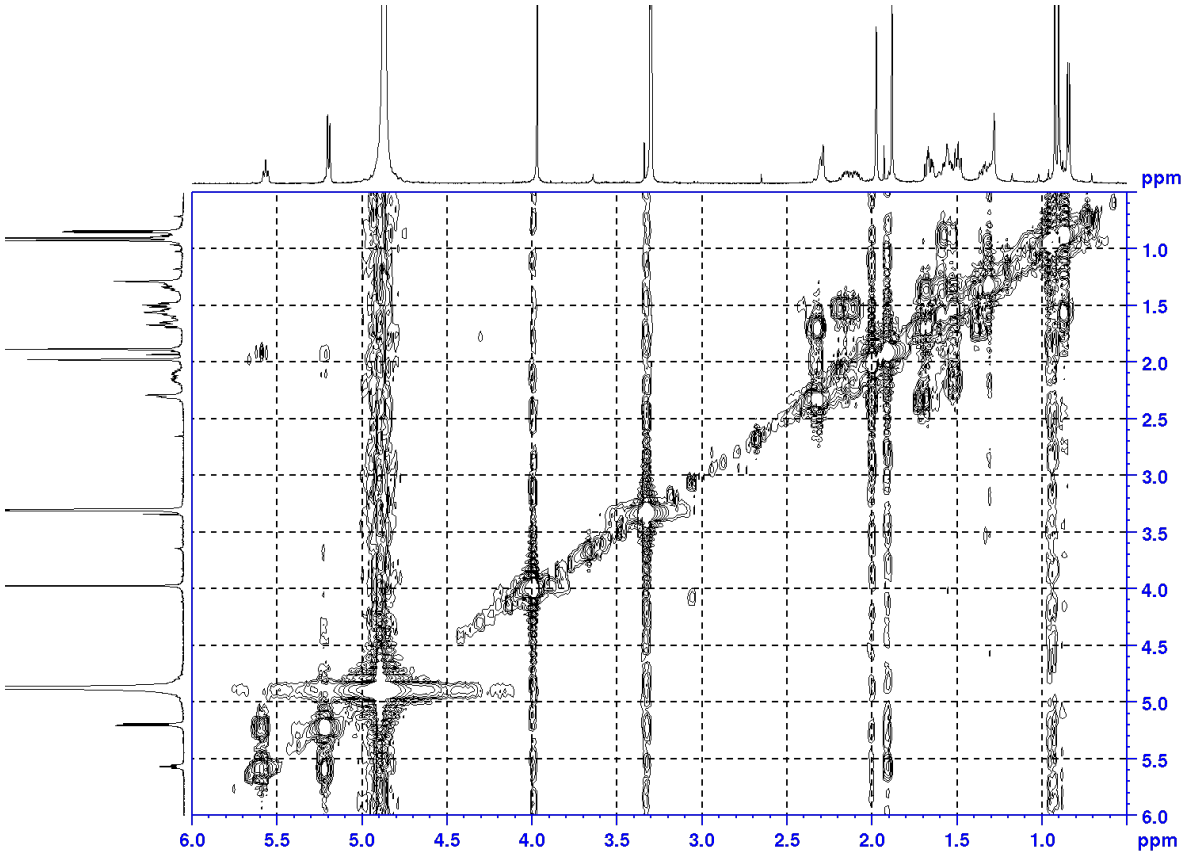

Figure S2. ^{1}H-^{1}H COSY spectrum of agelamasine A (**1**) as a TFA salt form in CD_3OD (500 MHz).

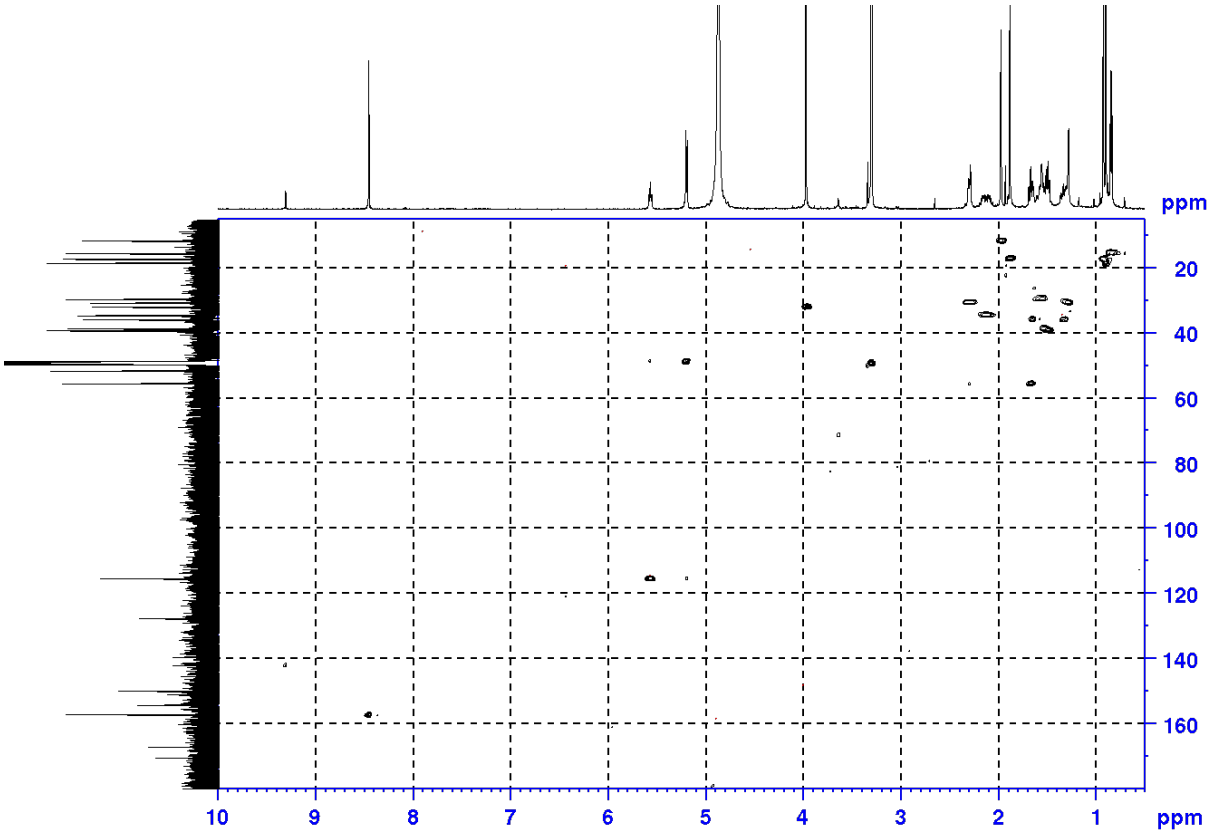

Figure S3. HSQC spectrum of agelamasine A (**1**) as a TFA salt form in CD_3OD (500 MHz).

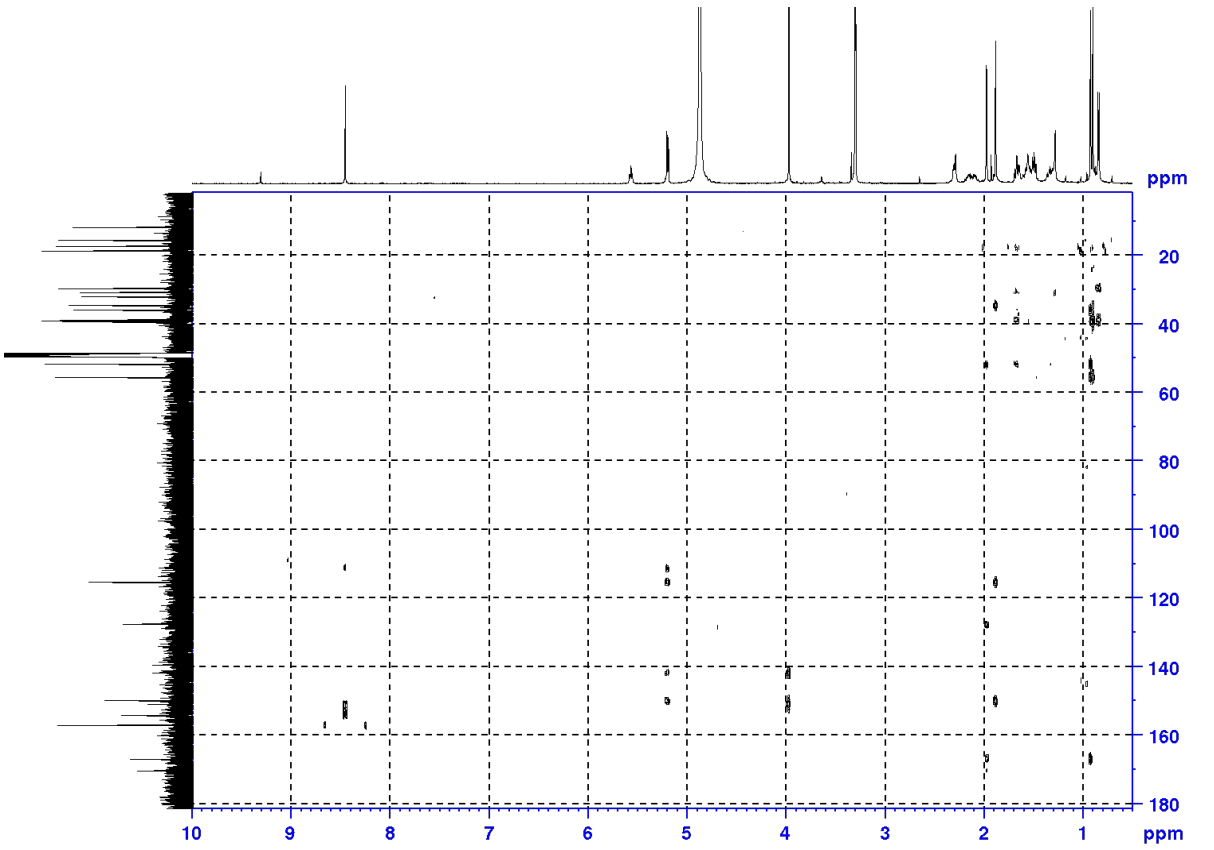

Figure S4. HMBC spectrum of agelamasine A (**1**) as a TFA salt form in CD_3OD (500 MHz).

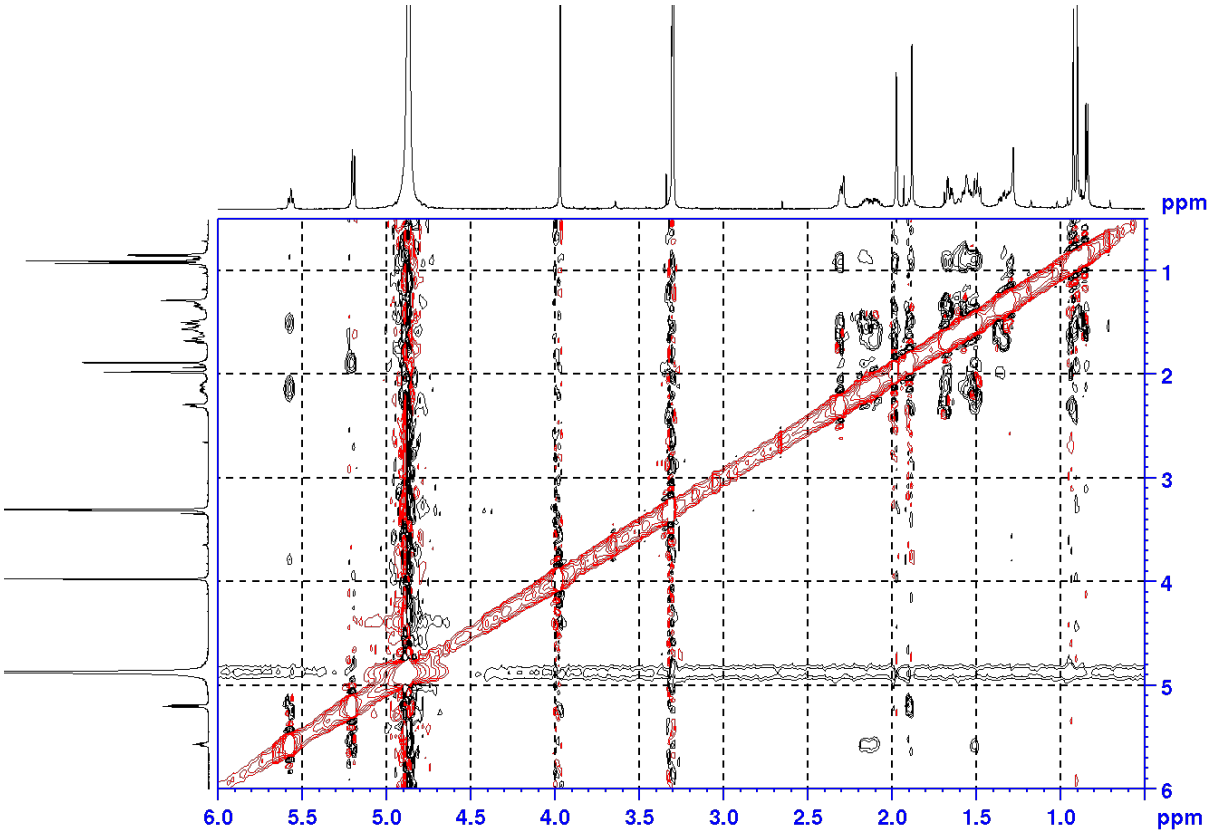

Figure S5. ROESY spectrum of agelamasine A (**1**) as a TFA salt form in CD_3OD (500 MHz).

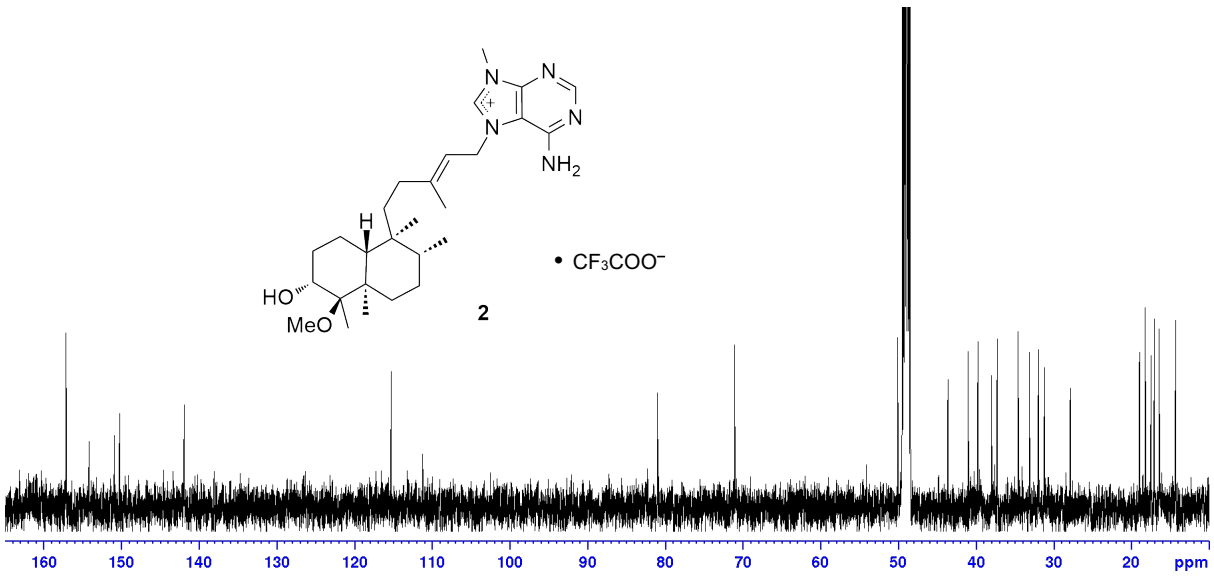

Figure S6. ^{13}C NMR spectrum of agelamasine B (**2**) as a TFA salt form in CD_3OD (125 MHz).

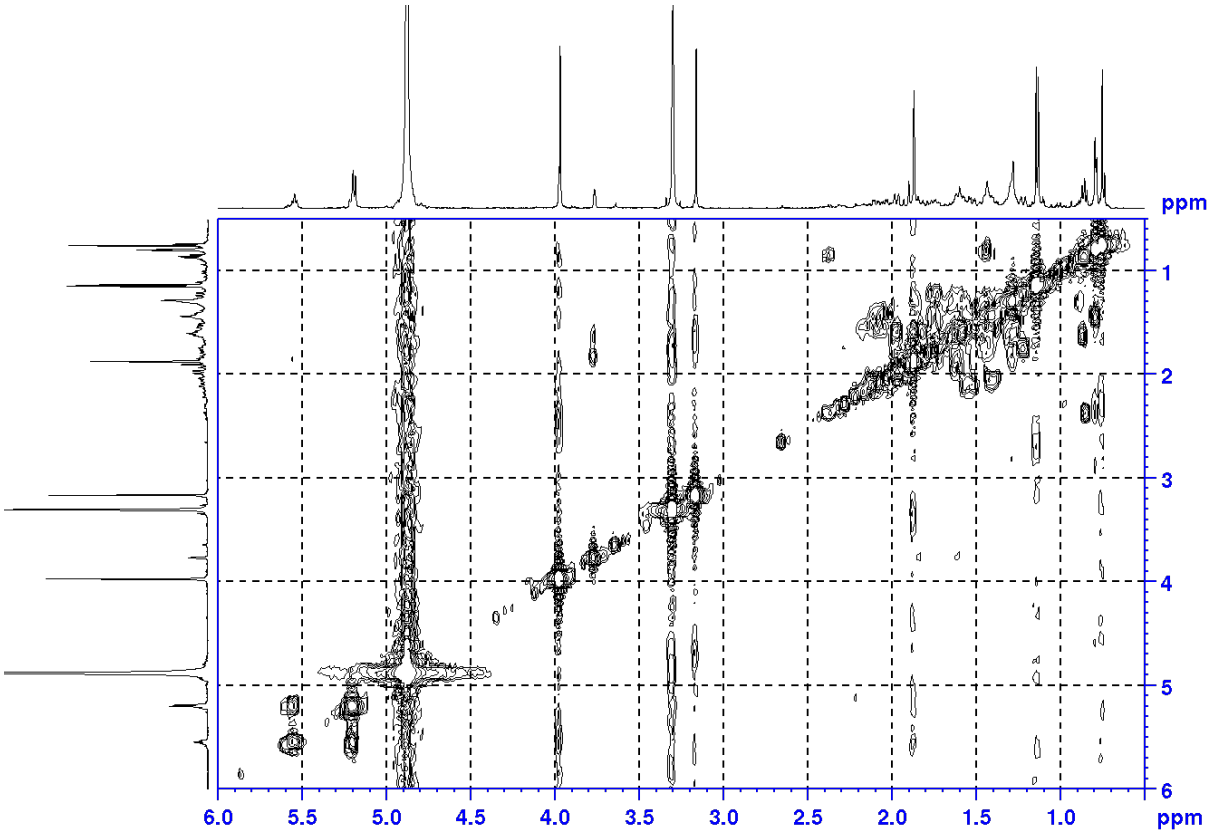

Figure S7. ^{1}H-^{1}H COSY spectrum of agelamasine B (**2**) as a TFA salt form in CD_3OD (500 MHz).

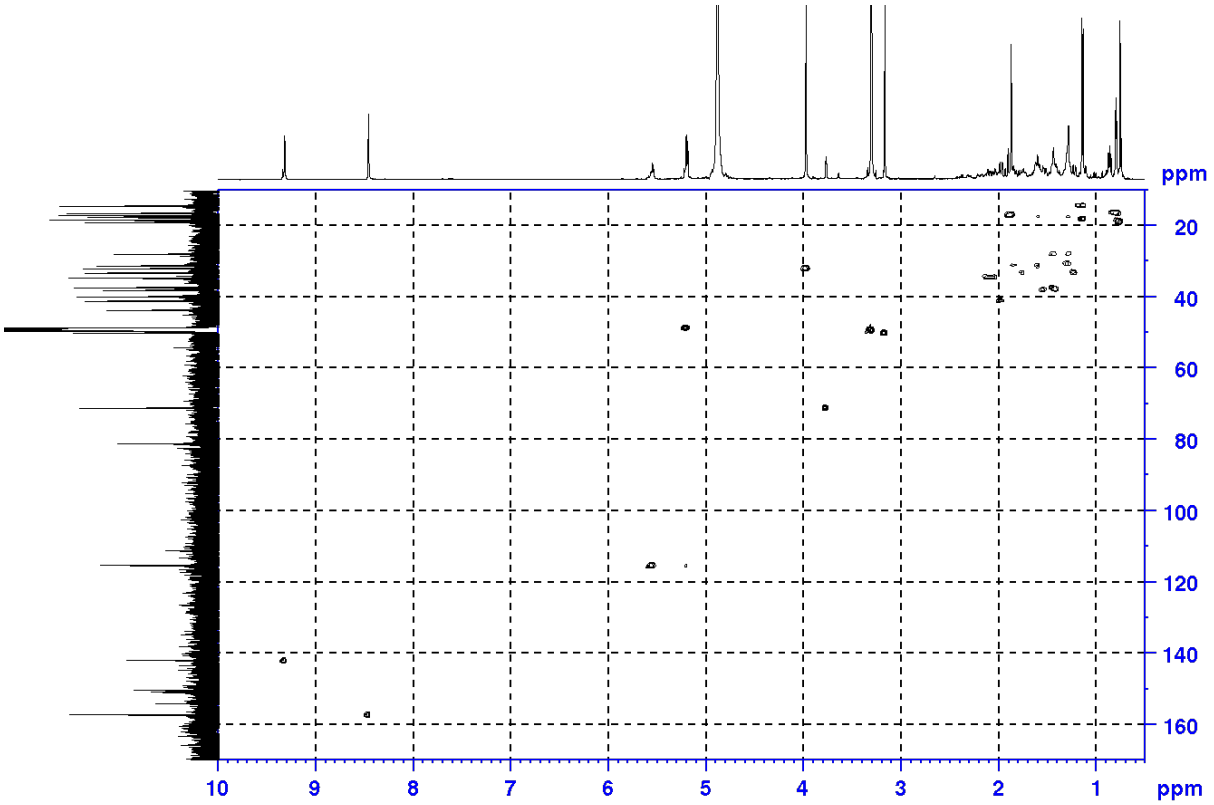

Figure S8. HSQC spectrum of agelamasine B (**2**) as a TFA salt form in CD_3OD (500 MHz).

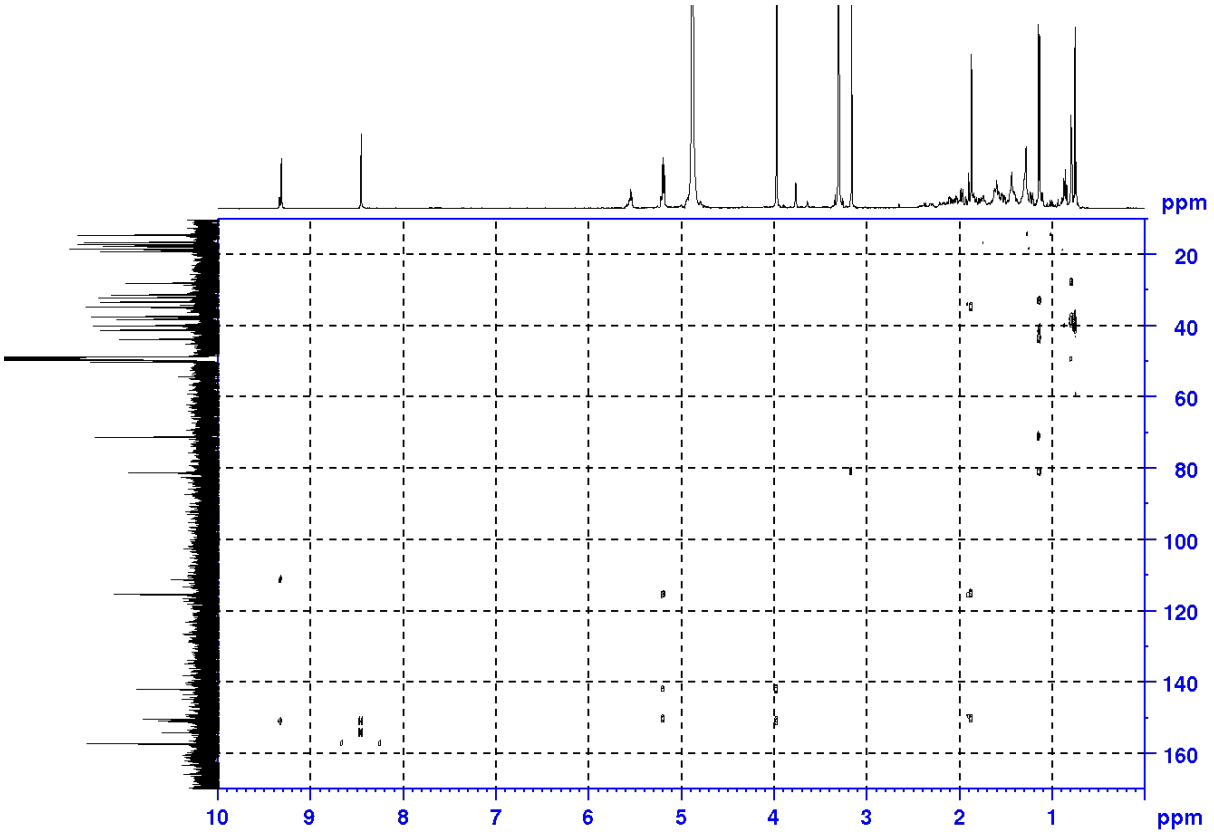

Figure S9. HMBC spectrum of agelamasine B (**2**) as a TFA salt form in CD_3OD (500 MHz).

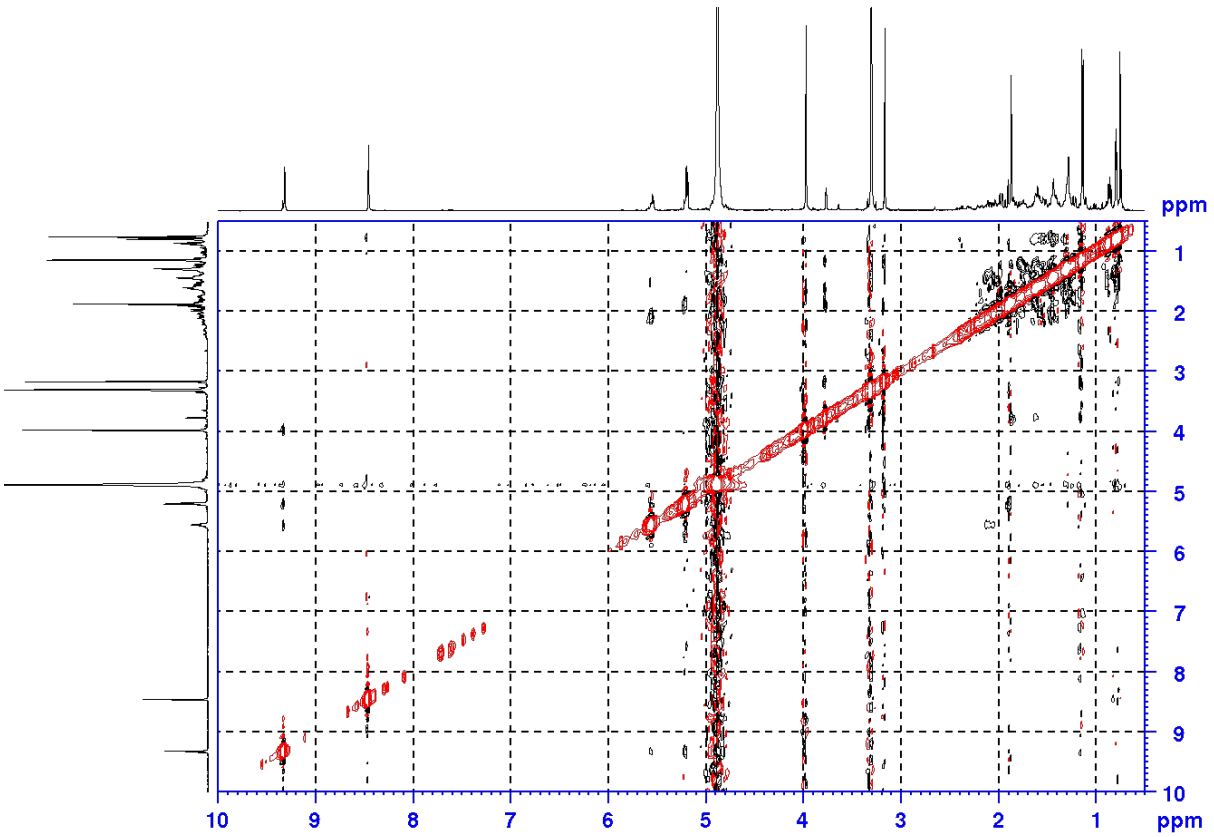

Figure S10. ROESY spectrum of agelamasine B (**2**) as a TFA salt form in CD_3OD (500 MHz).

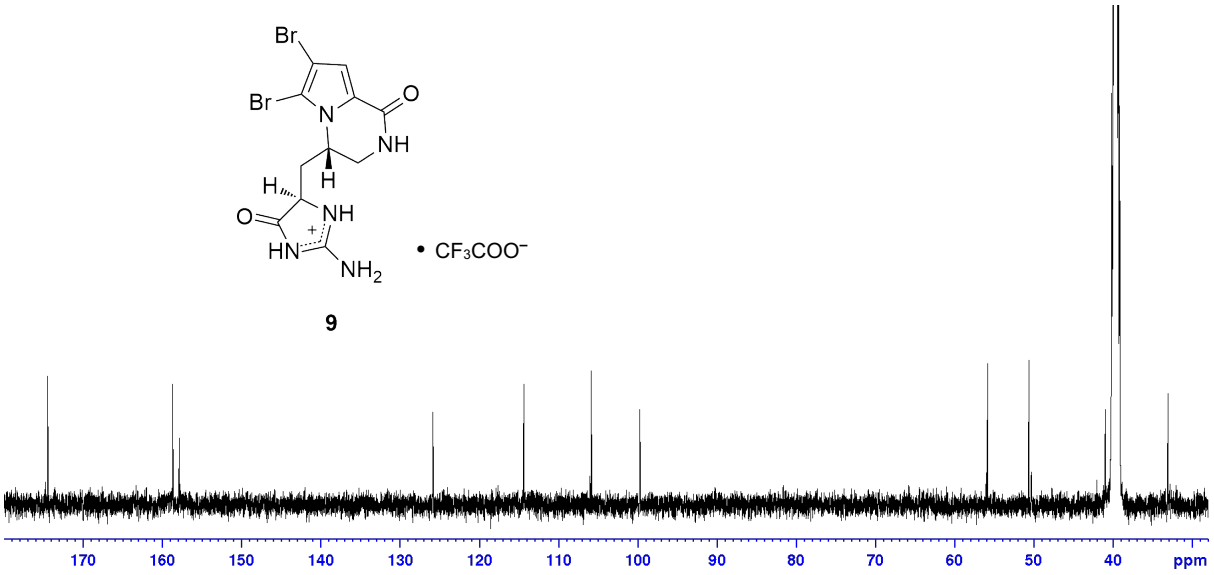

Figure S11. ^{13}C NMR spectrum of agesamide C (**9**) as a TFA salt form in DMSO-d_6 (125 MHz).

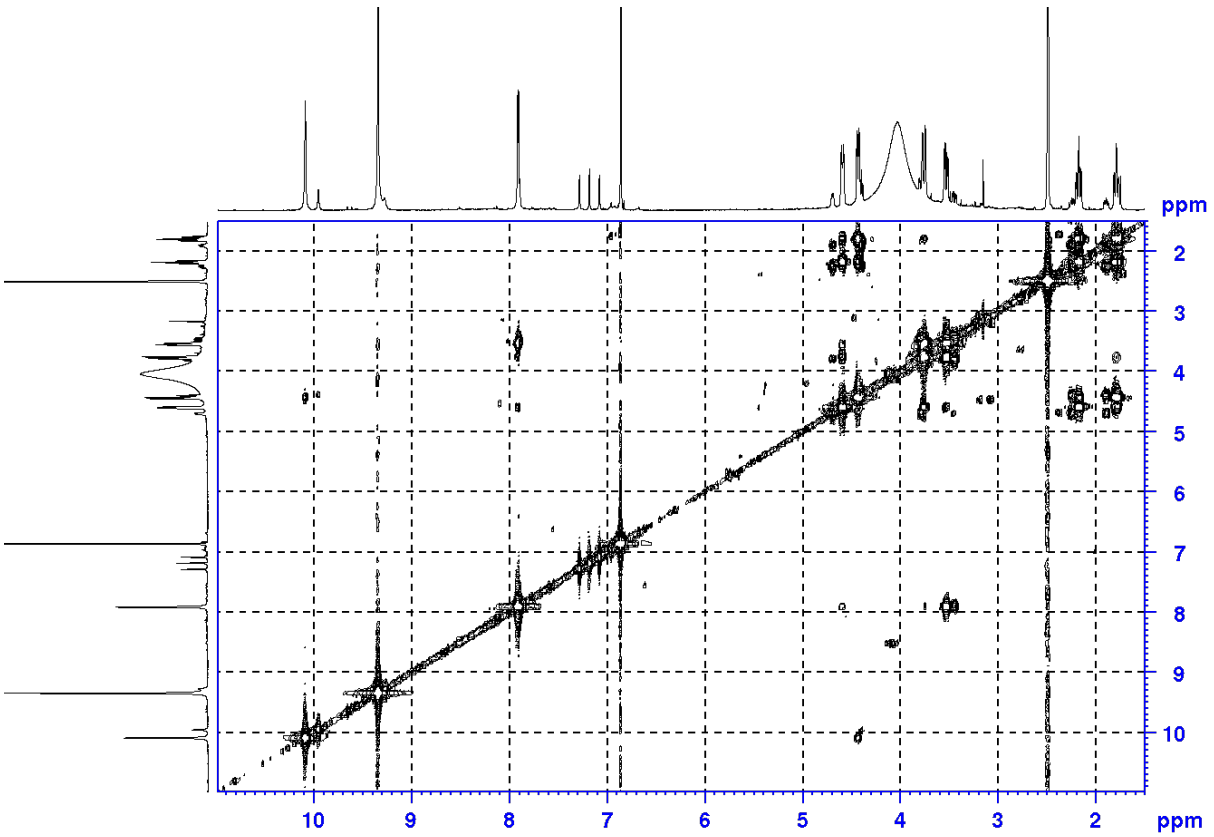

Figure S12. ^{1}H-^{1}H COSY spectrum of agesamide C (**9**) as a TFA salt form in DMSO-d_6 (500 MHz).

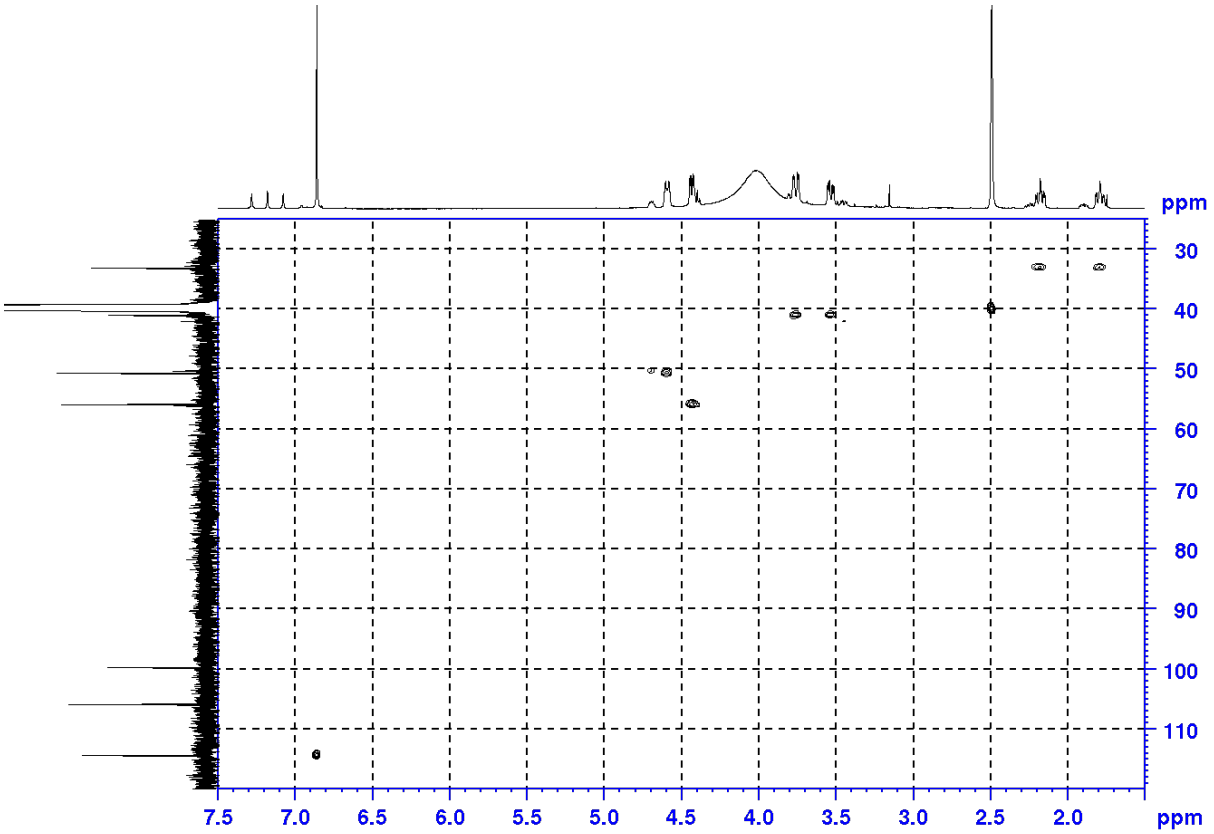

Figure S13. HSQC spectrum of agesamide C (**9**) as a TFA salt form in DMSO-d_6 (500 MHz).

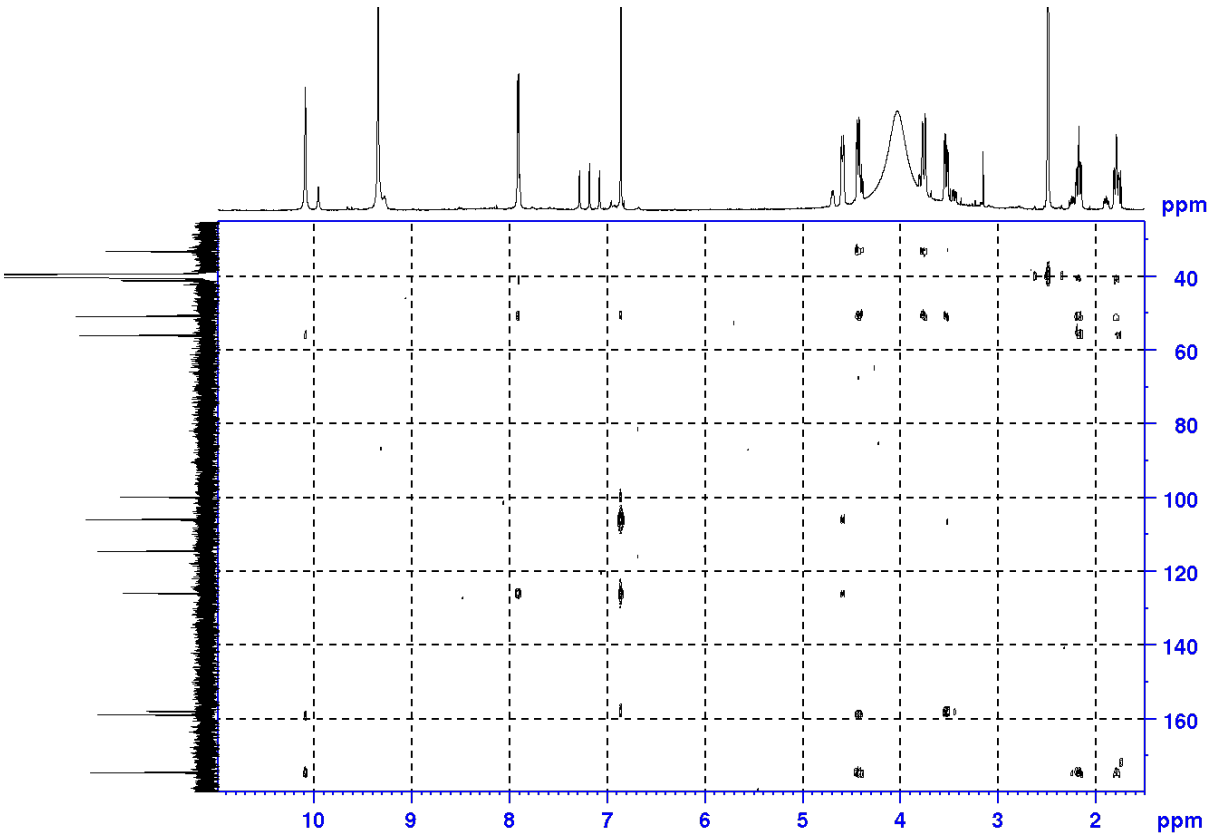

Figure S14. HMBC spectrum of agesamide C (**9**) as a TFA salt form in DMSO-d_6 (500 MHz).

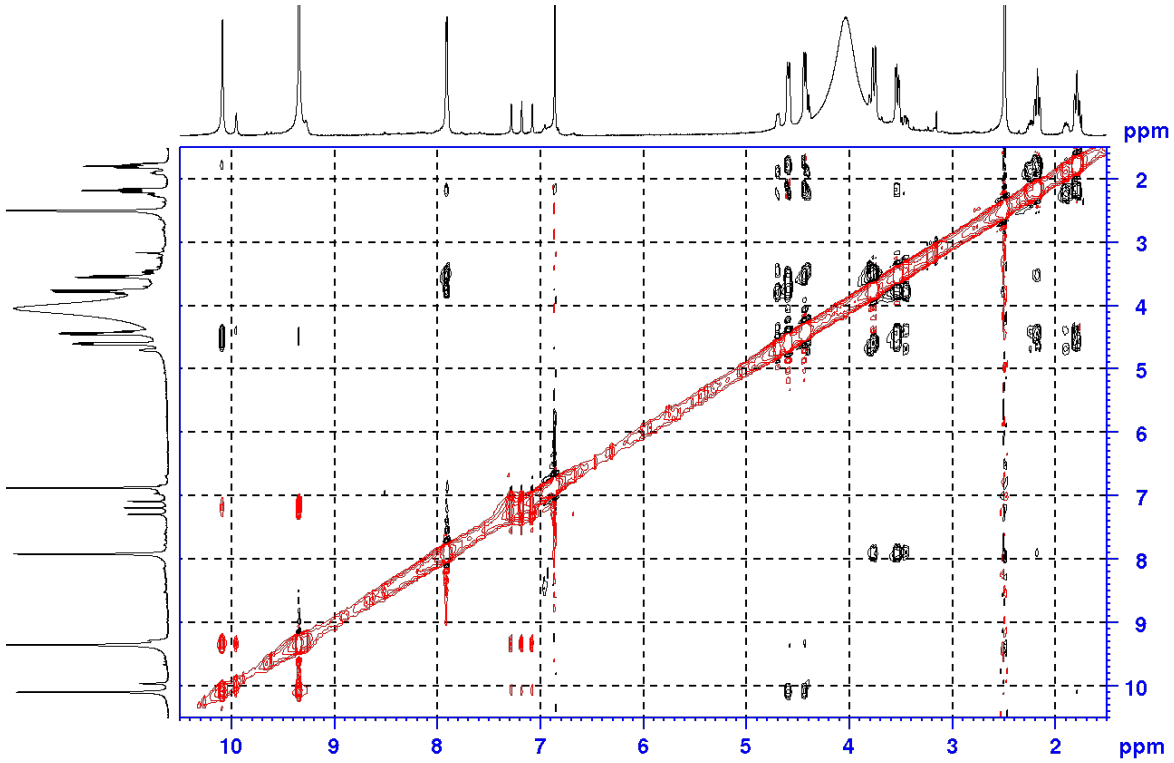

Figure S15. ROESY spectrum of agesamide C (**9**) as a TFA salt form in DMSO-d_6 (500 MHz).

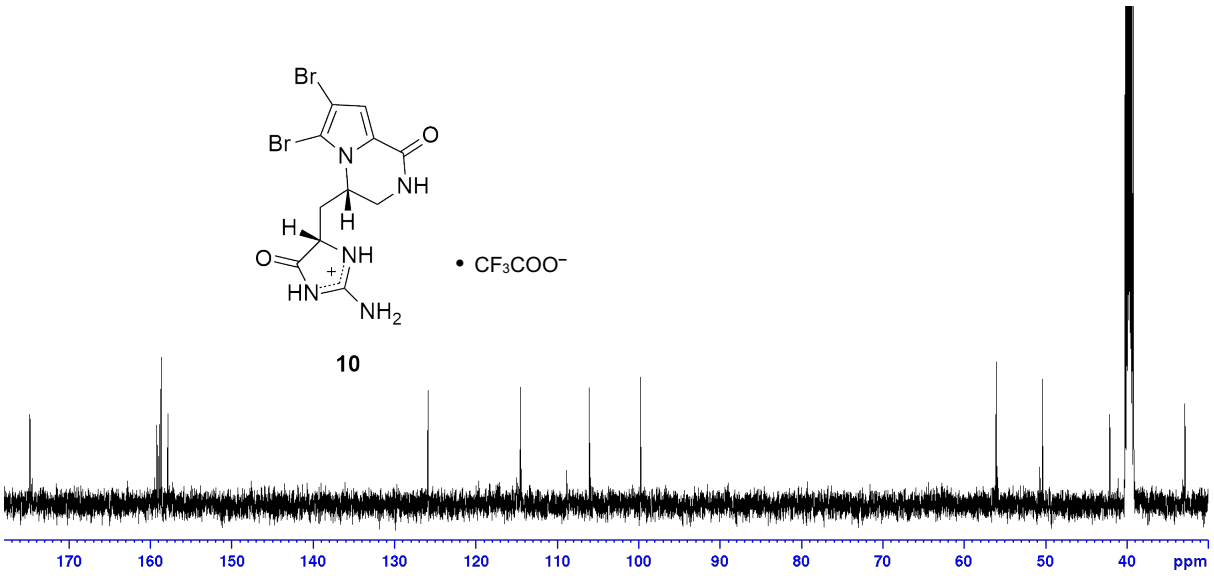

10

Figure S16. ^{13}C NMR spectrum of agesamide D (**10**) as a TFA salt form in DMSO-d_6 (125 MHz).

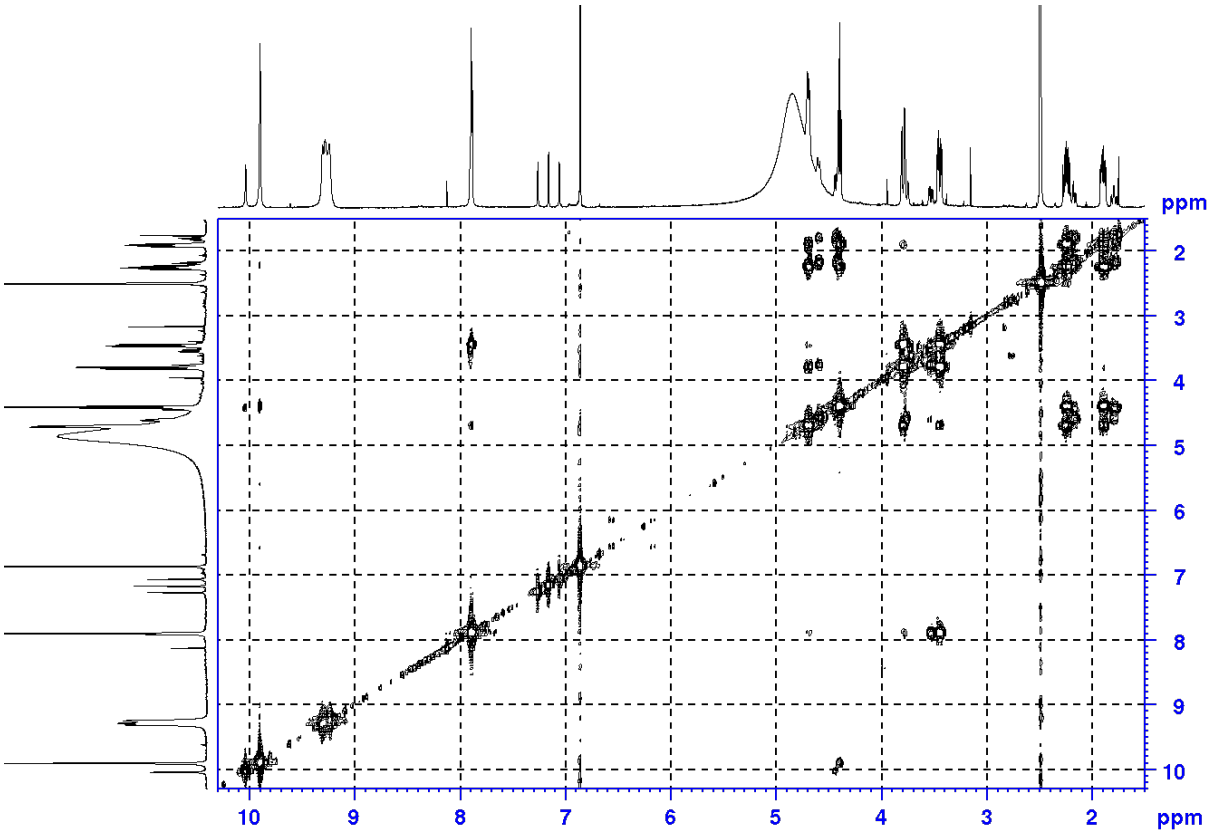

Figure S17. ^{1}H-^{1}H COSY spectrum of agesamide D (**10**) as a TFA salt form in DMSO-d_6 (500 MHz).

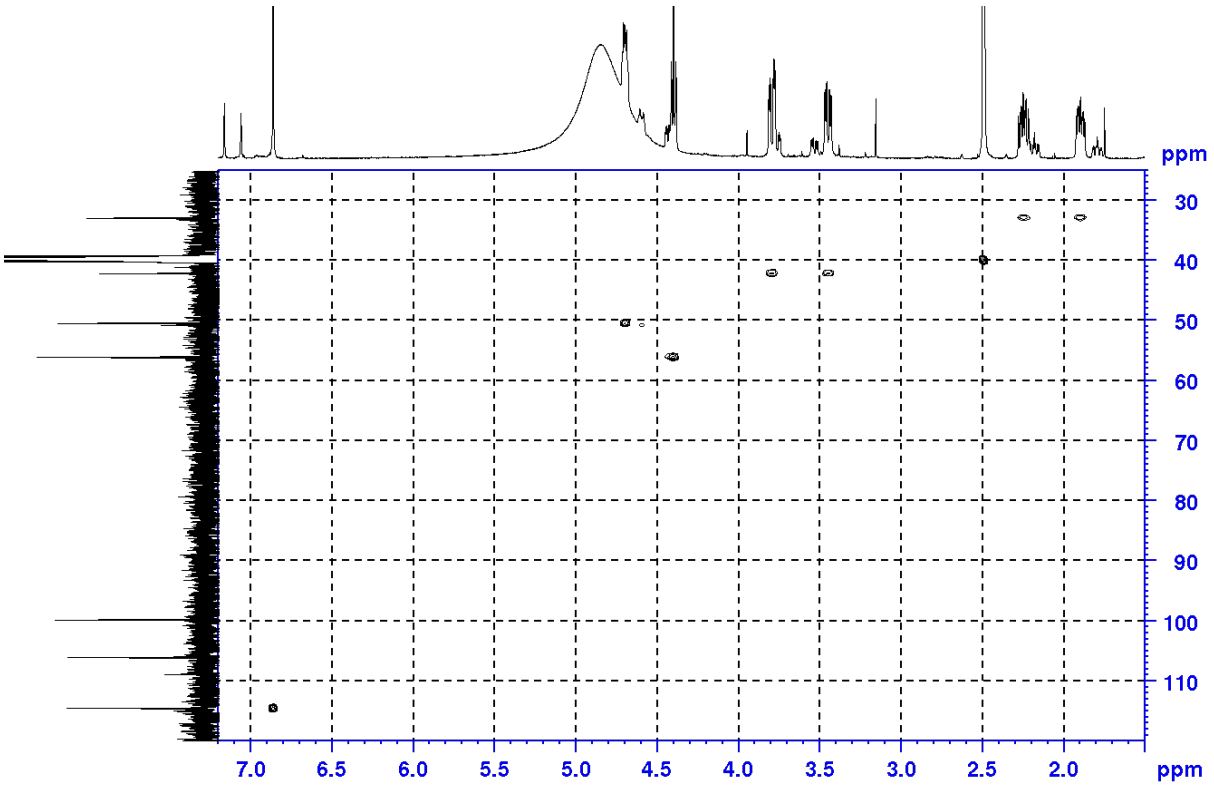

Figure S18. HSQC spectrum of agesamide D (**10**) as a TFA salt form in DMSO-d_6 (500 MHz).

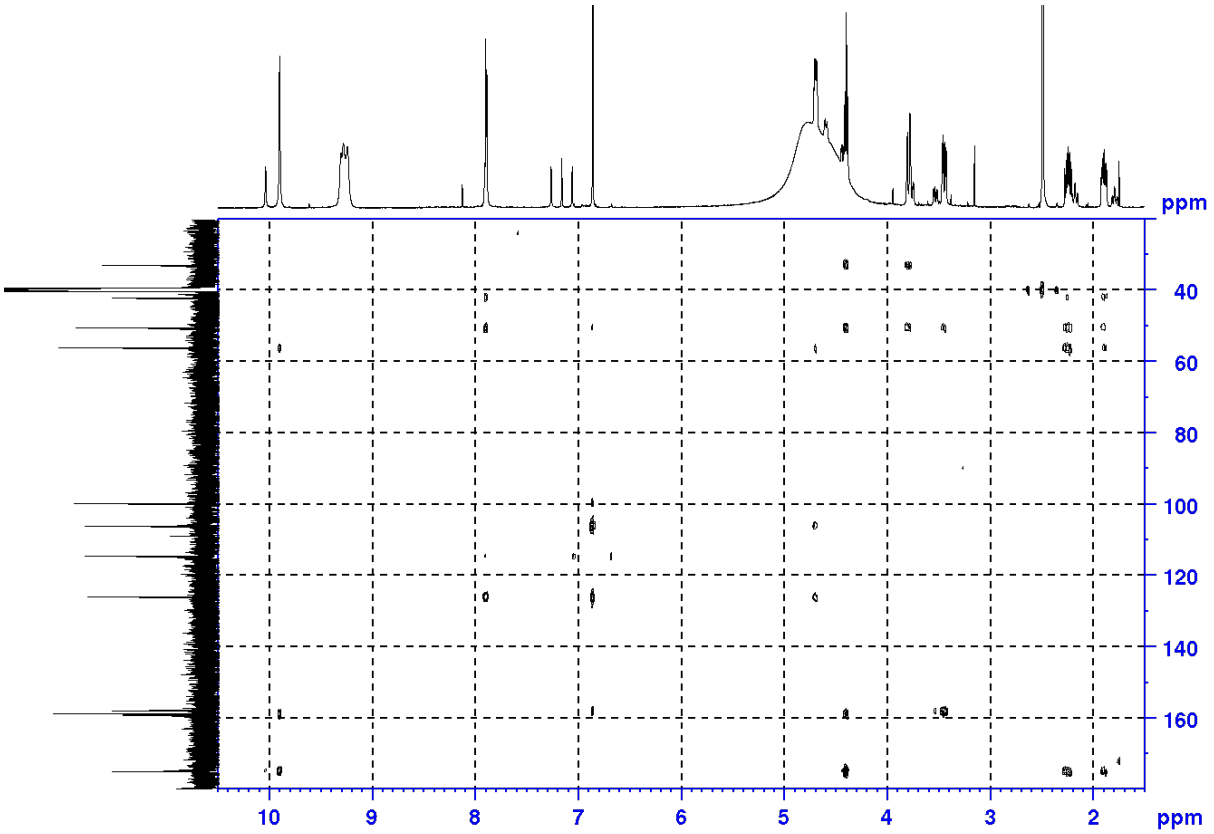

Figure S19. HMBC spectrum of agesamide D (**10**) as a TFA salt form in DMSO-d_6 (500 MHz).

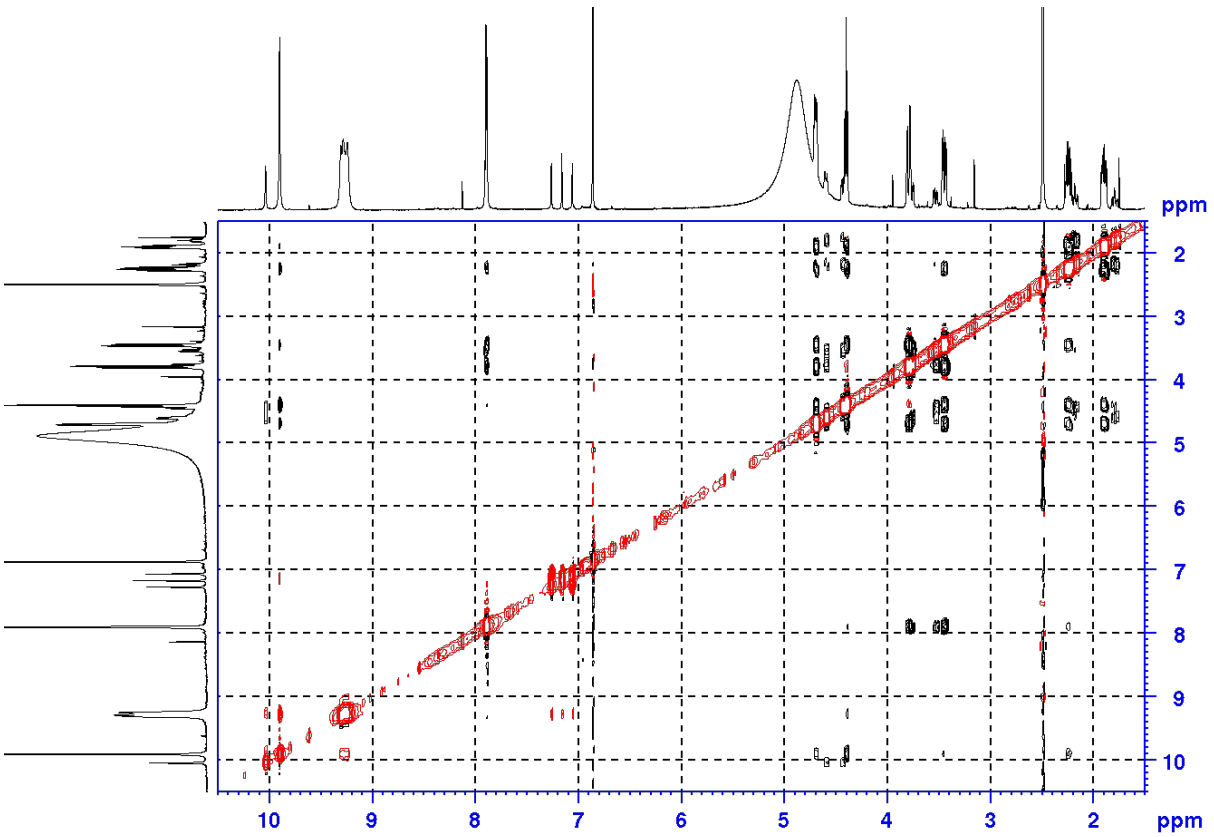

Figure S20. ROESY spectrum of agesamide D (**10**) as a TFA salt form in DMSO-d_6 (500 MHz).

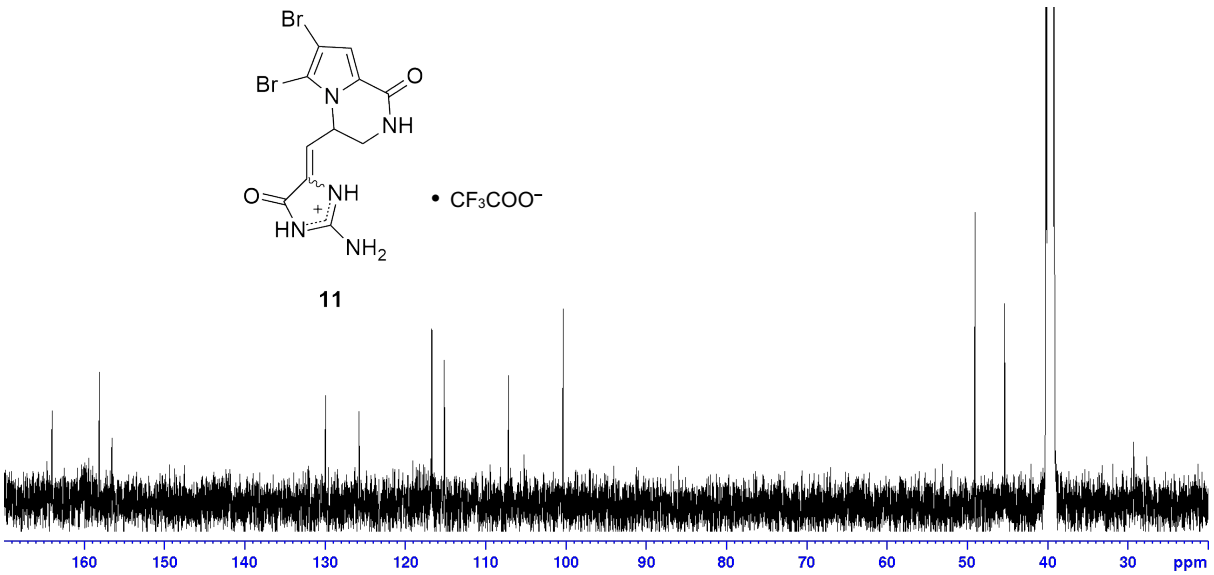

Figure S21. ^{13}C NMR spectrum of agesamide E (**11**) as a TFA salt form in DMSO-d_6 (125 MHz).

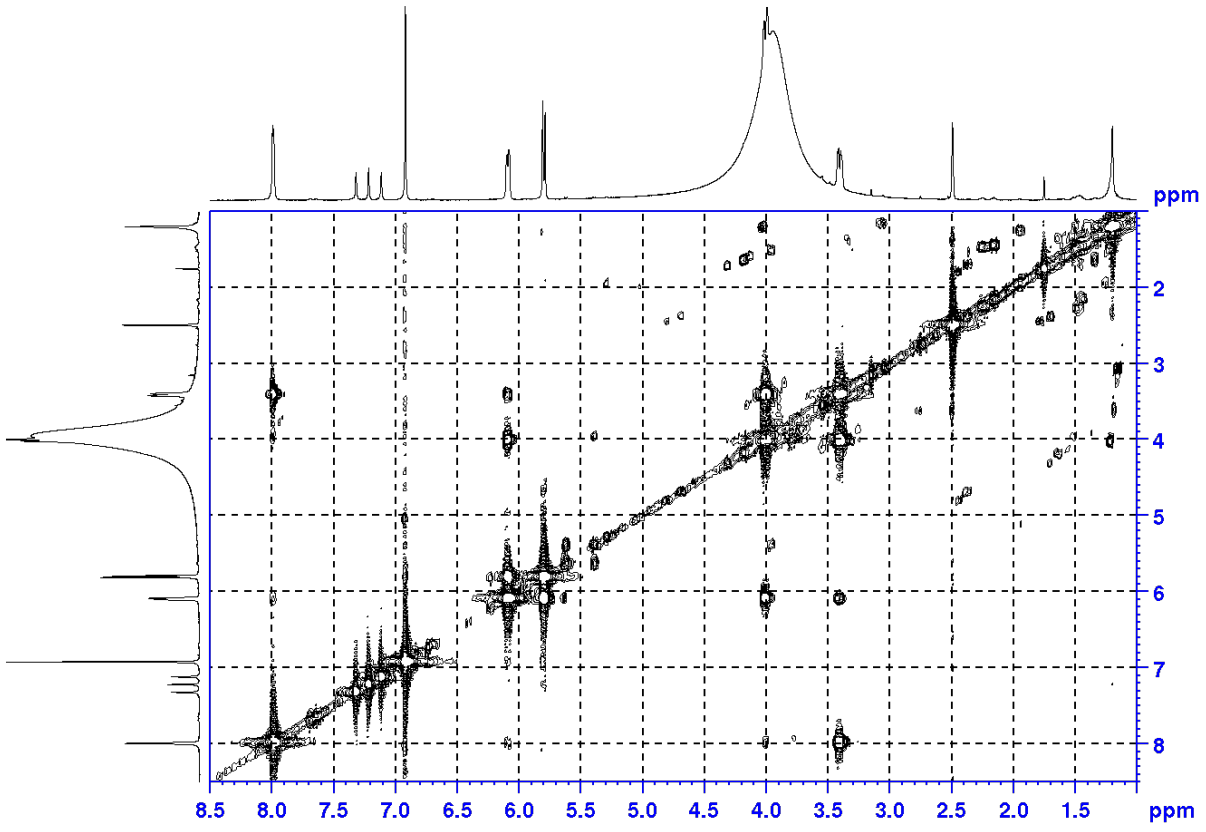

Figure S22. ^{1}H-^{1}H COSY spectrum of agesamide E (**11**) as a TFA salt form in DMSO-d_6 (500 MHz).

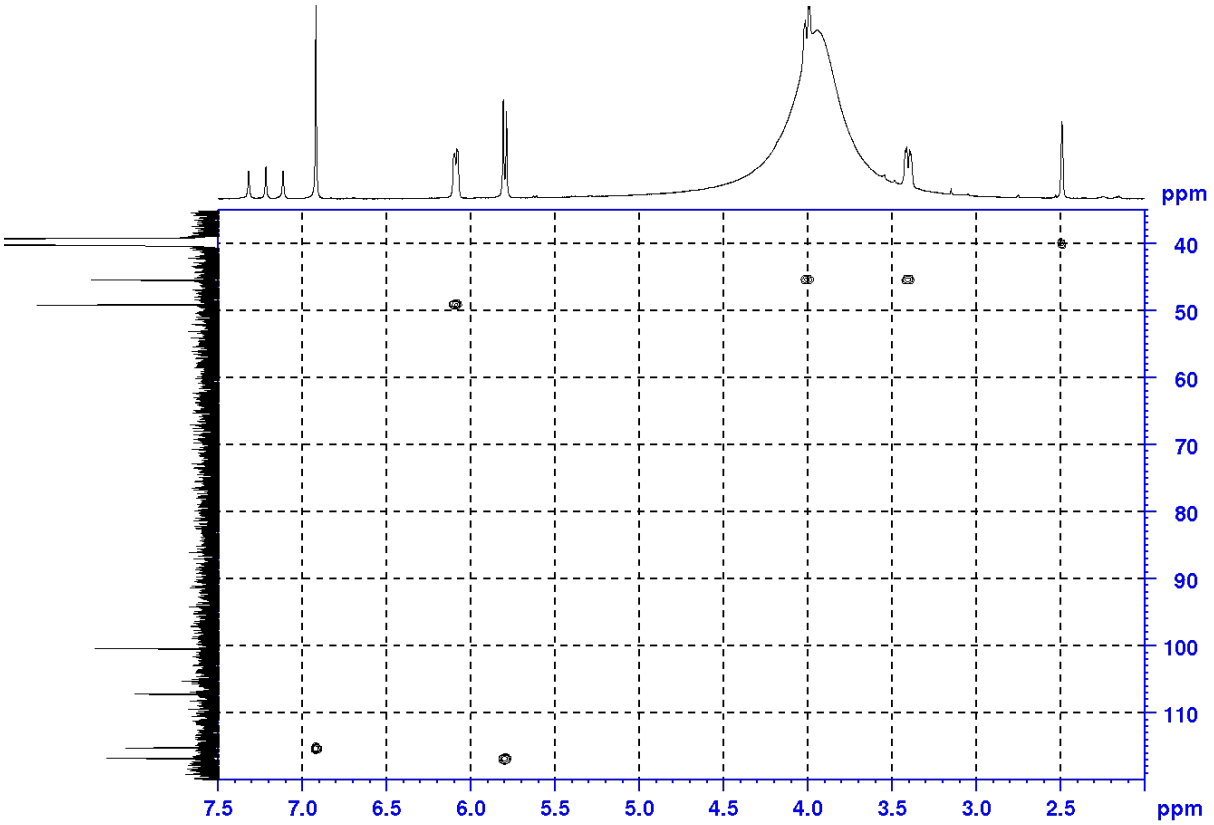

Figure S23. HSQC spectrum of agesamide E (**11**) as a TFA salt form in DMSO-d_6 (500 MHz).

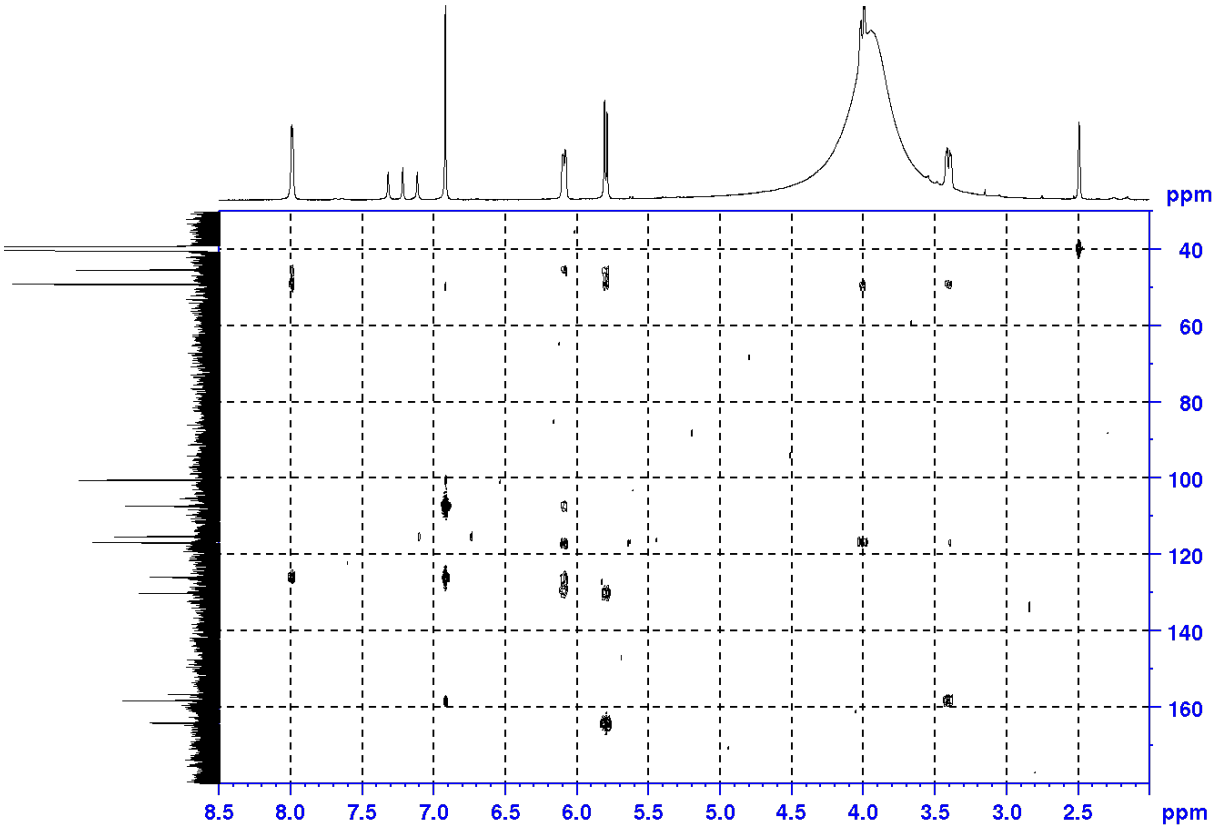

Figure S24. HMBC spectrum of agesamide E (**11**) as a TFA salt form in DMSO-d_6 (500 MHz).

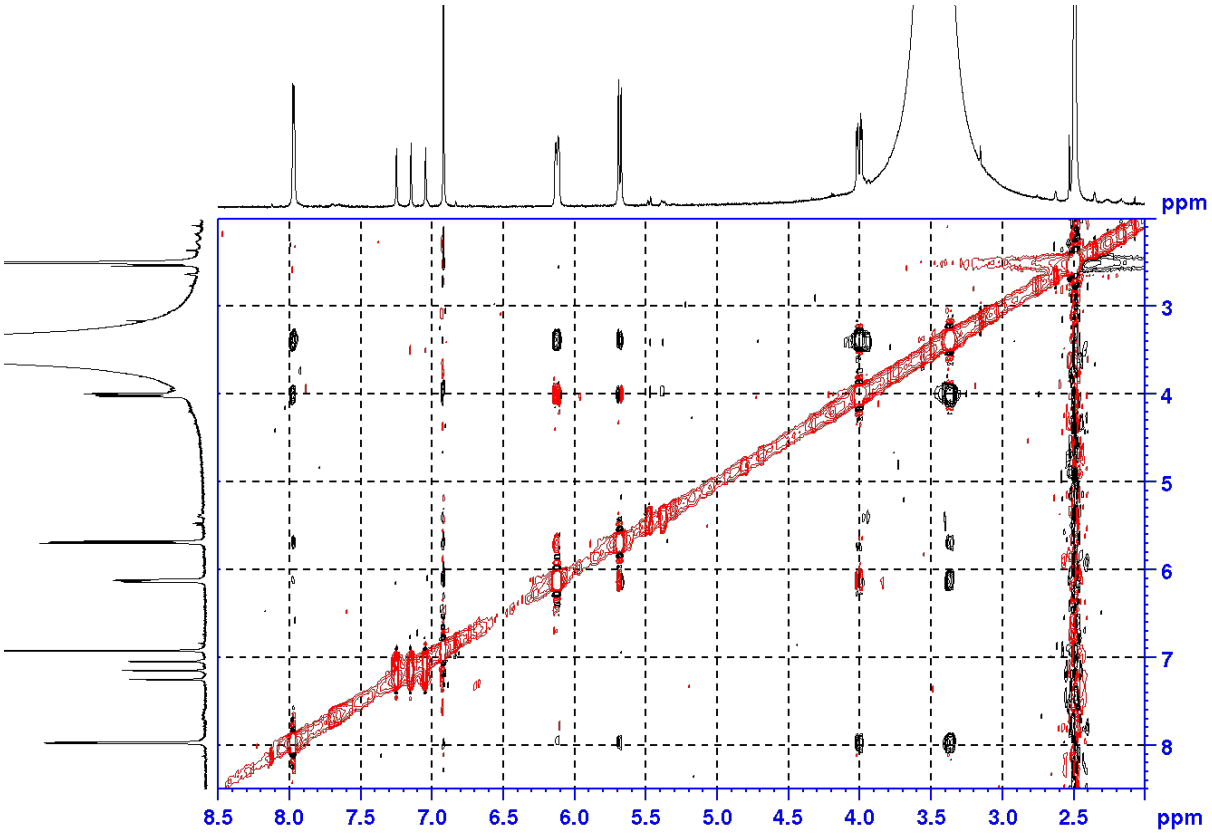

Figure S25. ROESY spectrum of agesamide E (**11**) as a TFA salt form in DMSO-d_6 (500 MHz).

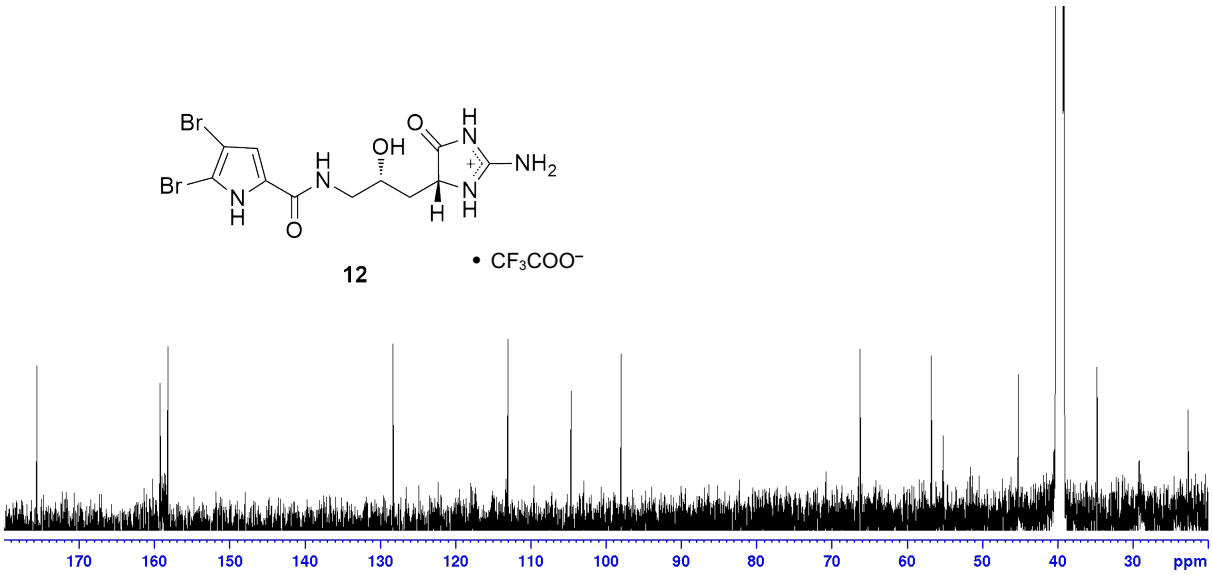

12

Figure S26. ^{13}C NMR spectrum of 9-hydroxydihydrodispacamide (**12**) as a TFA salt form in DMSO-d_6 (125 MHz).

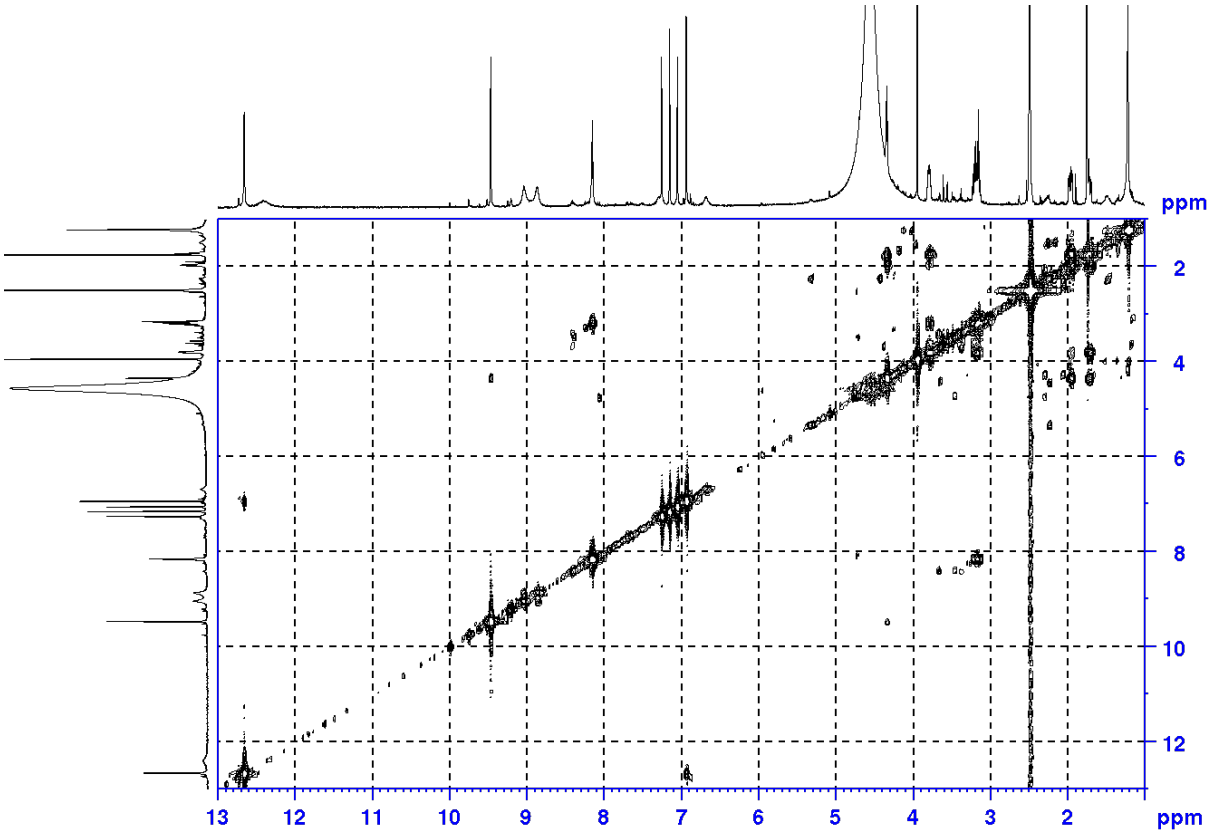

Figure S27. ^{1}H-^{1}H COSY spectrum of 9-hydroxydihydrodispacamide (**12**) as a TFA salt form in DMSO-d_6 (500 MHz).

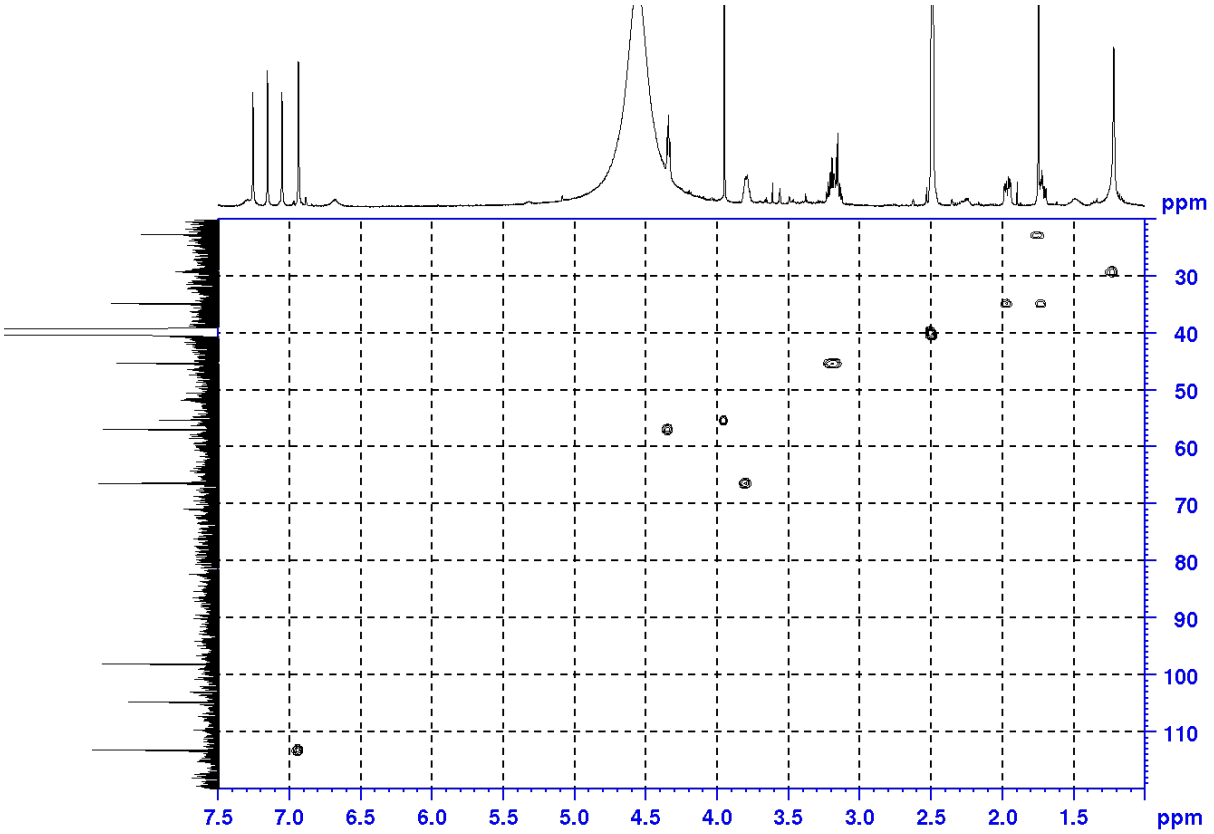

Figure S28. HSQC spectrum of 9-hydroxydihydrodispacamide (**12**) as a TFA salt form in DMSO-d_6 (500 MHz).

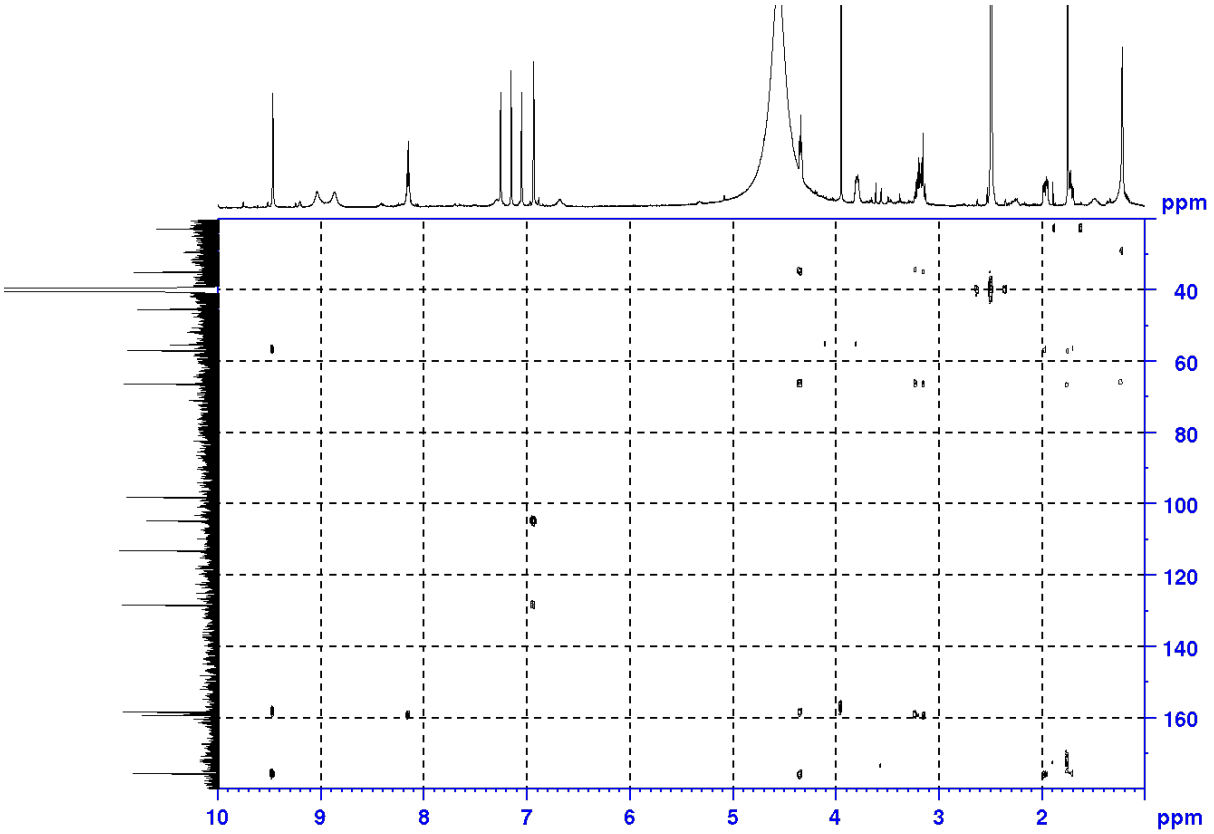

Figure S29. HMBC spectrum of 9-hydroxydihydrodispacamide (**12**) as a TFA salt form in DMSO-d_6 (500 MHz).

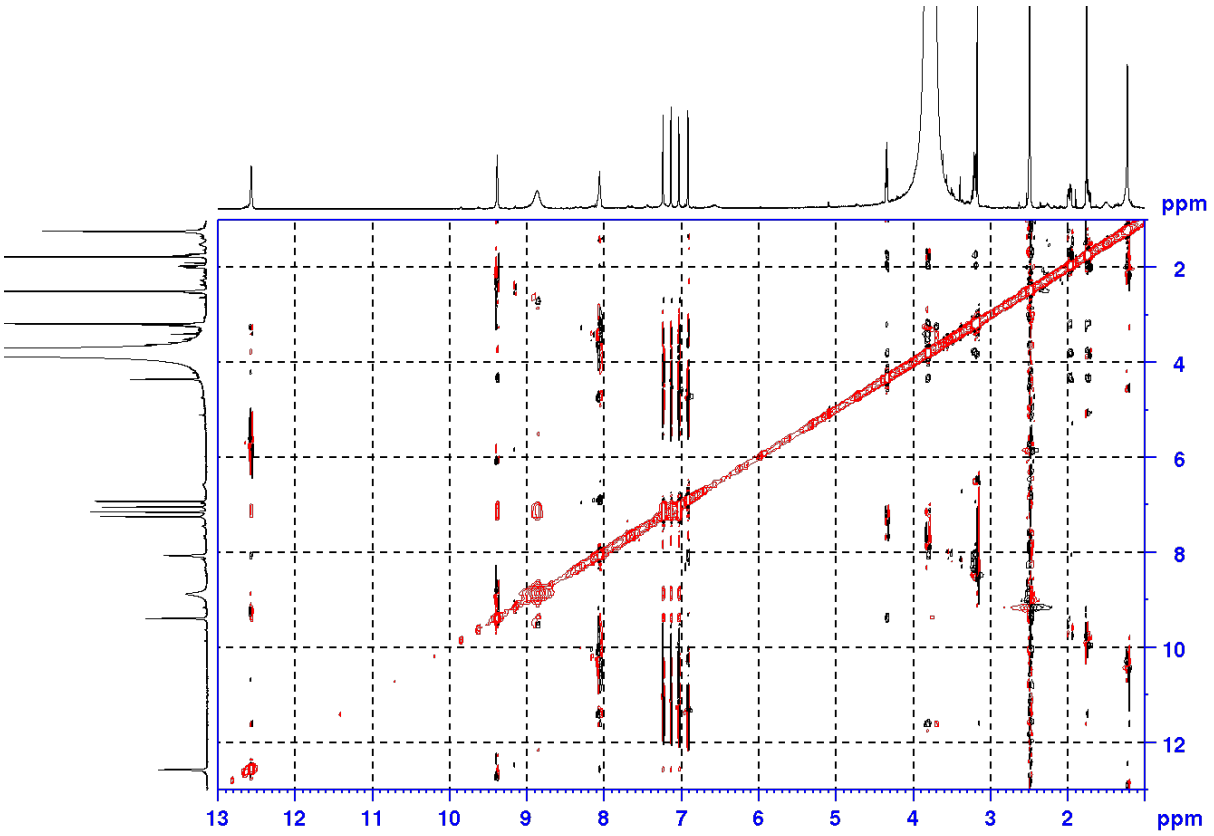

Figure S30. ROESY spectrum of 9-hydroxydihydrodispacamide (**12**) as a TFA salt form in DMSO-d_6 (500 MHz).

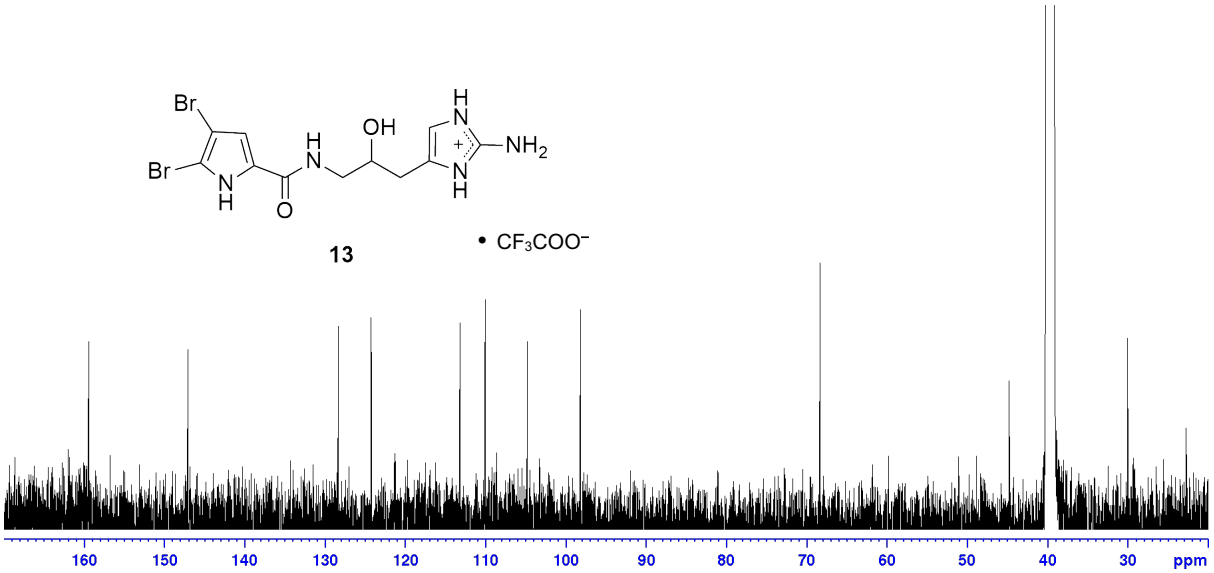

Figure S31. ^{13}C NMR spectrum of 9-hydroxydihydrooroidin (**13**) as a TFA salt form in DMSO-d_6 (125 MHz).

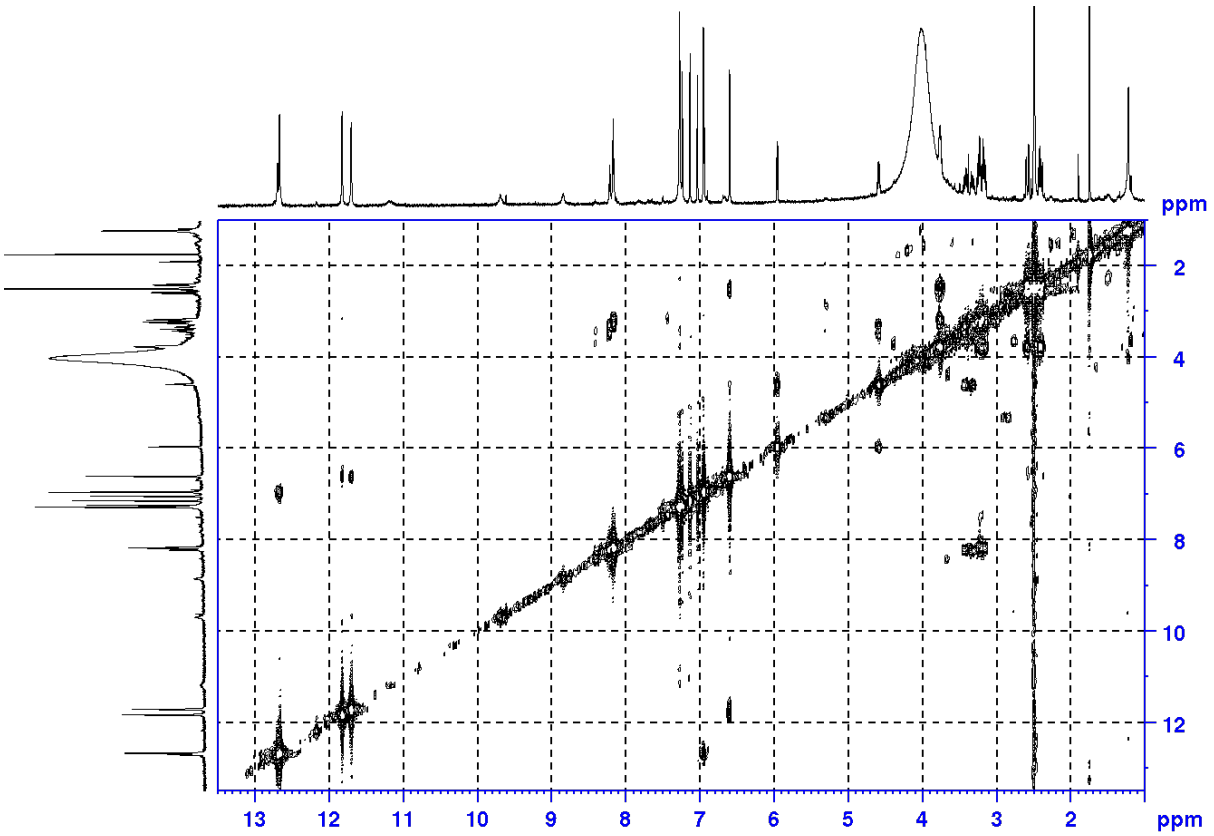

Figure S32. ^{1}H-^{1}H COSY spectrum of 9-hydroxydihydrooroidin (**13**) as a TFA salt form in DMSO-d_6 (500 MHz).

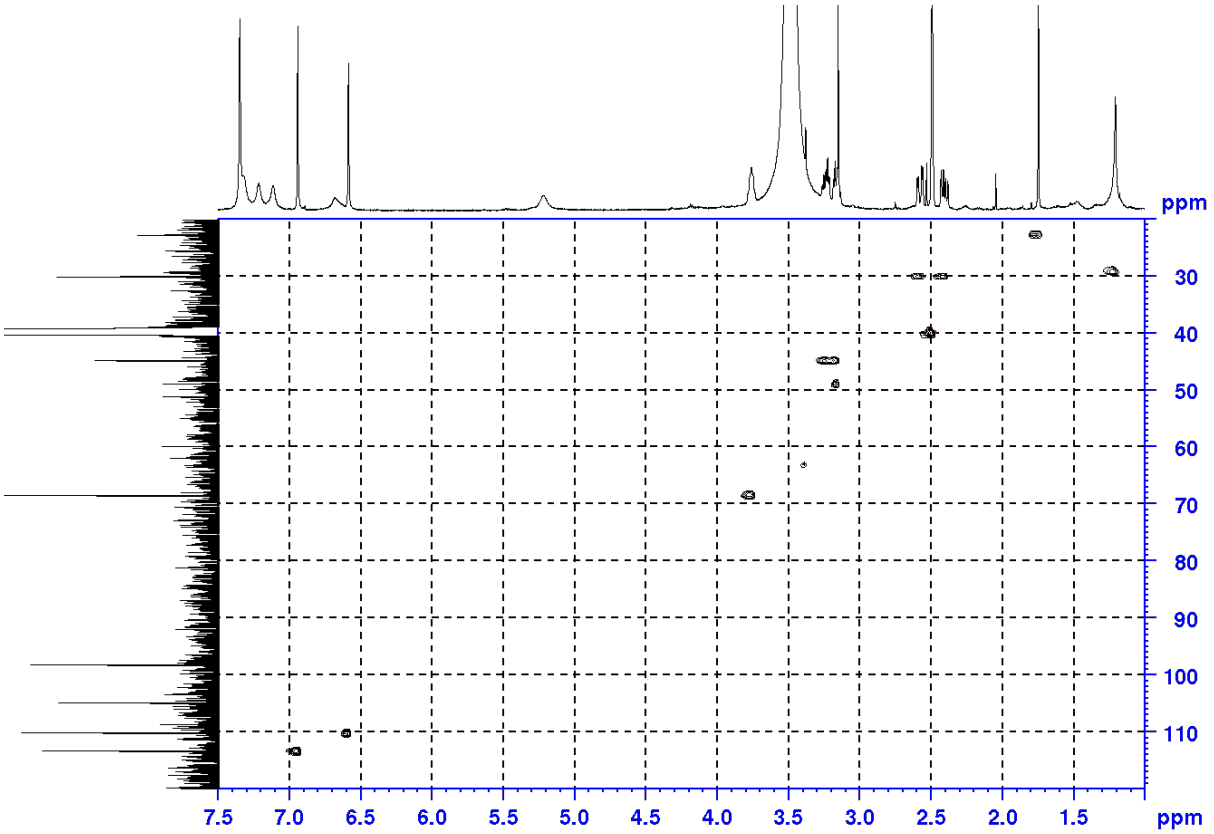

Figure S33. HSQC spectrum of 9-hydroxydihydrooroidin (**13**) as a TFA salt form in DMSO-d_6 (500 MHz).

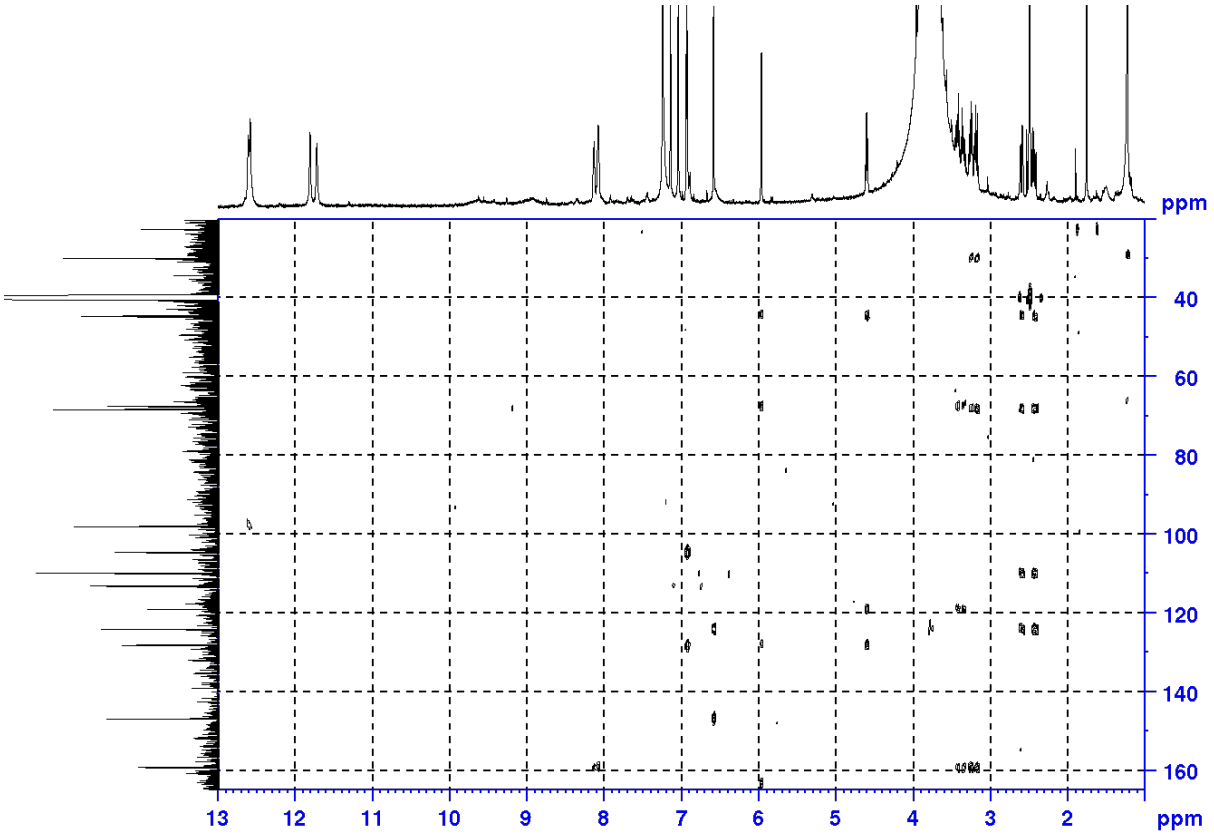

Figure S34. HMBC spectrum of 9-hydroxydihydrooroidin (**13**) as a TFA salt form in DMSO-d_6 (500 MHz).

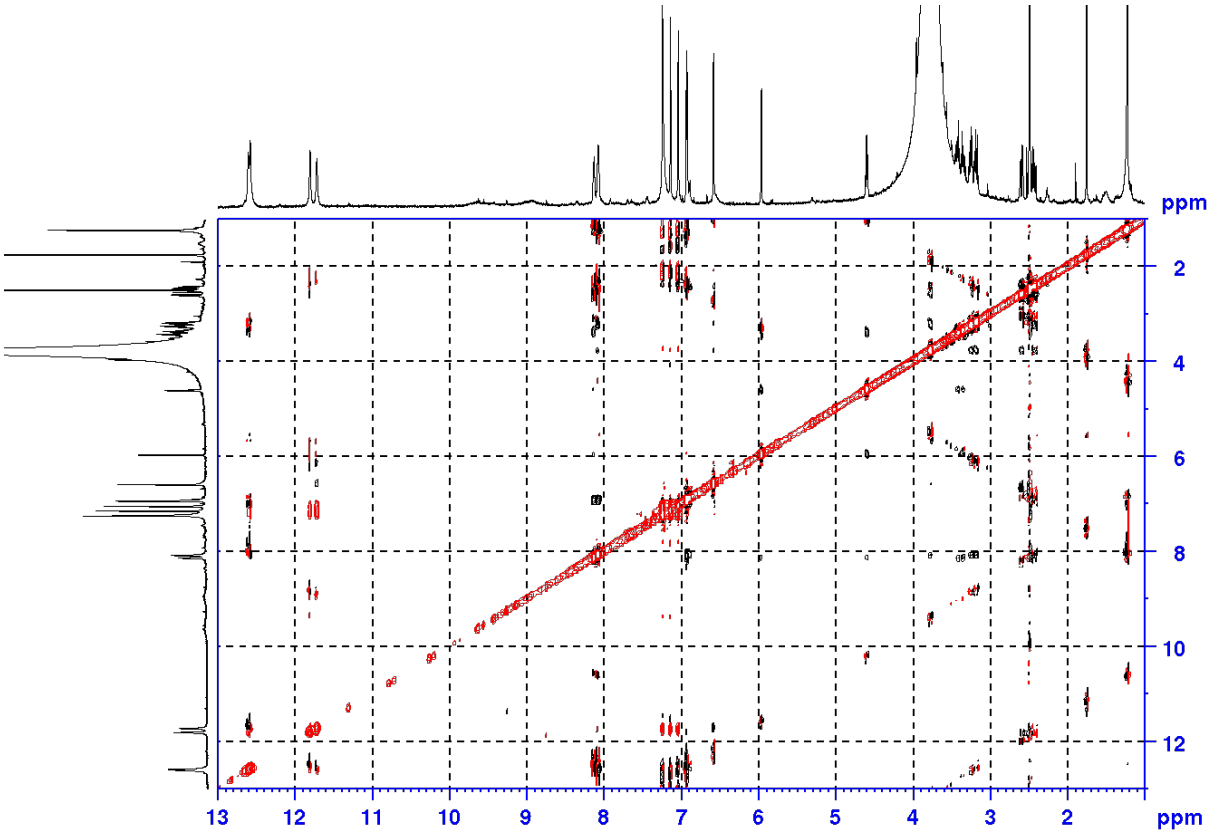

Figure S35. ROESY spectrum of 9-hydroxydihydrooroidin (**13**) as a TFA salt form in DMSO-d_6 (500 MHz).

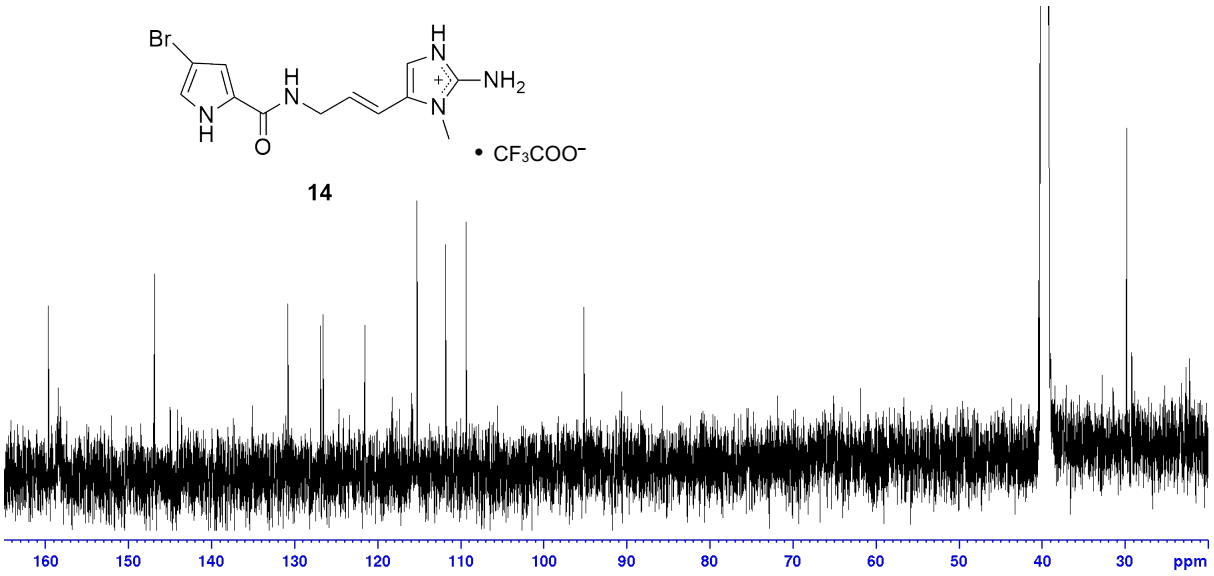

14

Figure S36. ^{13}C NMR spectrum of 9-(*E*)-keramadine (**14**) as a TFA salt form in DMSO-d_6 (125 MHz).

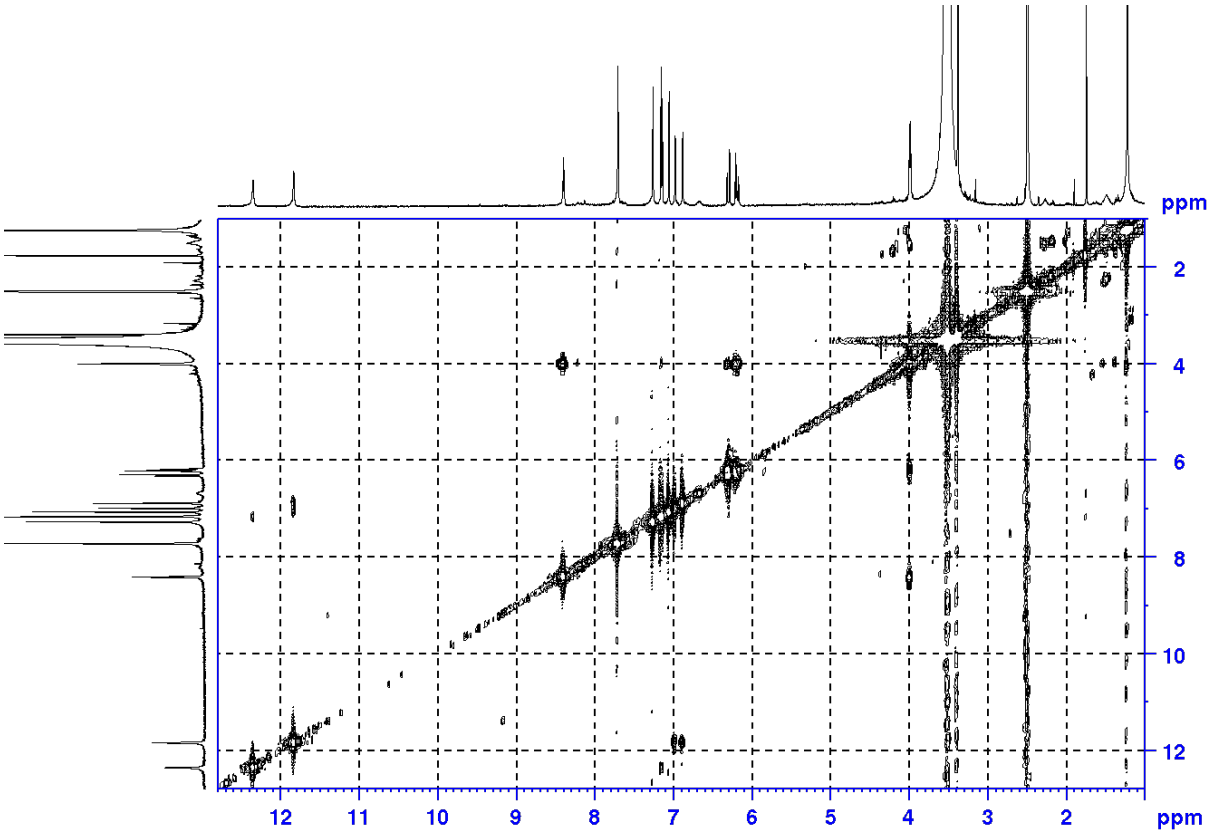

Figure S37. ^{1}H-^{1}H COSY spectrum of 9-(*E*)-keramadine (**14**) as a TFA salt form in DMSO-d_6 (500 MHz).

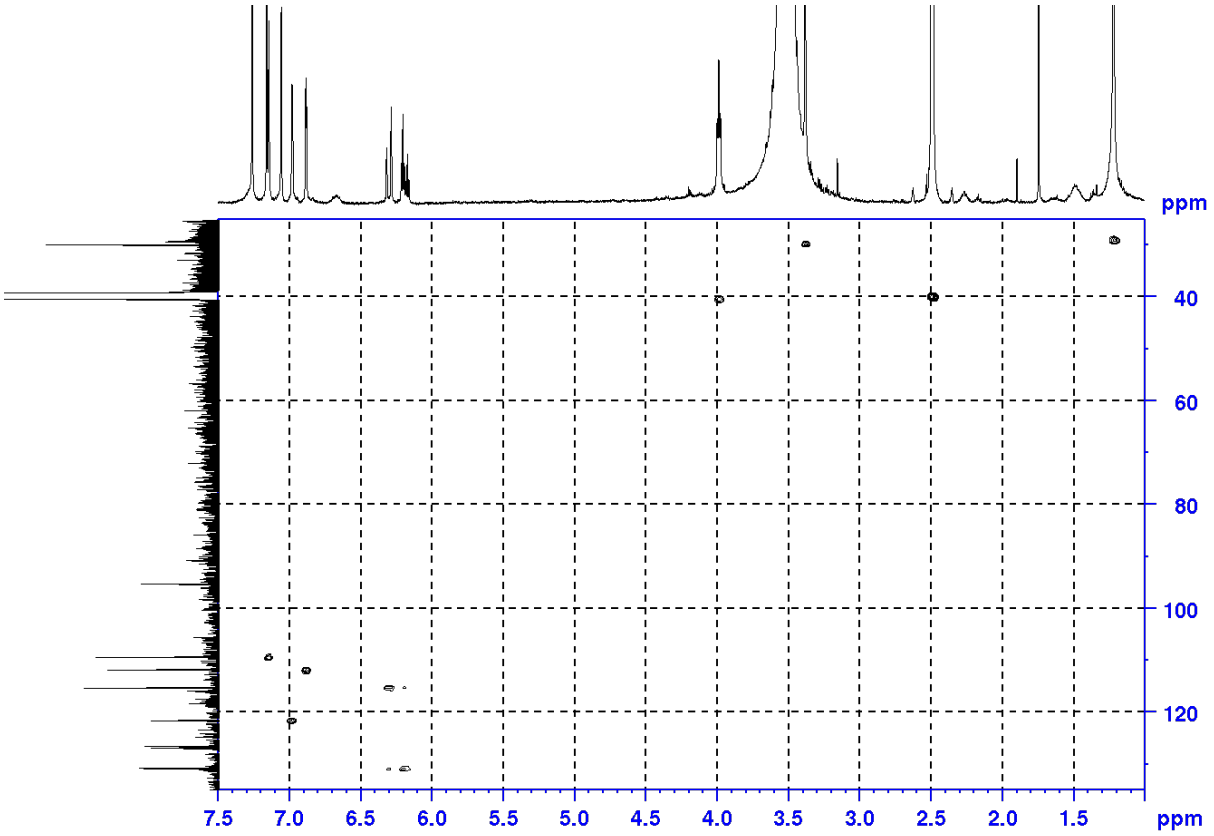

Figure S38. HSQC spectrum of 9-(*E*)-keramadine (**14**) as a TFA salt form in DMSO-d_6 (500 MHz).

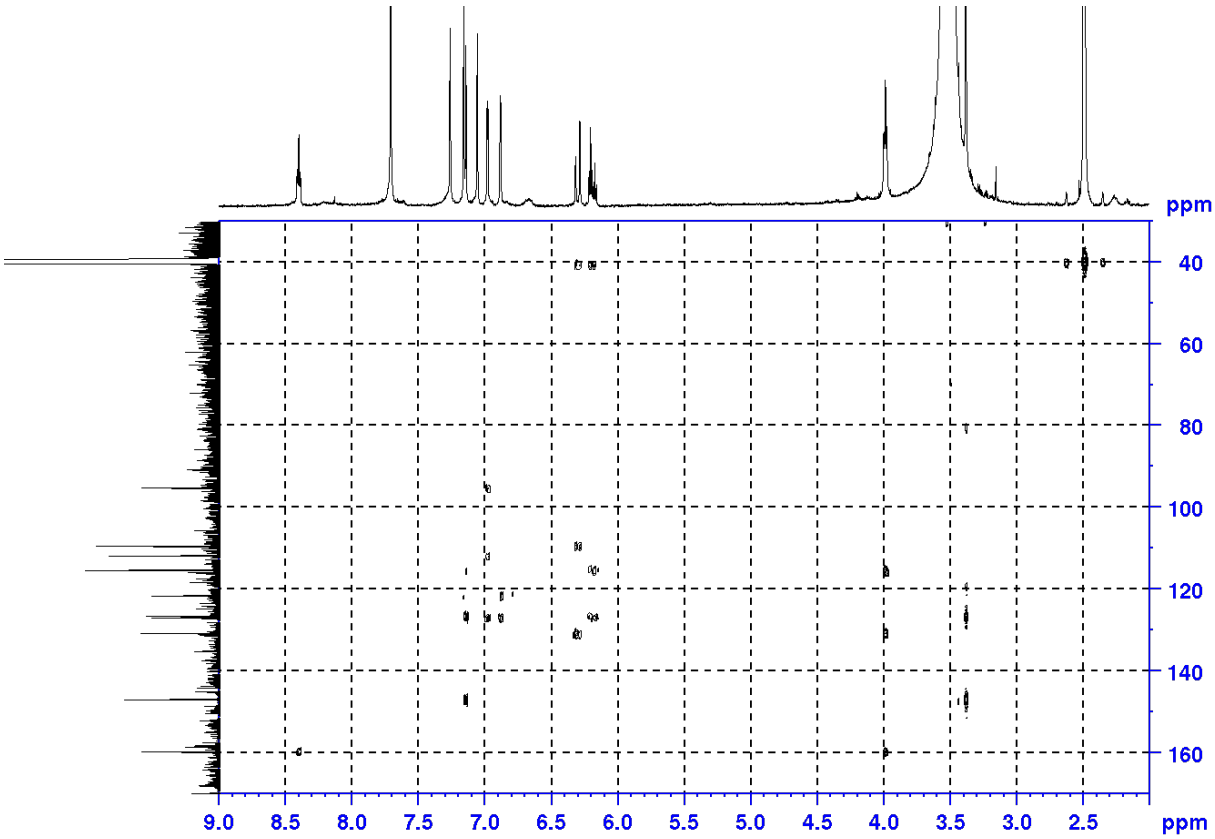

Figure S39. HMBC spectrum of 9-(*E*)-keramadine (**14**) as a TFA salt form in DMSO-d_6 (500 MHz).

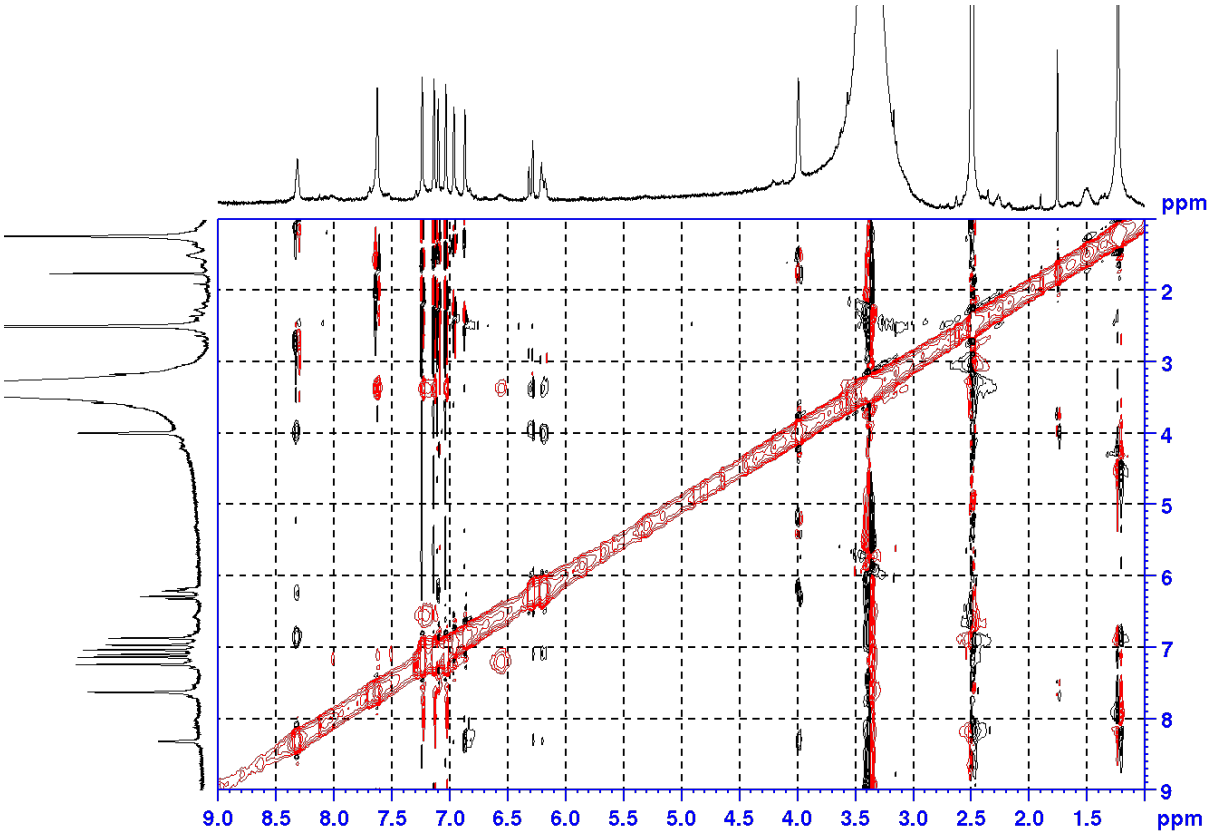

Figure S40. ROESY spectrum of 9-(*E*)-keramadine (**14**) as a TFA salt form in DMSO-d_6 (500 MHz).

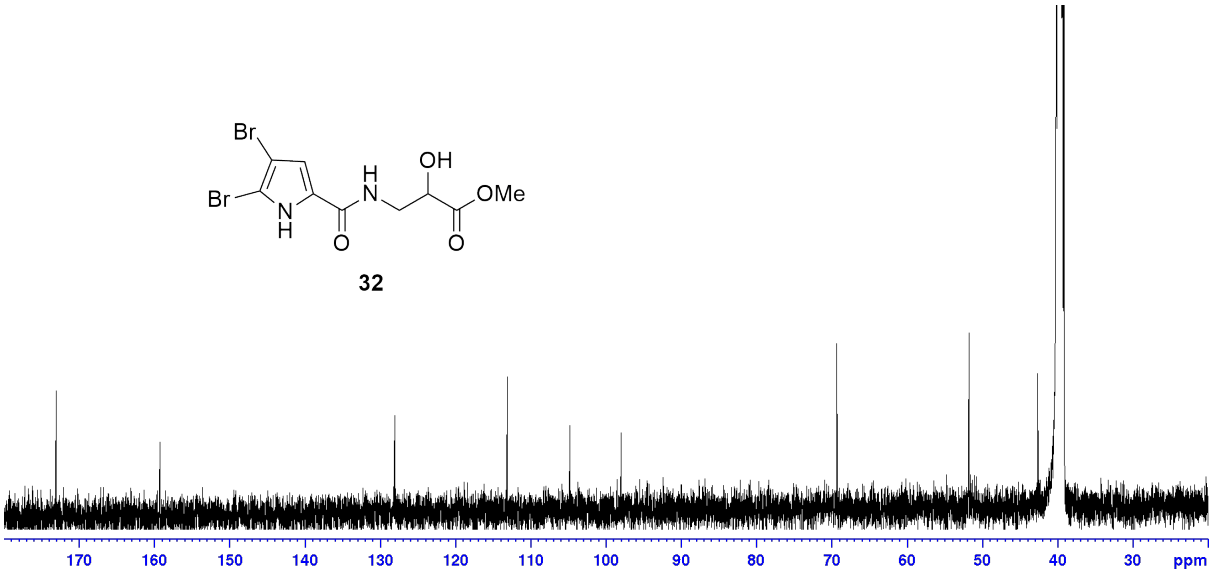

Figure S41. ^{13}C NMR spectrum of agesasine A (**32**) in DMSO-d_6 (125 MHz).

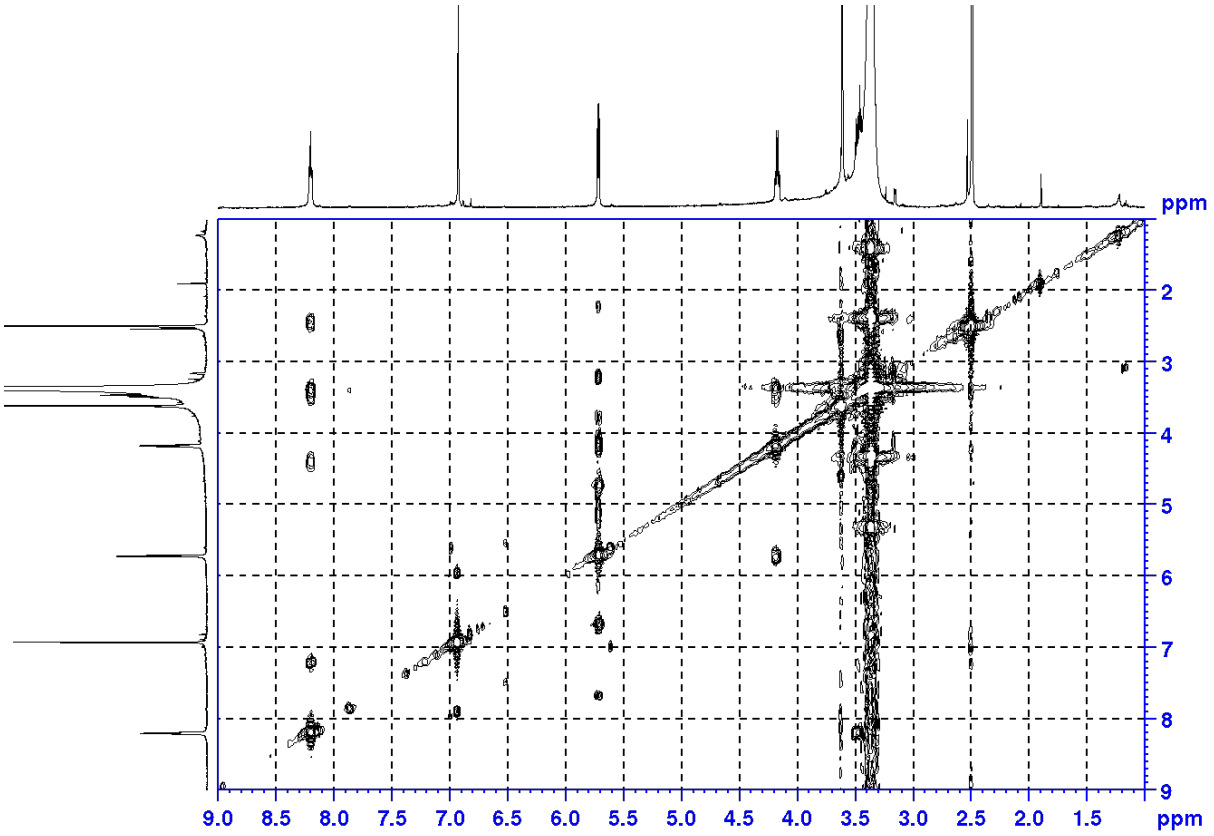

Figure S42. ^{1}H-^{1}H COSY spectrum of agesasine A (**32**) in DMSO-d_6 (500 MHz).

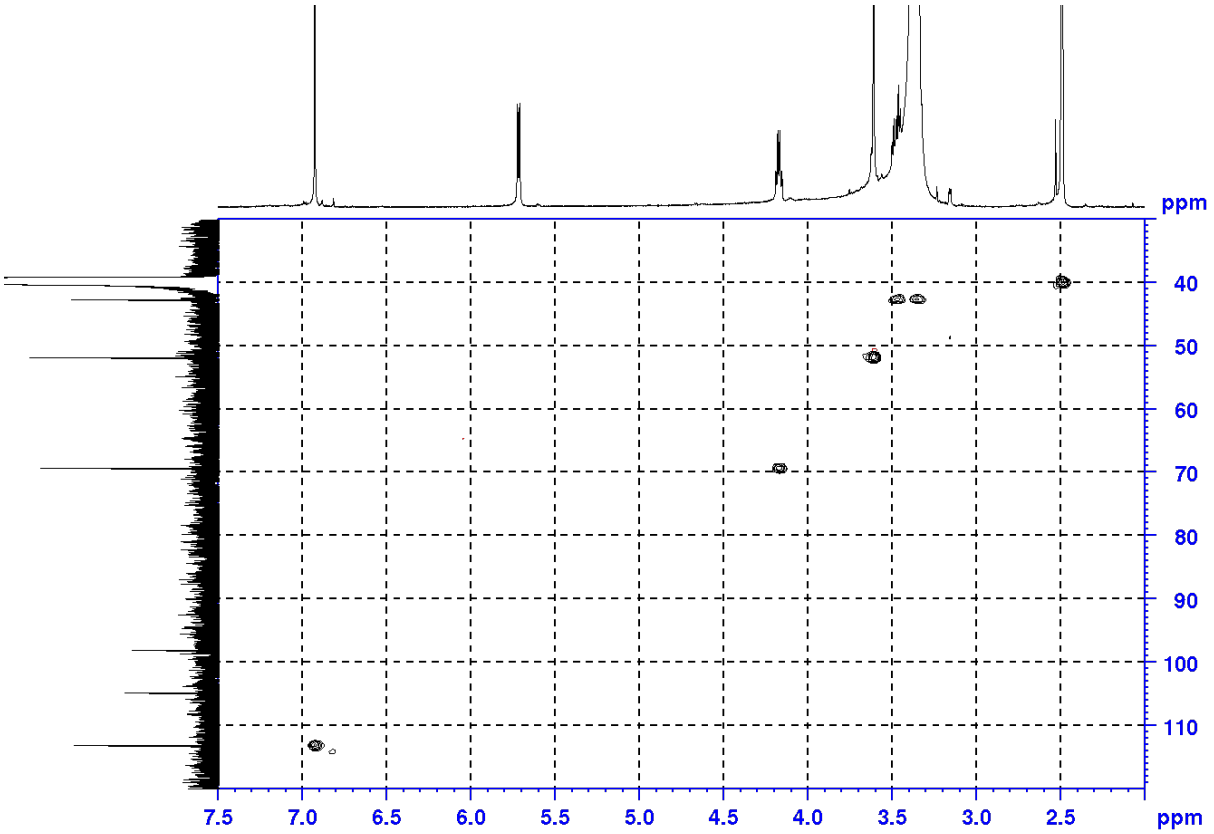

Figure S43. HSQC spectrum of agesasine A (**32**) in DMSO-d_6 (500 MHz).

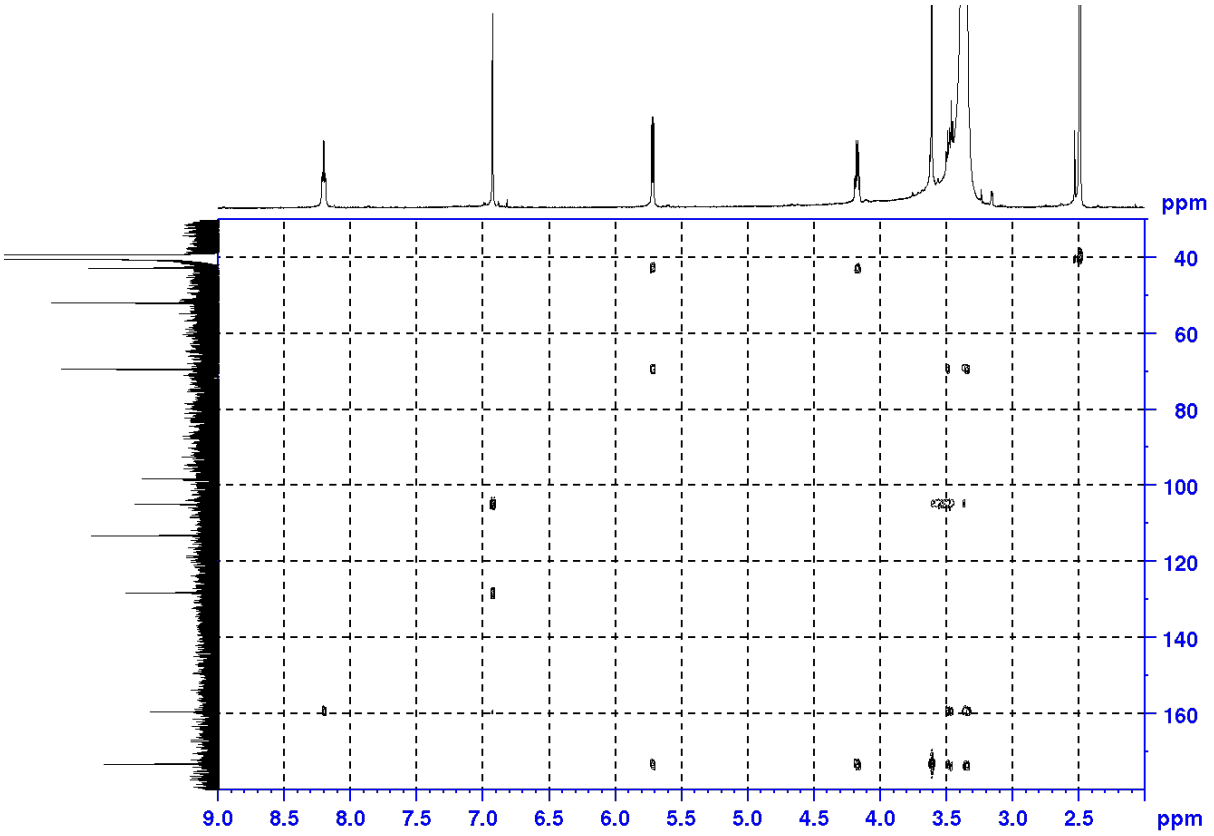

Figure S44. HMBC spectrum of agesasine A (**32**) in DMSO-d_6 (500 MHz).

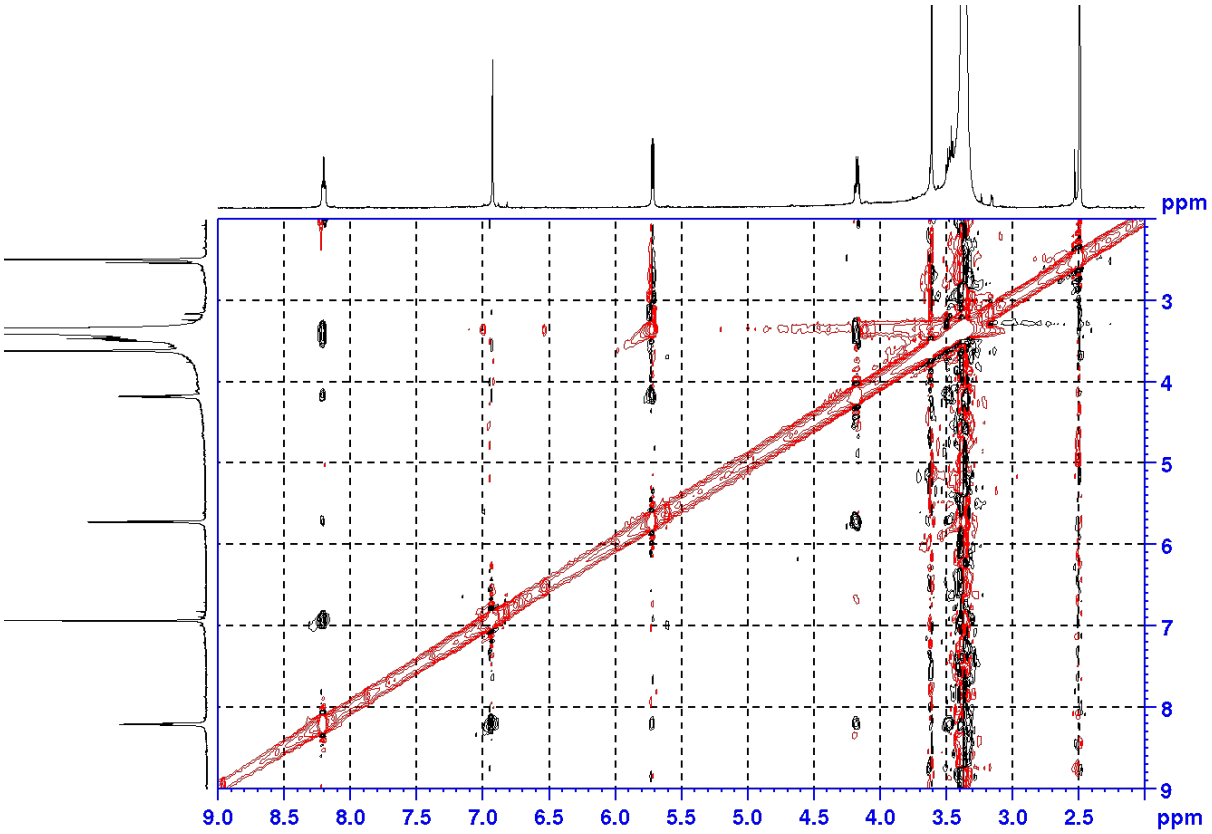

Figure S45. ROESY spectrum of agesasine A (**32**) in DMSO-d_6 (500 MHz).

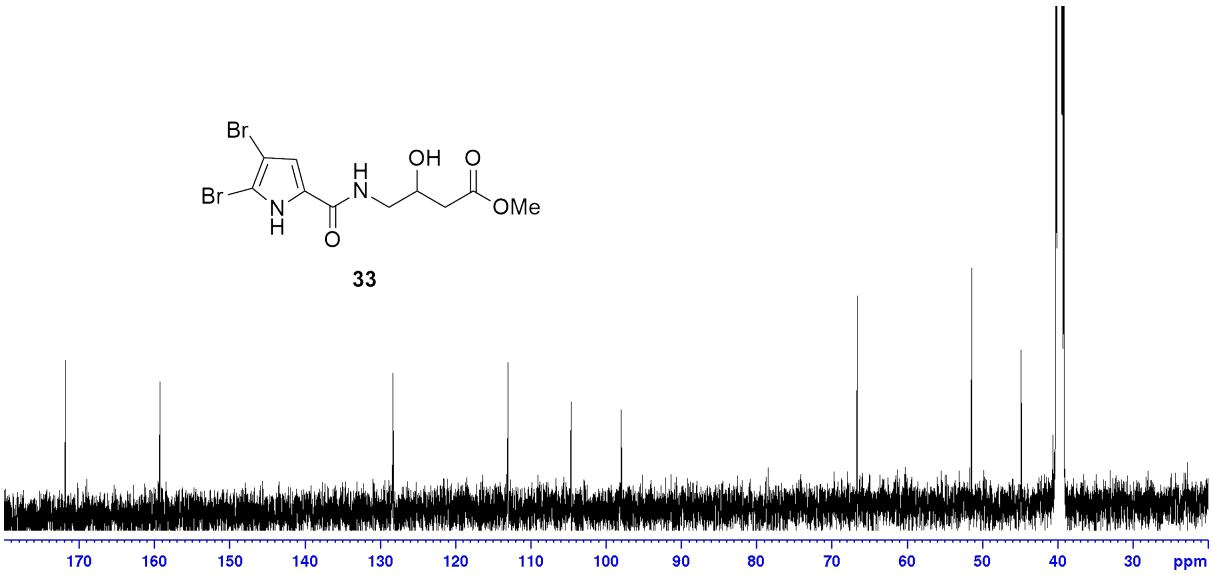

33

Figure S46. ^{13}C NMR spectrum of agesasine B (**33**) in DMSO-d_6 (125 MHz).

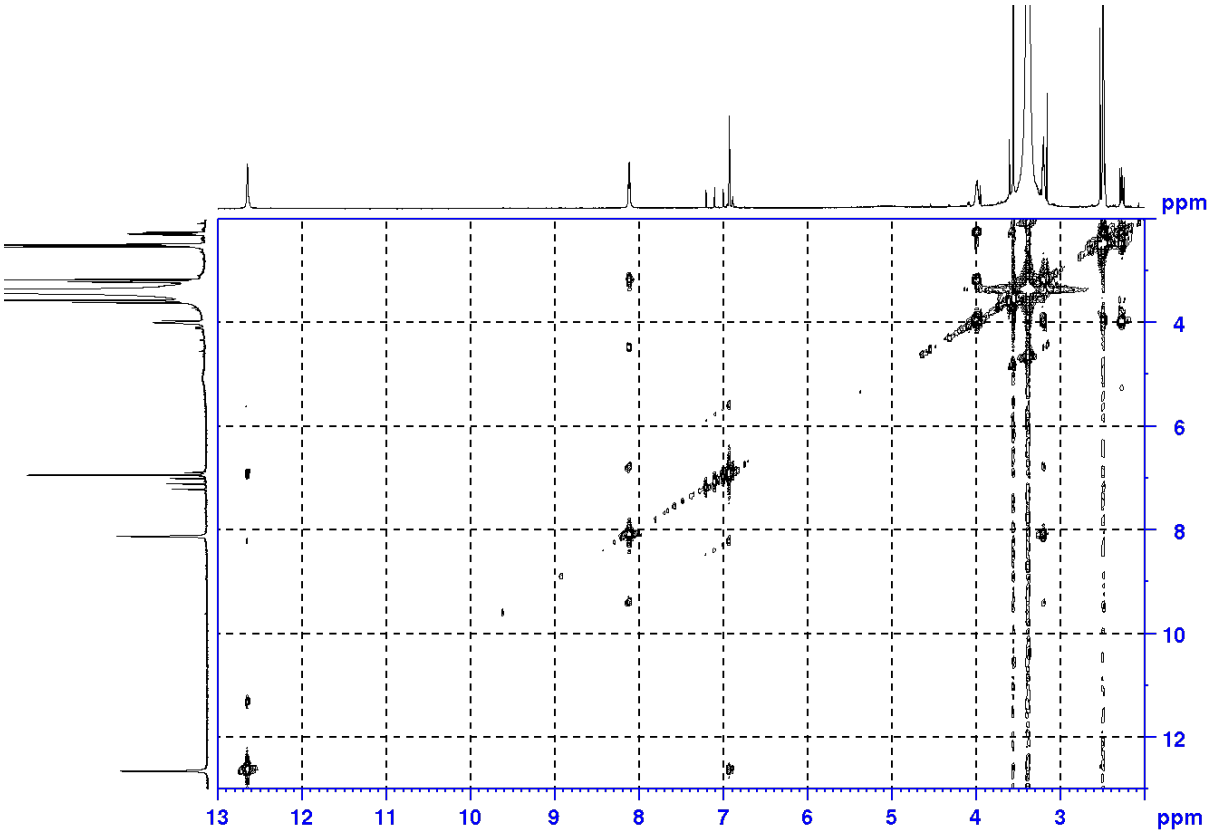

Figure S47. ^{1}H-^{1}H COSY spectrum of agesasine B (**33**) in DMSO-d_6 (500 MHz).

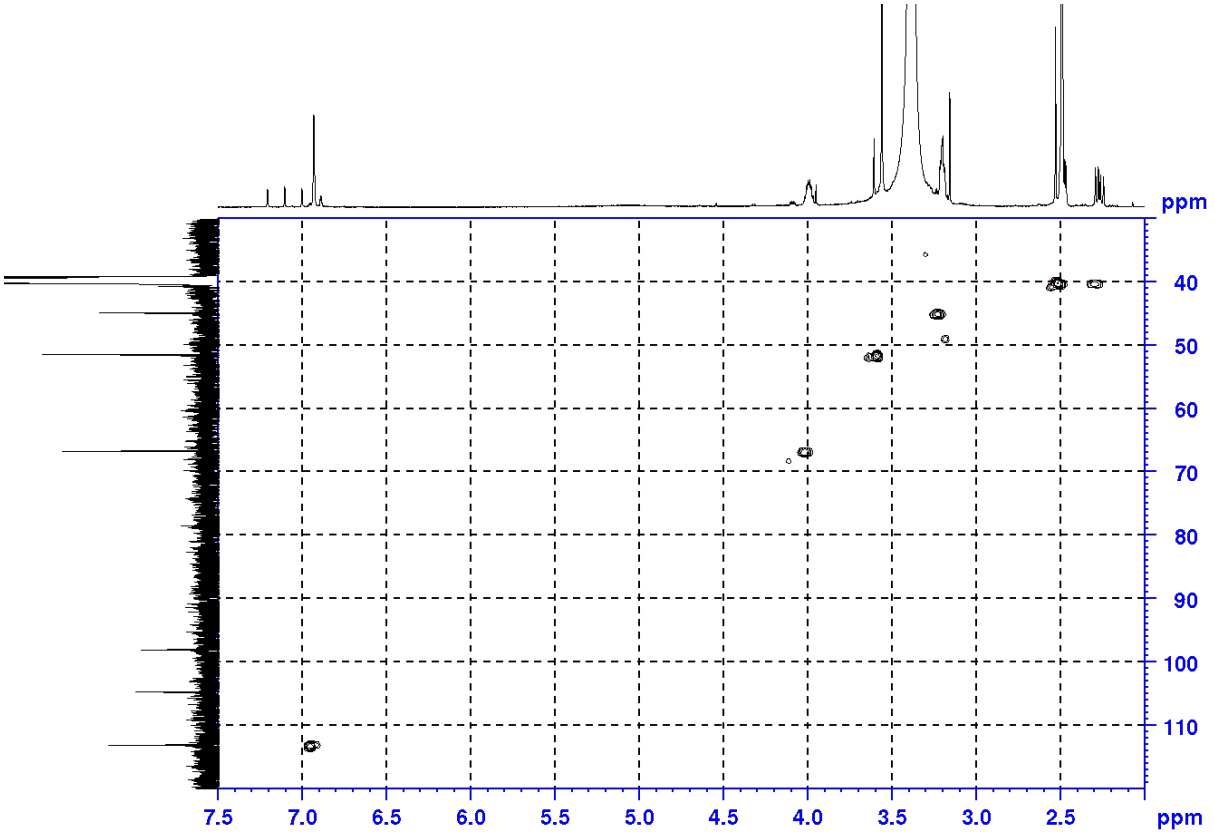

Figure S48. HSQC spectrum of agesasine B (**33**) in DMSO-d_6 (500 MHz).

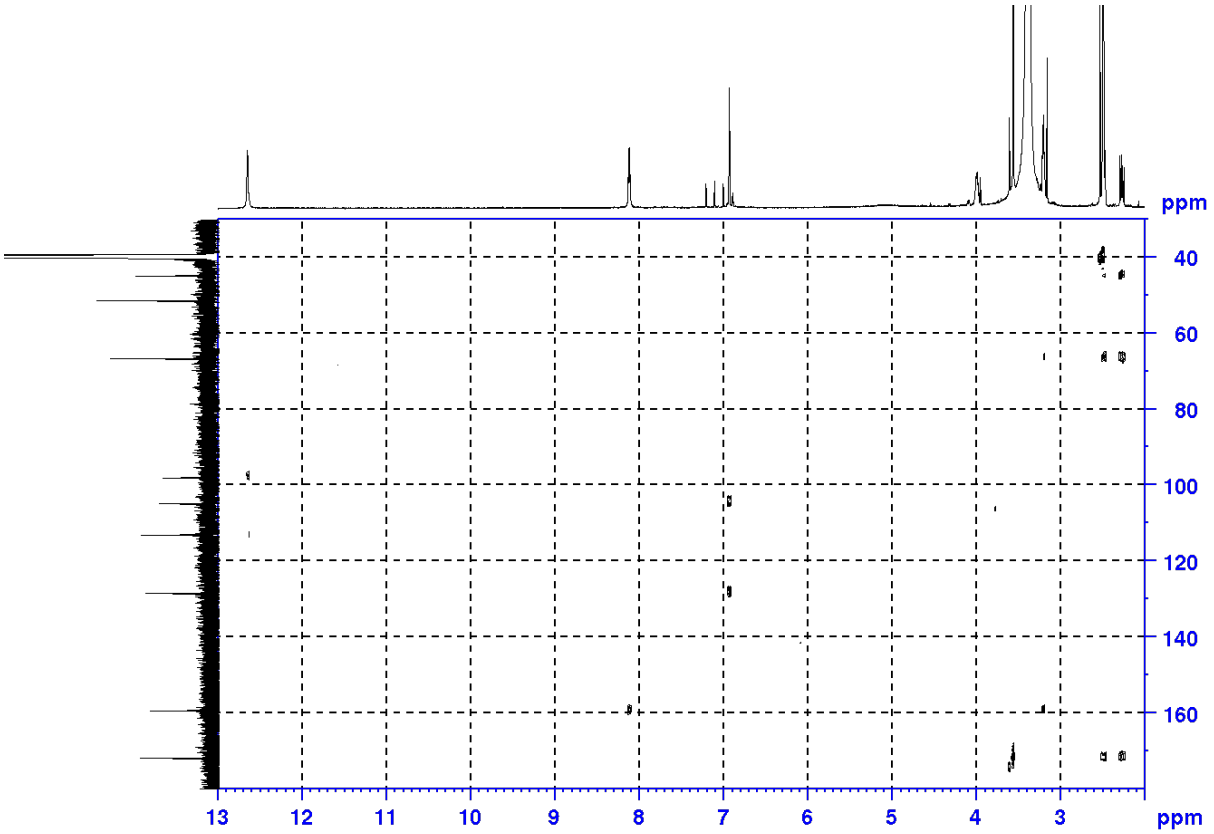

Figure S49. HMBC spectrum of agesasine B (**33**) in DMSO-d_6 (500 MHz).

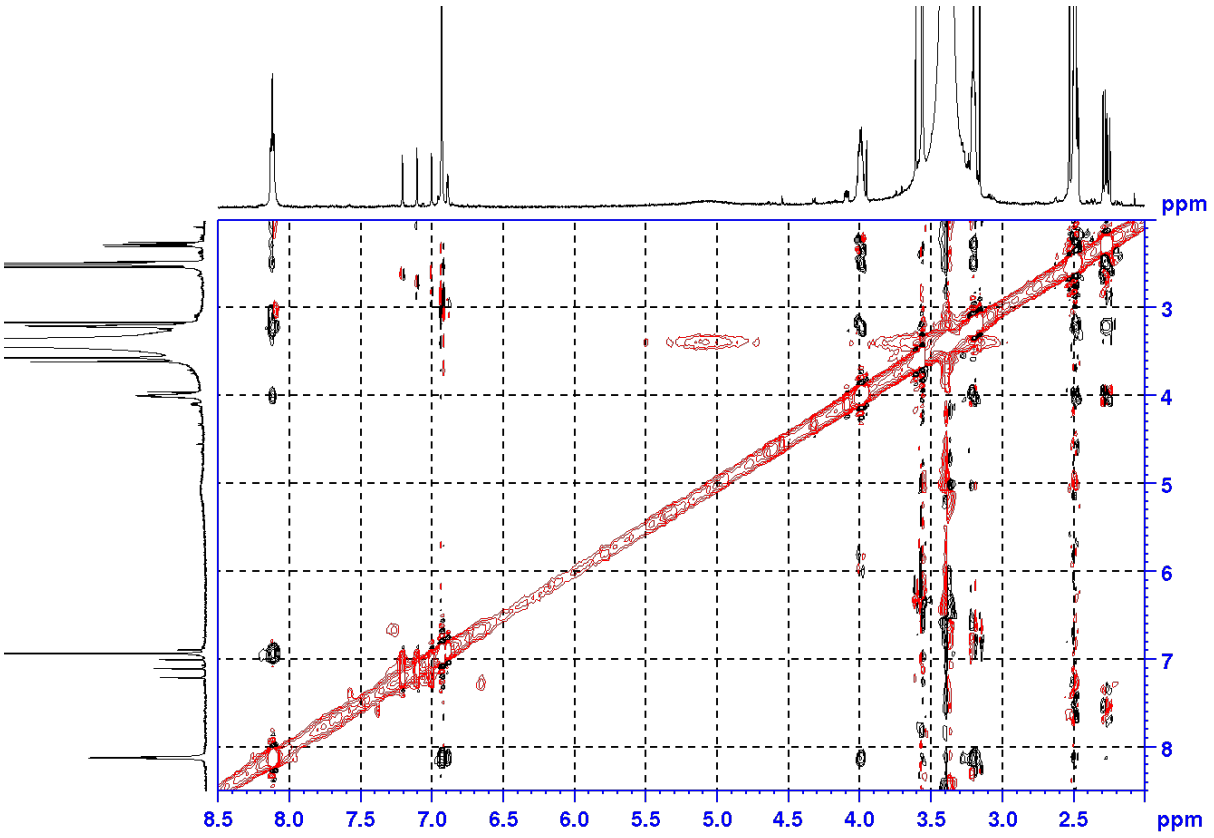

Figure S50. ROESY spectrum of agesasine B (**33**) in DMSO-d_6 (500 MHz).

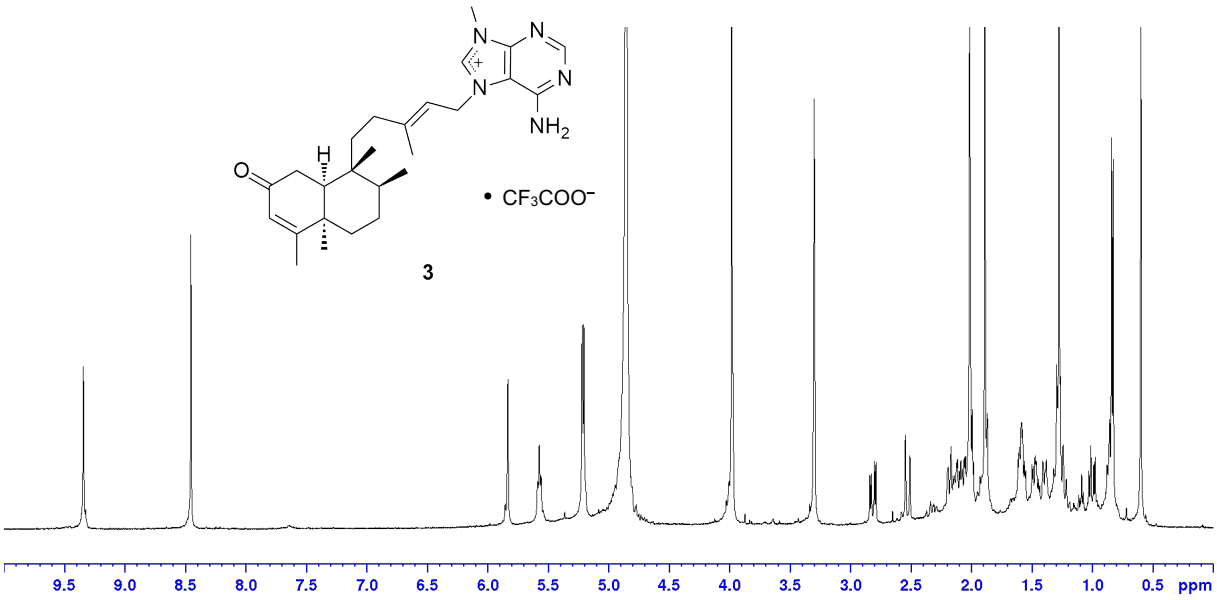

Figure S51. ^{1}H NMR spectrum of 2-oxo-agelasine A (**3**) as a TFA salt form in CD_3OD (500 MHz).

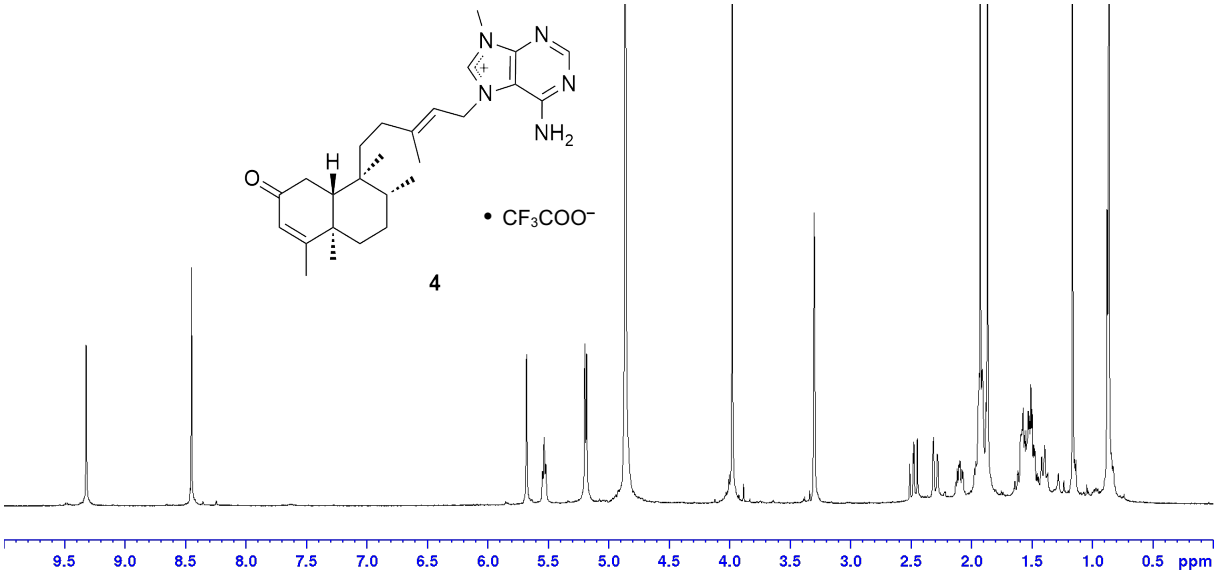

Figure S52. ^{1}H NMR spectrum of 2-oxo-agelasine B (**4**) as a TFA salt form in CD_3OD (500 MHz).

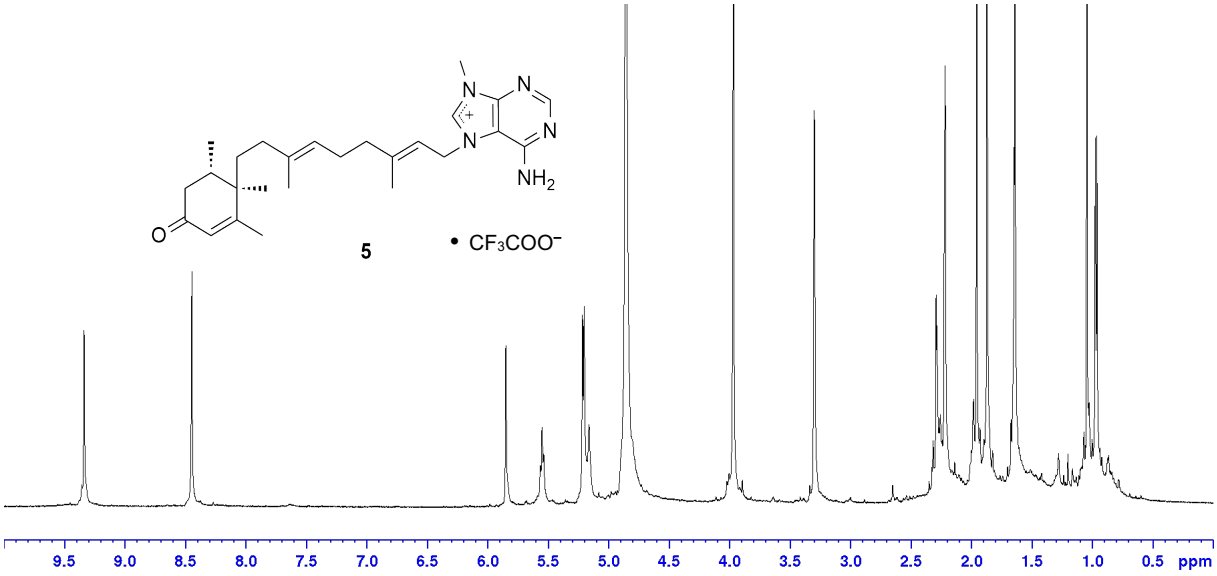

Figure S53. ^{1}H NMR spectrum of 2-oxo-agelasine F (**5**) as a TFA salt form in CD_3OD (500 MHz).

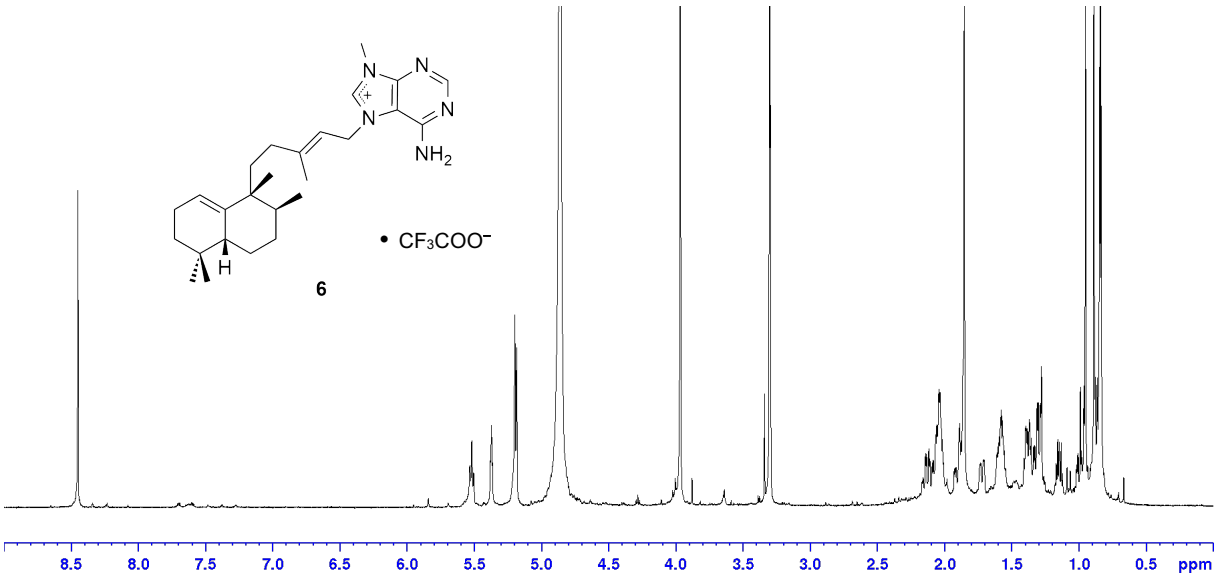

Figure S54. ^{1}H NMR spectrum of agelasine C (**6**) as a TFA salt form in CD_3OD (500 MHz).

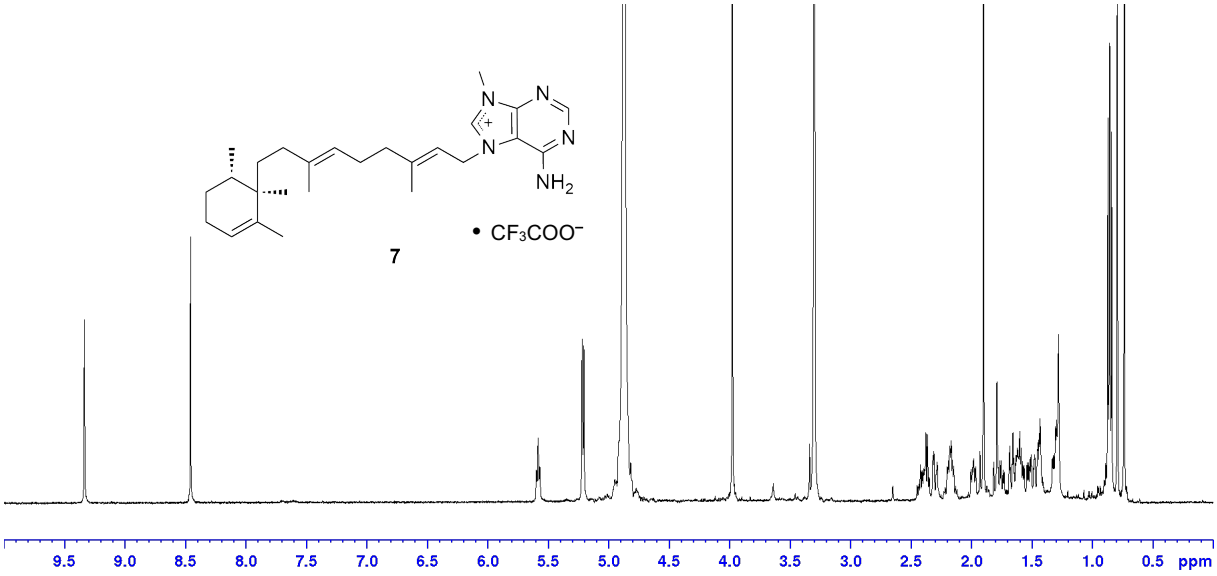

Figure S55. ^{1}H NMR spectrum of nemoechine F (**7**) as a TFA salt form in CD_3OD (500 MHz).

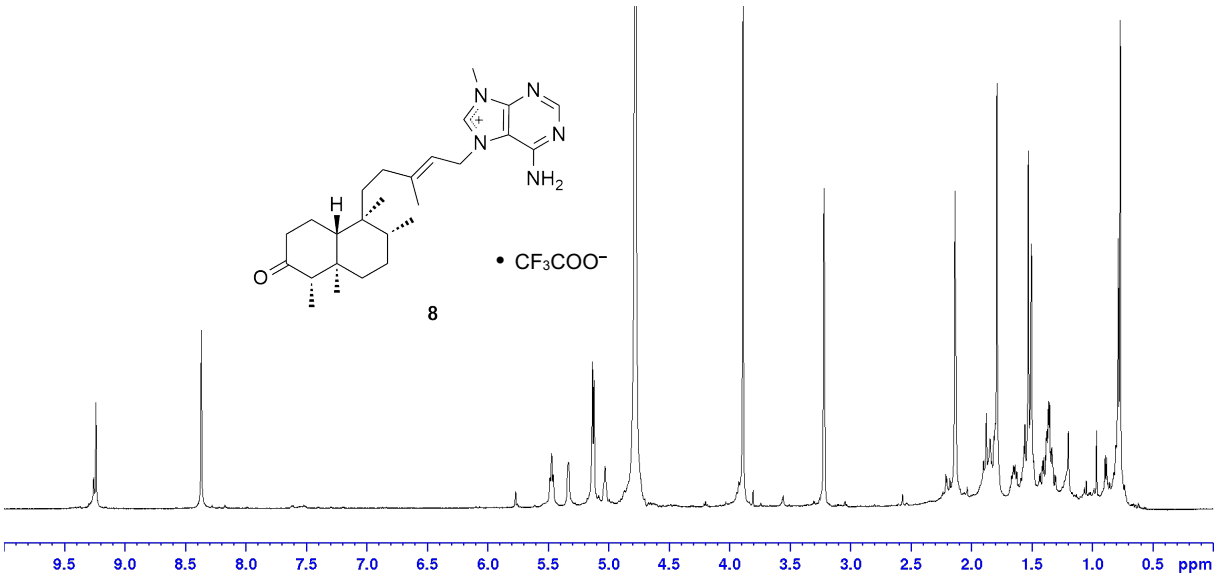

Figure S56. ^{1}H NMR spectrum of agelasine F (**8**) as a TFA salt form in CD_3OD (500 MHz).

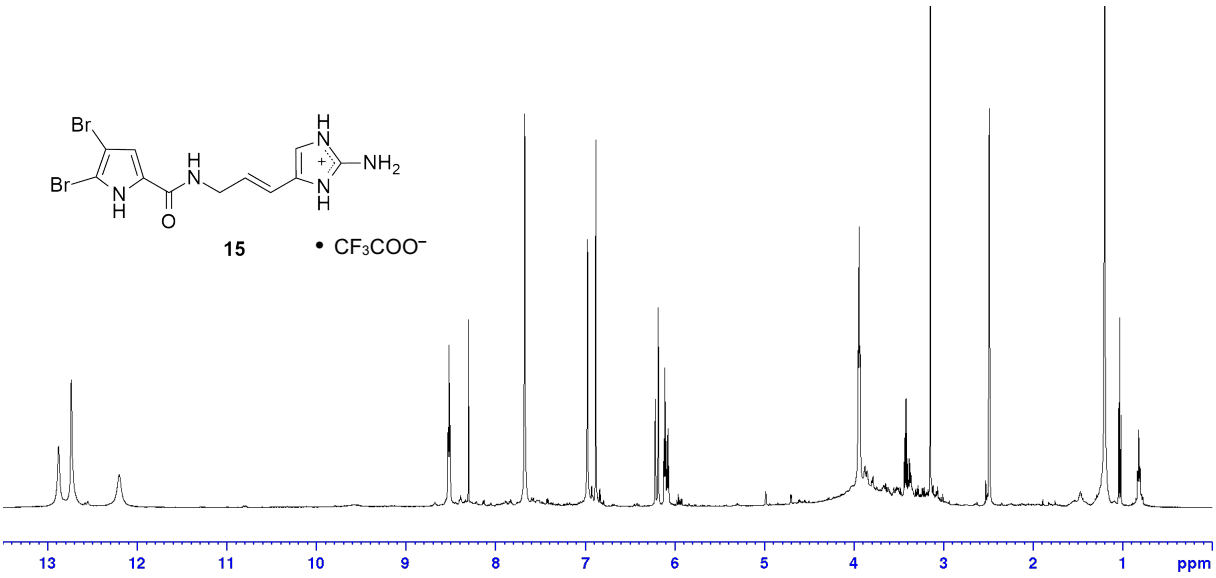

Figure S57. ^{1}H NMR spectrum of oroidin (**15**) as a TFA salt form in DMSO-d_6 (500 MHz).

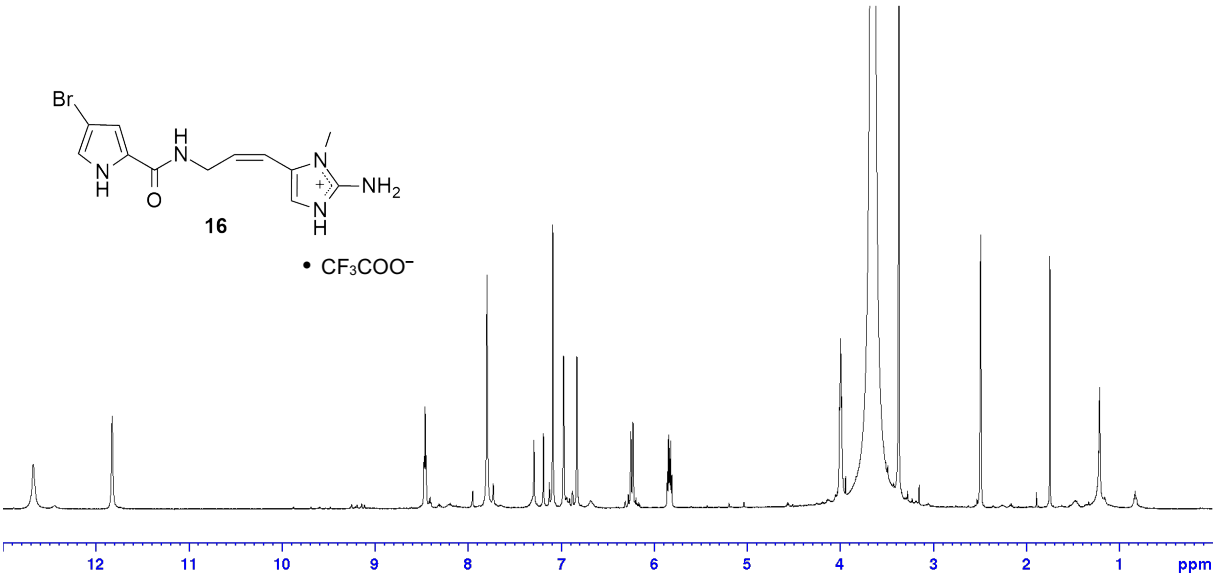

Figure S58. ^{1}H NMR spectrum of keramadine (**16**) as a TFA salt form in DMSO-d_6 (500 MHz).

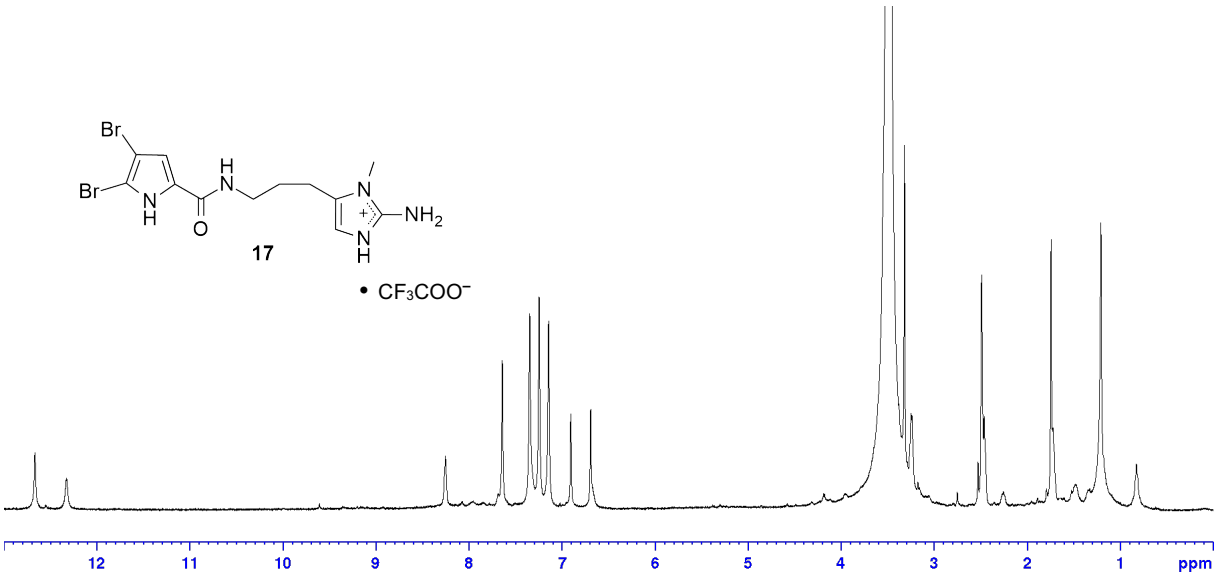

Figure S59. ^{1}H NMR spectrum of 2-bromo-9,10-dihydrokeramadine (**17**) as a TFA salt form in DMSO-d_6 (500 MHz).

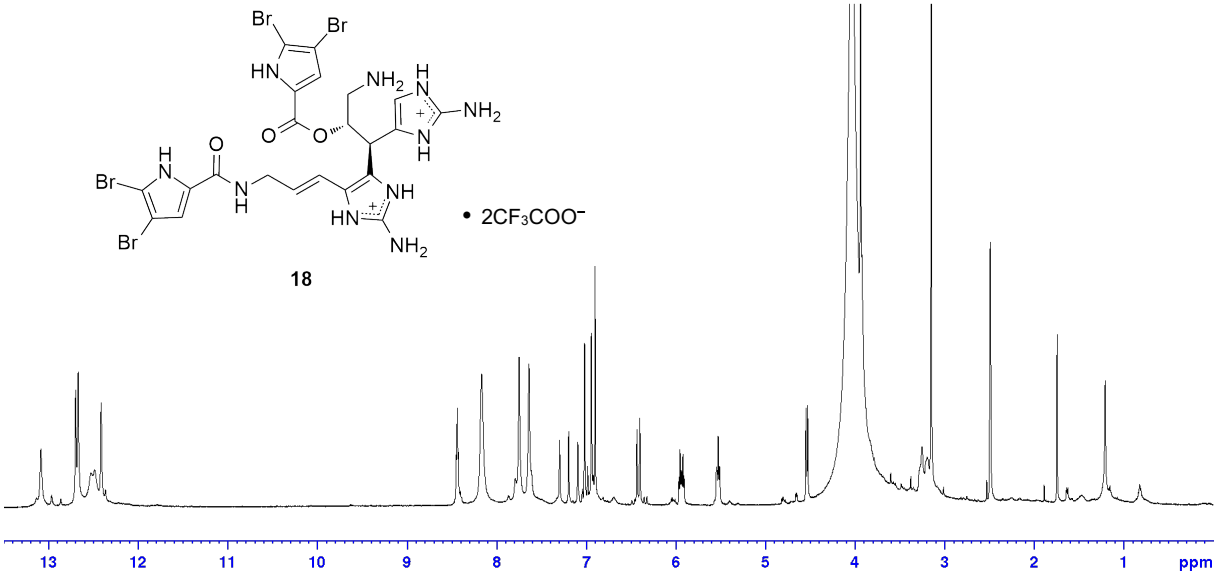

Figure S60. ^{1}H NMR spectrum of nagelamide L (**18**) as a TFA salt form in DMSO-d_6 (500 MHz).

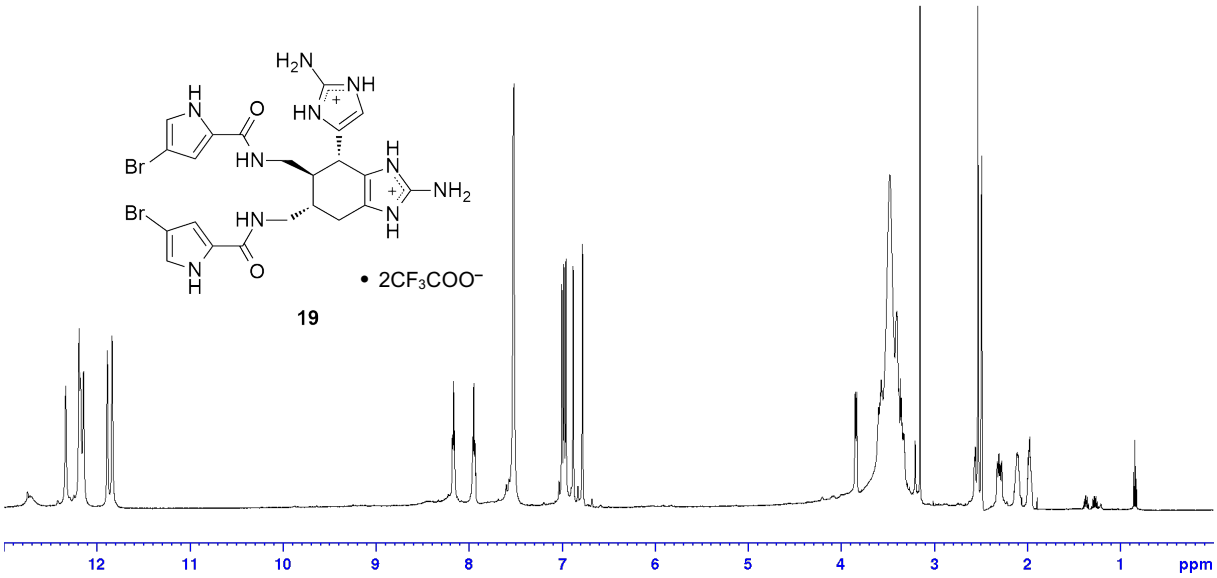

Figure S61. ^{1}H NMR spectrum of ageliferin (**19**) as a TFA salt form in DMSO-d_6 (500 MHz).

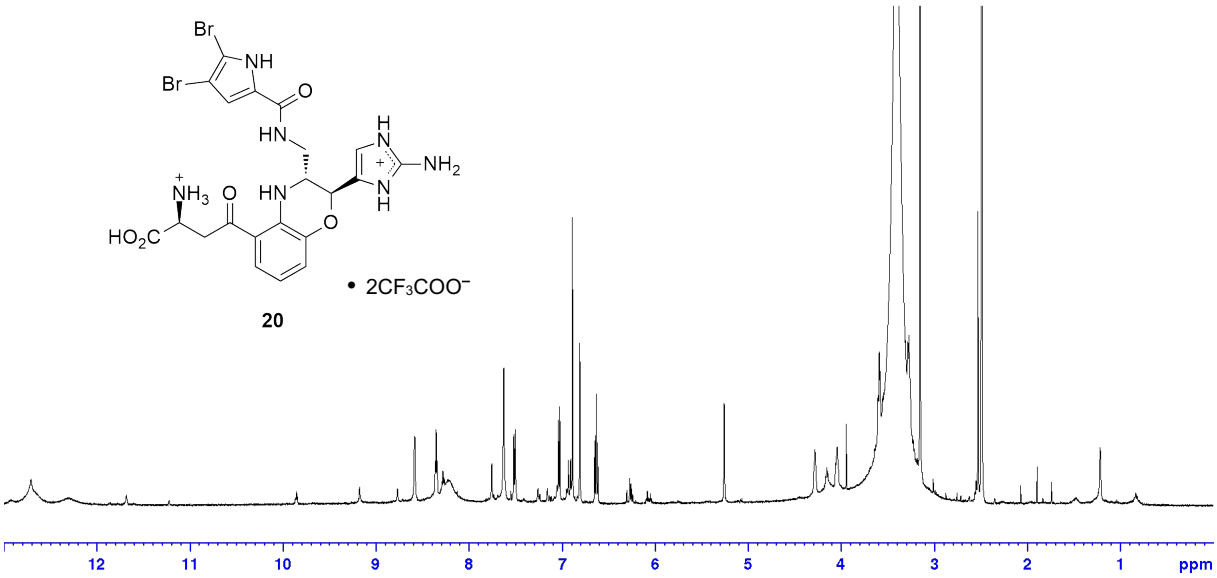

Figure S62. ^{1}H NMR spectrum of agelamadin C (**20**) as a TFA salt form in DMSO-d_6 (500 MHz).

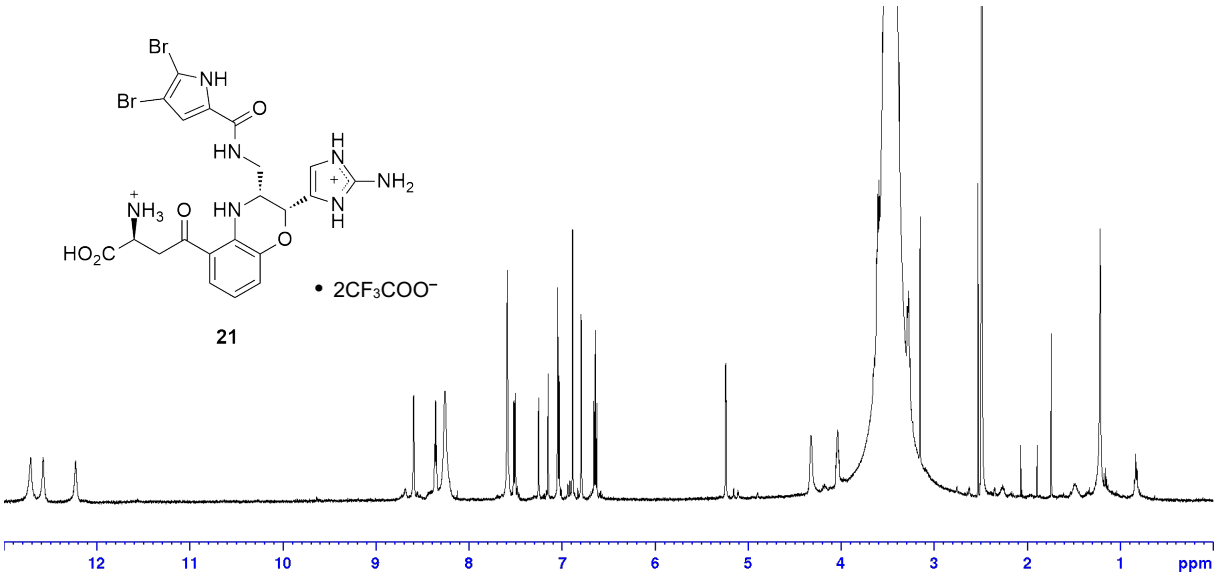

Figure S63. [1]H NMR spectrum of agelamadin E (**21**) as a TFA salt form in DMSO-d_6 (500 MHz).

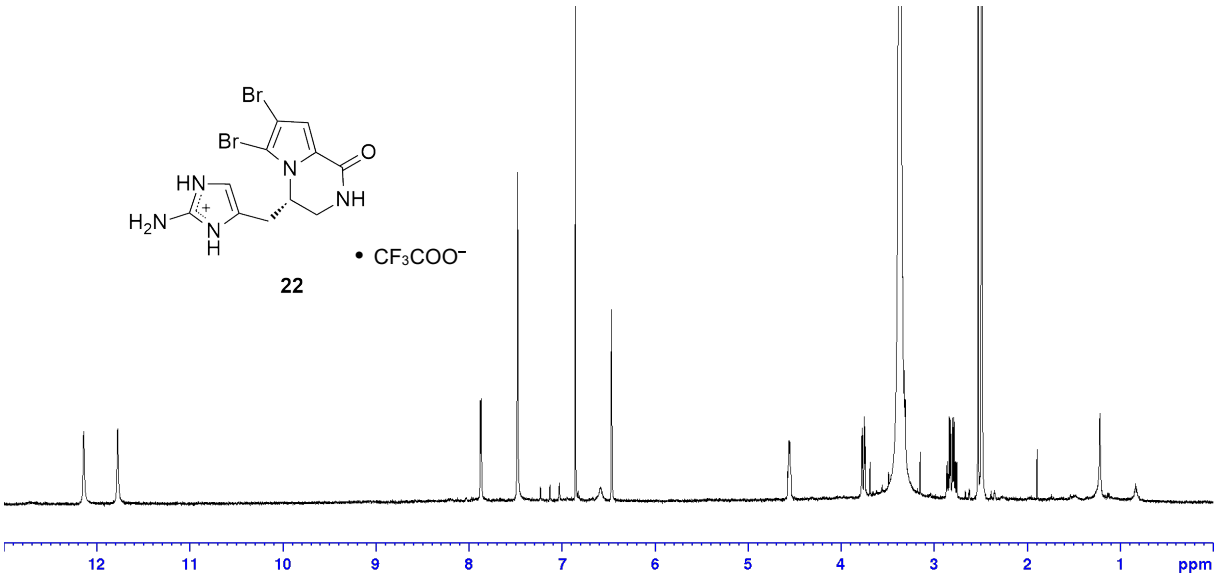

Figure S64. [1]H NMR spectrum of cyclooroidin (**22**) as a TFA salt form in DMSO-d_6 (500 MHz).

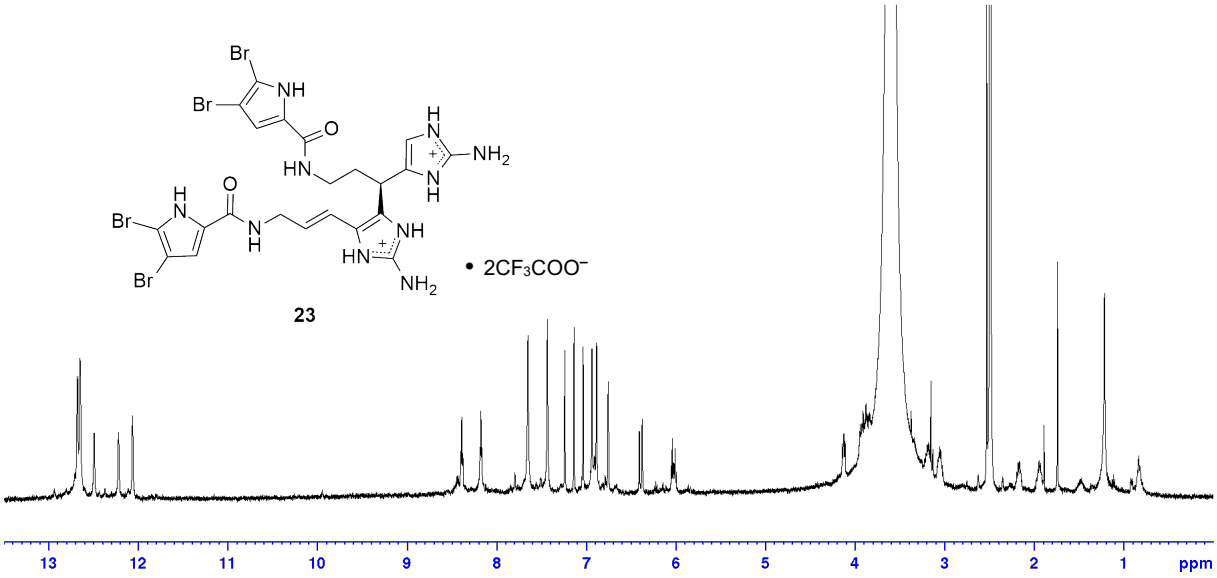

Figure S65. ^{1}H NMR spectrum of nagelamide A (**23**) as a TFA salt form in DMSO-d_6 (500 MHz).

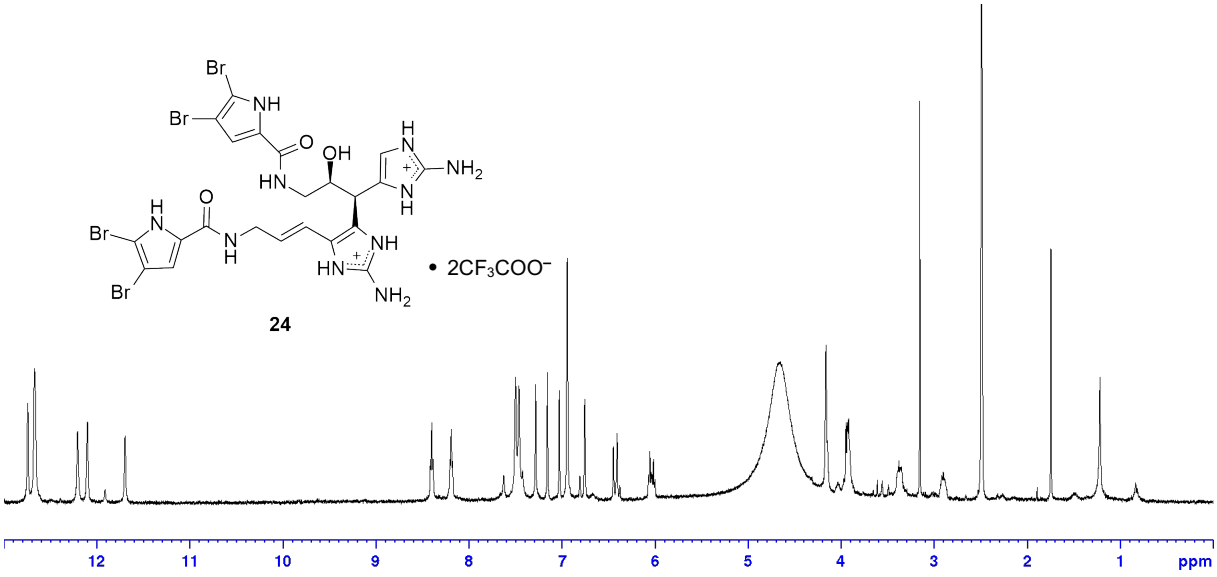

Figure S66. ^{1}H NMR spectrum of nagelamide B (**24**) as a TFA salt form in DMSO-d_6 (500 MHz).

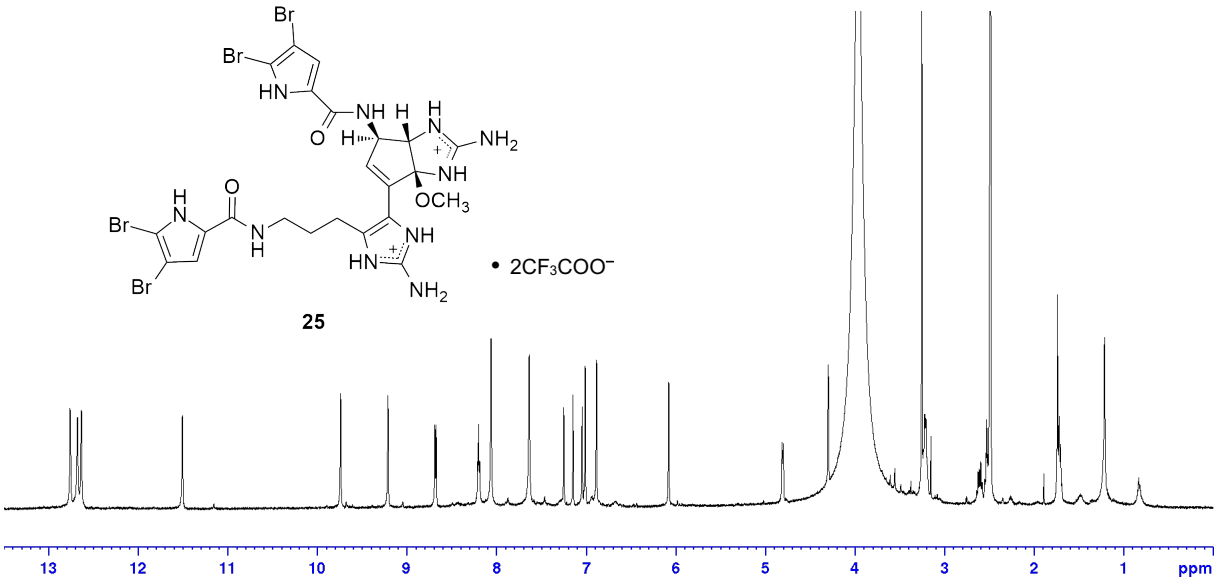

Figure S67. ^{1}H NMR spectrum of nagelamide J (**25**) as a TFA salt form in DMSO-d_6 (500 MHz).

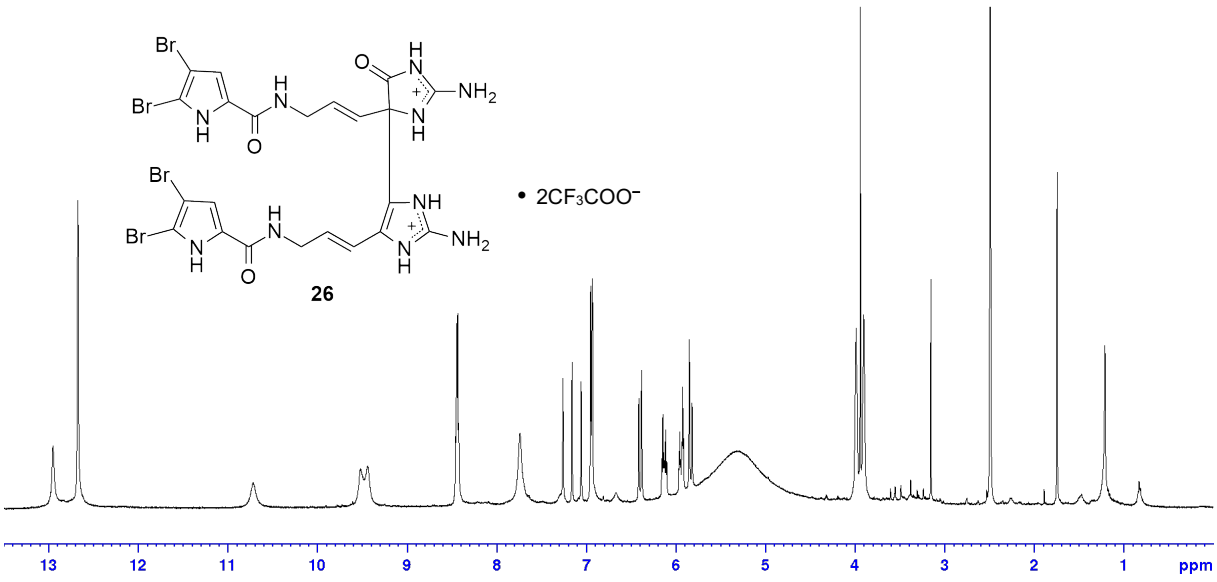

Figure S68. ^{1}H NMR spectrum of mauritiamine (**26**) as a TFA salt form in DMSO-d_6 (500 MHz).

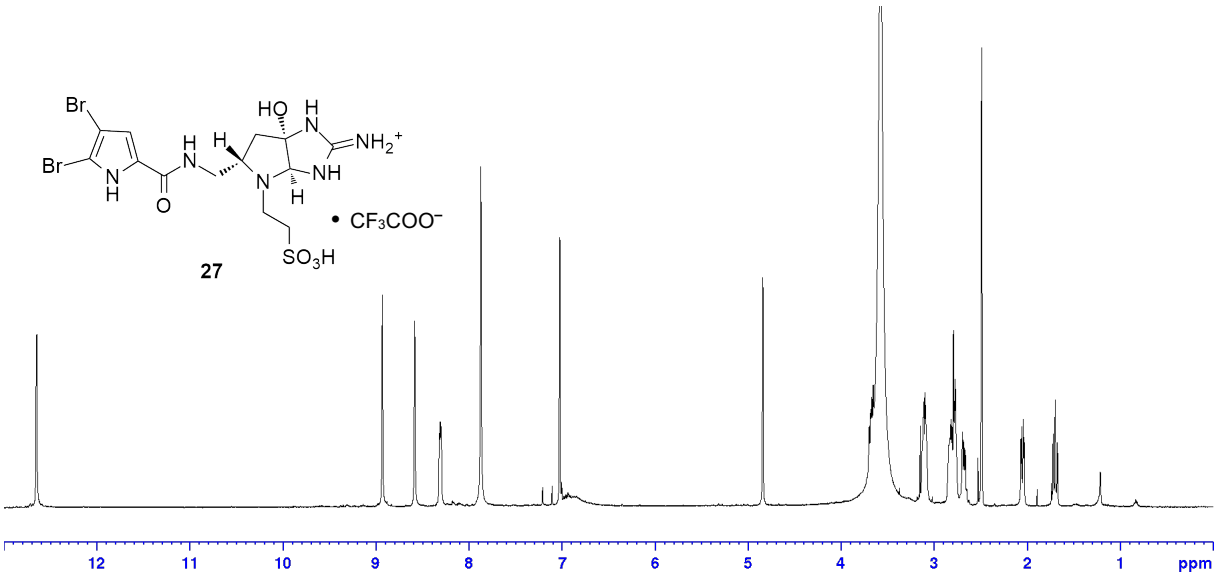

Figure S69. ^{1}H NMR spectrum of nagelamide M (**27**) as a TFA salt form in DMSO-d_6 (500 MHz).

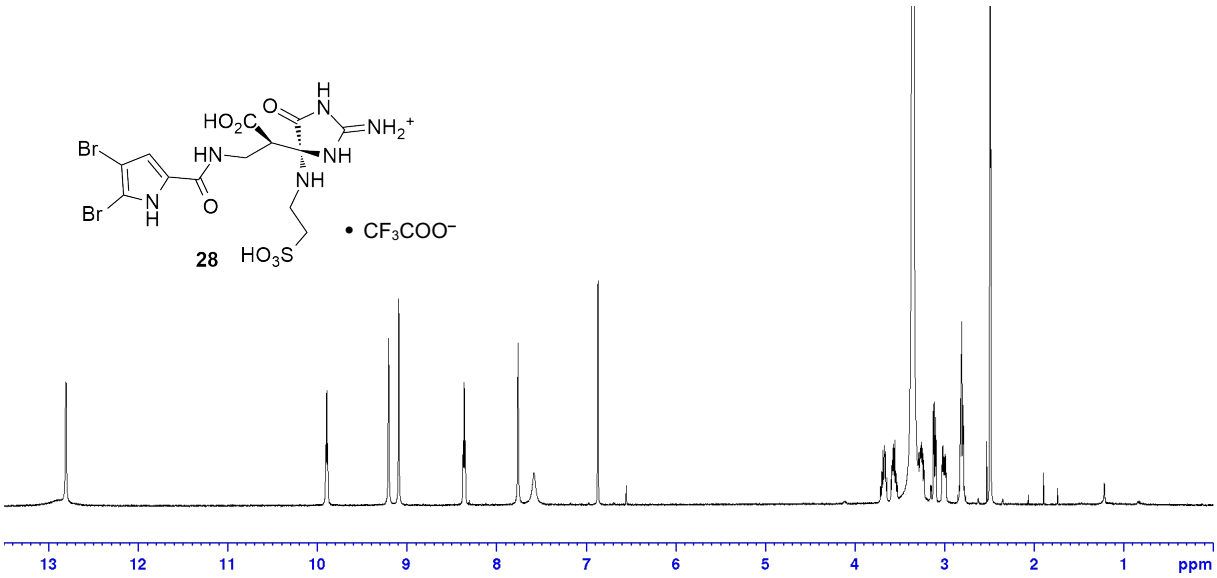

Figure S70. ^{1}H NMR spectrum of nagelamide N (**28**) as a TFA salt form in DMSO-d_6 (500 MHz).

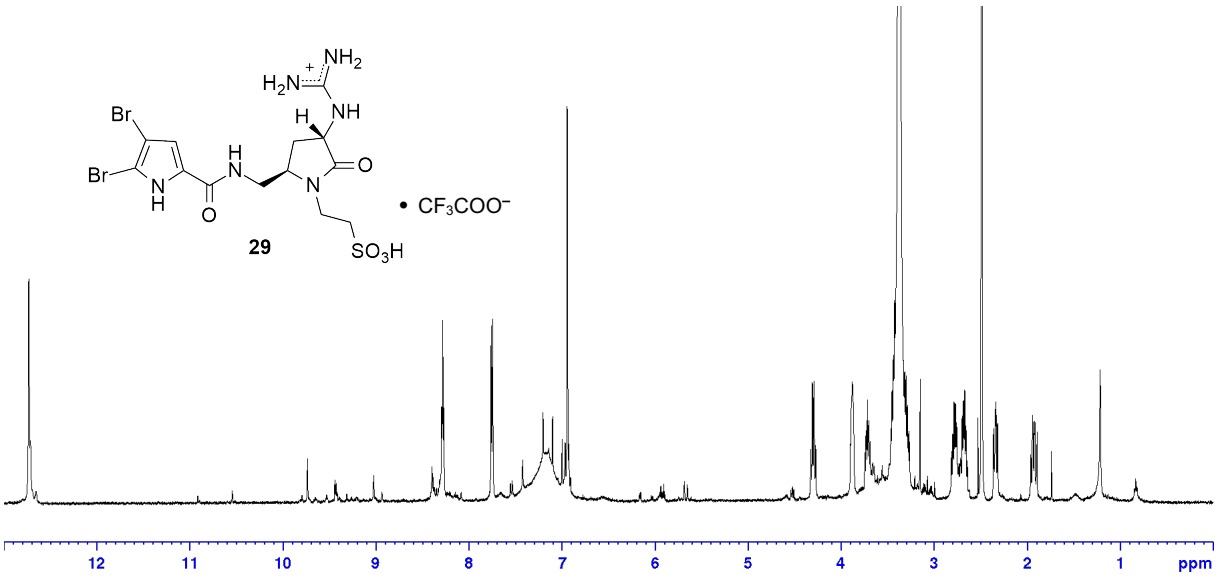

Figure S71. ^{1}H NMR spectrum of nagelamide U (**29**) as a TFA salt form in DMSO-d_6 (500 MHz).

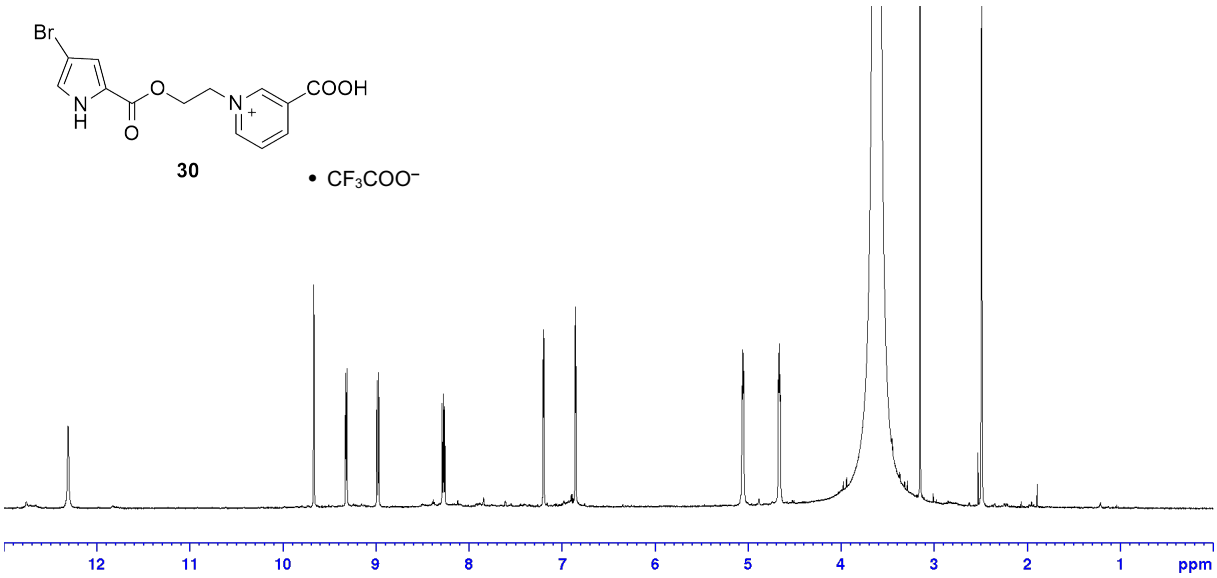

Figure S72. ^{1}H NMR spectrum of agelongine (**30**) as a TFA salt form in DMSO-d_6 (500 MHz).

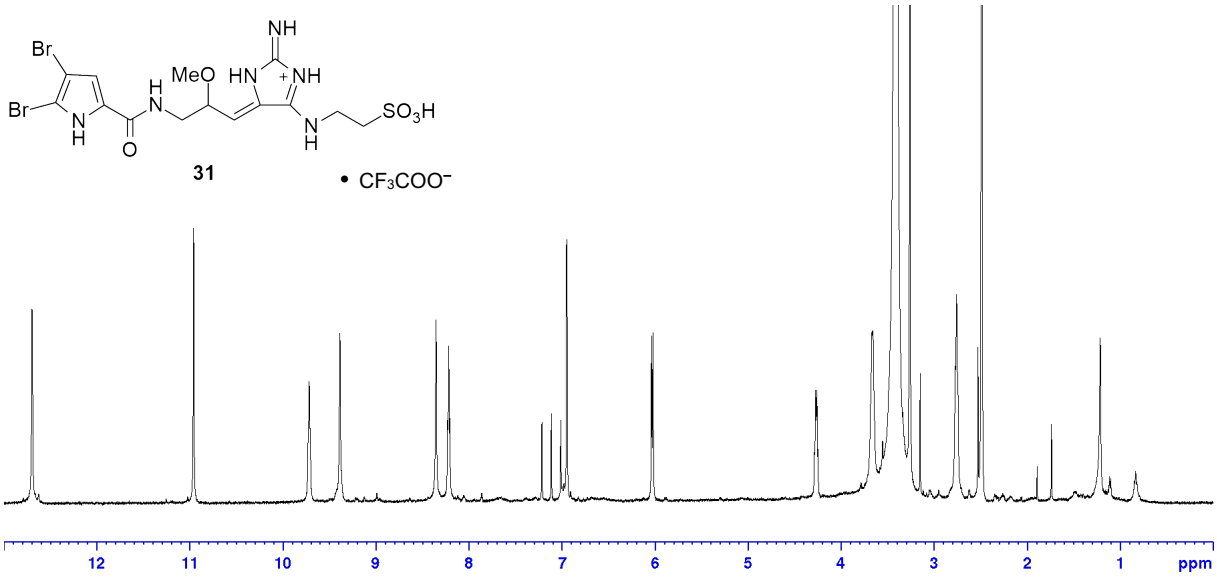

Figure S73. ^{1}H NMR spectrum of tauroacidin C (**31**) as a TFA salt form in DMSO-d_6 (500 MHz).

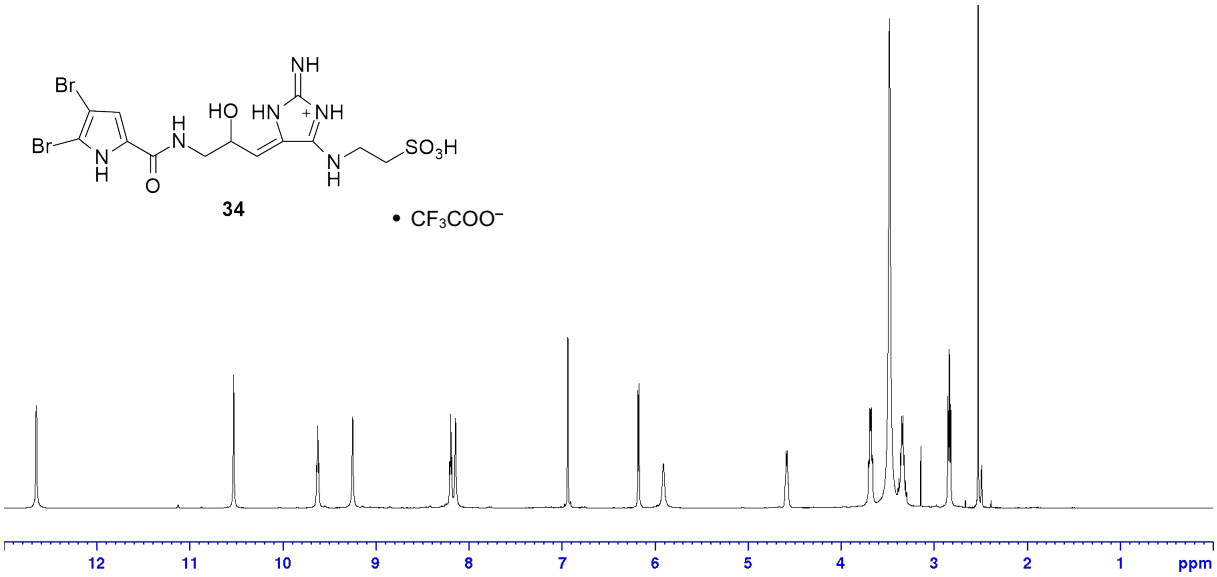

Figure S74. ^{1}H NMR spectrum of tauroacidin A (**34**) as a TFA salt form in DMSO-d_6 (500 MHz).

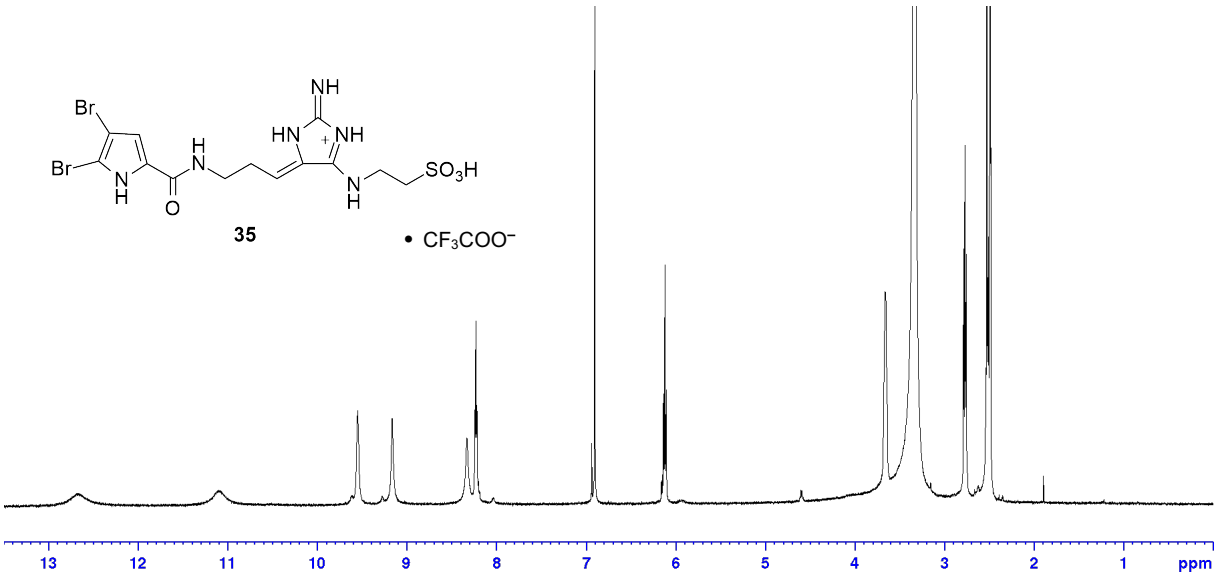

Figure S75. ^{1}H NMR spectrum of taurodispacamide A (**35**) as a TFA salt form in DMSO-d_6 (500 MHz).